

SECRETOME AND GLYCOME OF MAMMALIAN ADIPOCYTES UNDER INSULIN
RESISTANT CONDITIONS

by

JAE-MIN LIM

(Under the Direction of Lance Wells)

ABSTRACT

Insulin resistance defines the metabolic syndrome and precedes type 2 diabetes, thus is considered as the hallmark for type 2 diabetes. Prolonged hyperglycemia and hyperinsulinemia are both required for the development of classical insulin resistance. In recent years, accumulative evidence has established that elevated O-GlcNAc levels via either genetic or pharmacological methods lead to insulin resistance in both cultured adipocytes and animal models. Adipocytes, besides being a major site for energy storage, are endocrine in nature and secrete a variety of proteins (adipocytokines) that can modulate insulin sensitivity, hypertension, food intake, and general energy homeostasis. The link between O-GlcNAc levels, insulin resistance, and adipocytokine secretion is further explored in this dissertation.

First, by using immortalized and primary rodent adipocytes, the secreted proteome of differentiated adipocytes under insulin responsive and two insulin resistant conditions is explicitly elucidated via shotgun proteomics leading to the identification of 97 and 203 secreted proteins, respectively. More than 80 N-linked glycosylation sites on adipocytokines released by these adipocytes were also mapped. Moreover, we took a step further to address the quantitative secretome of human primary adipocytes with the same technique. Of the 190 secreted proteins

identified, we report 20 up-regulated and 6 down-regulated proteins detected in both insulin resistant conditions. Moreover, we applied glycomic techniques to examine (1) the N-linked sites from the pool of secreted proteins and (2) the characterization and relative abundance of complex N- and O-glycans released from adipocytes exposed to different conditions. We identified 91 N-glycosylation sites on the secreted proteins derived from 51 proteins, as well as 155 and 29 released N- and O-glycans respectively. There were moderate alterations in the observed N- and O-linked glycans under the different conditions considered.

In short, our studies have provided a list of adipocytokines whose secreted levels vary under insulin resistant conditions. These proteins bear the potential to be prognostic/diagnostic biomarkers for the detection of metabolic syndrome and type 2 diabetes. Also, comparing the results compiled from both classical and non-canonical insulin resistance provides further insights for the role of the O-GlcNAc modification on intracellular proteins in the disease progression of type 2 diabetes.

INDEX WORDS: O-GlcNAc, insulin resistance, type 2 diabetes, metabolic syndrome, adipocytokine, tandem mass spectrometry, shotgun proteomics, glycosylation, glycomics, N-linked, O-linked

SECRETOME AND GLYCOME OF MAMMALIAN ADIPOCYTES UNDER INSULIN
RESISTANT CONDITIONS

by

JAE-MIN LIM

B.S., Changwon National University, Republic of Korea, 1998

M.S., Changwon National University, Republic of Korea, 2000

M.S., Western Carolina University, 2003

A Dissertation Submitted to the Graduate Faculty of The University of Georgia in Partial

Fulfillment of the Requirements for the Degree

DOCTOR OF PHILOSOPHY

ATHENS, GEORGIA

2009

© 2009

JAE-MIN LIM

All Rights Reserved

SECRETOME AND GLYCOME OF MAMMALIAN ADIPOCYTES UNDER INSULIN
RESISTANT CONDITIONS

by

JAE-MIN LIM

Major Professor: Lance Wells

Committee: I. Jonathan Amster
Ron Orlando

Electronic Version Approved:

Maureen Grasso
Dean of the Graduate School
The University of Georgia
May 2009

DEDICATION

I would like to thank my wife, Seongha Park, and my daughters, Yejin and Yena, for their unconditional love, patience and support. Words can not express my gratitude for their sacrifice. I would like to thank my parents, parents-in-law, brothers, sisters, brothers-in-law, sisters-in-law, nieces and nephews who have always encouraged me.

May 2009
Jae-Min Lim

ACKNOWLEDGEMENTS

I would like to acknowledge the following people for the professional and personal assistance during the research and the preparation of this dissertation.

I would like to thank my advisor, Dr. Lance Wells, for his encouragement, guidance and assistance as well as for providing me with great experiences and facilities. My most sincere appreciation goes to Dr. Lance Wells and his family. Many thanks also go to my committee, Dr. I. Jonathan Amster and Dr. Ron Orlando, for their invaluable time and expertise.

I would like to thank Dr. Dorothy Hausman, Dr. Michael Tiemeyer, Dr. Carl Bergmann, Dr. Jin-Kyu Lee, Dr. Kazuhiro Aoki and Dr. James Atwood III for their expertise and countless help.

I would like to thank Dr. David J. Butcher (Professor, Department of Chemistry and Physics, Western Carolina University), Dr. Yong-Ill Lee (Professor, Department of Chemistry, Changwon National University) and Dr. Young-Jae Yoo (Professor, Department of Chemistry, Changwon National University) for providing their encouragement during the study.

Special thanks goes to my laboratory members, Enas Gad Elkarim, Dan Sherling, Chin Fen Teo, Stephanie Hammond, Peng (Linda) Zhao, Anu Rajesh Koppikar, Sandii Brimble, Edith

Hayden, Meng Fang, Krithika Vaidyanathan and Sean Durning for their friendship, kindness and assistance in the laboratory. Best wishes in their future endeavors.

I would also like to thank the administrative staff of the Chemistry Department and the Complex Carbohydrate Research Center.

May 2009
Jae-Min Lim

TABLE OF CONTENTS

	Page
ACKNOWLEDGEMENTS	v
LIST OF TABLES	ix
LIST OF FIGURES	x
CHAPTER	
1 CHAPTER 1: INTRODUCTION AND LITERATURE REVIEW	1
1.1. INSULIN RESISTANCE AND O-GlcNAc MODIFICATION	1
1.2. ADIPOCYTES AND ADIPOCYTOKINES.....	3
1.3. QUANTITATIVE PROTEOMICS AND GLYCOMICS.....	5
REFERENCES.....	9
2 CHAPTER 2: DEFINING THE REGULATED SECRETED PROTEOME OF RODENT ADIPOCYTES UPON THE INDUCTION OF UNSULIN RESISTANCE.....	30
ABSTRACT	31
2.1. INTRODUCTION.....	32
2.2. EXPERIMENTAL PROCEDURES	34
2.3. RESULTS.....	39
2.4. DISCUSION.....	43
REFERENCES.....	48
SUPPORTING INFORAMTION	71

3	CHAPTER 3: QUANTITATIVE SECRETOME AND GLYCOME OF PRIMARY HUMAN ADIPOCYTES UNDER INSULIN RESISTANT CONDITIONS	93
	ABSTRACT	94
	3.1. INTRODUCTION.....	95
	3.2. EXPERIMENTAL PROCEDURES	99
	3.3. RESULTS.....	107
	3.4. DISCUSSION	112
	REFERENCES.....	116
	SUPPORTING INFORMATION	148
4	CHAPTER 4: CONCLUSION	158
	APPENDICES	161
A	APPENDIX A: MAPPING GLYCANS ONTO SPECIFIC N-LINKED GLYCOSYLATION SITES OF <i>PIRUS COMMUNIS</i> PGIP REDEFINES THE INTERFACE FOR EPG-PGIP INTERACTIONS.....	161
	ABSTRACT	162
	A.1. INTRODUCTION.....	162
	A.2. EXPERIMENTAL PROCEDURES	165
	A.3. RESULTS.....	168
	A.4. DISCUSSION.....	170
	REFERENCES.....	173

LIST OF TABLES

	Page
Table 1-1: Summary of the quantification technologies for proteomics and glycomics experiments	27
Table 2-1: Calculation of false-discovery rates	56
Table 2-2: Novel secreted proteins from immortalized mouse adipocytes.....	57
Table 2-3: Mouse adipocytokines regulated by insulin resistance	59
Table 2-4: Novel secreted proteins from primary rat adipocytes	60
Table 2-5: Rat adipocytokines regulated by insulin resistance.....	63
Table 2-6: Sites of N-linked glycosylation in rodent adipocytes.....	64
Table 3-1: Total secreted proteins from human adipose tissue by LC-MS/MS	126
Table 3-2: Human adipocytokines regulated a minimum of 150% under both insulin resistant conditions	132
Table 3-3: Identification of N-linked glycosylation sites using PNGase F with the incorporation of ¹⁸ O water in human adipocytokines	133
Table 3-4: Relative quantification of N-linked glycans from human adipocytes between insulin resistant conditions and insulin response condition by ¹³ C/ ¹² C ratio and prevalence ratio.....	137
Table 3-5: Relative quantification of O-linked glycans from human adipocytes between insulin resistant conditions and insulin responsive condition by ¹³ C/ ¹² C ratio and prevalence ratio.....	140

LIST OF FIGURES

	Page
Figure 1-1: Glucose metabolism and insulin transduction in adipocytes.	28
Figure 1-2: Images of fat droplets in mammalian adipocytes.....	29
Figure 2-1: O-GlcNAc levels are elevated under insulin resistant conditions.....	67
Figure 2-2: Schematic diagram of experimental approach.....	68
Figure 2-3: Assigning the secreted proteome of adipocytes.....	69
Figure 2-4: Differential secretion of adipocytokines determined by reconstructed ion chromatograms	70
Figure 3-1: Detection of O-GlcNAc levels from nucleocytosolic proteins of human adipocytes	141
Figure 3-2: Schematic flow diagram of the experimental procedure	142
Figure 3-3: The functional categories of secretome from human adipocytes.....	143
Figure 3-4: Characterization of glycome from human adipocytes by NS-MS and TIM scan.....	144
Figure 3-5: Relative quantification of glycome from human adipocytes with insulin resistant conditions using $^{13}\text{C}/^{12}\text{C}$ labeling.....	145

CHAPTER 1

INTRODUCTION AND LITERATURE REVIEW

1.1. INSULIN RESISTANCE AND O-GlcNAc MODIFICATION

Diabetes mellitus (commonly referred to as diabetes) is a chronic metabolic disorder that affects about 5% of the population in industrialized nations and the global incidence of diabetes is increasing as to be characterized as an epidemic. Most cases of diabetes are one of two categories, which are very distinct in their etiologies and pathogenesis (1). Type 1 diabetes is due to beta-cell dysfunction in the pancreatic islets of Langerhans. Type 2 diabetes accounts for the vast majority cases of diabetes from defects in both insulin resistance and pancreatic insulin secretion. Insulin resistance is associated with type 2 diabetes, hypertension and cardiovascular disease and related to various metabolic and physiological disorders known as Syndrome X or metabolic syndrome (2-4). Insulin resistance, a hallmark of type 2 diabetes, results from a stepwise progression of hyperglycemia to hyperinsulinemia along with glucose toxicity (5). Nutrient excess, particularly glucose, have been shown to decrease insulin sensitivity, with potential association with insulin resistance (6-8). Insulin sensitivity has been shown to be regulated by the hexosamine biosynthetic pathway (HBP) due to excess glucose flux shown in Figure 1-1 (9). Direct association between insulin resistance and the HBP due to glucose flux was first established by Marshall *et al.* (6, 7) and further supported by subsequent studies in which impairing HBP by blocking the rate limiting enzyme, glutamine:fructose-6-phosphate amidotransferase (GFAT), can reverse the effect of insulin resistance (10-12). In fact, only 2 to 5% of incoming glucose will be shuffled into the HBP compared to other major routes for

glucose utilization such as glycolysis, glycogen synthesis and the pentose phosphate shunt. The end product of the HBP is the sugar nucleotide UDP-GlcNAc which is utilized as a donor substrate for the ubiquitous intracellular glycosylation of nuclear and cytosolic proteins known as O-linked β -N-acetylglucosamine (O-GlcNAc) modification as well as complex glycosylation of proteins and lipids (13).

First discovered by Torres CR and Hart GW in 1984 (14), O-GlcNAc modification of cytosolic and nuclear proteins results from the enzymatic addition of the N-acetyl glucosamine (GlcNAc) moiety of UDP-N-acetylglucosamine (UDP-GlcNAc) to serines or threonines by the O-linked β -N-acetylglucosamine transferase (OGT) (15-17). O-GlcNAc glycosylated proteins can be deglycosylated by another enzyme, β -D-N acetylglucosaminidase (O-GlcNAcase) (18-20). O-GlcNAc modification on the serine and threonine residues of polypeptides has been shown to be a ubiquitous regulatory post-translational modification (PTM) in biological systems. The regulatory O-GlcNAc post-translational modification is more analogous to phosphorylation than to other types of glycosylation (21-25). O-GlcNAc competes with phosphorylation at specific sites (21, 26-29) and a reciprocal relationship between phosphorylation and O-GlcNAc has been observed globally (25, 30). In models of hyperglycemia, elevated levels of O-GlcNAc antagonize insulin signaling and promote insulin resistance associated with postreceptor defects in the potential interplay between O-GlcNAc and phosphate in signaling cascades (24, 31-33). From these researches, increasing global O-GlcNAc levels can induce insulin resistance without the prerequisite for hyperglycemia and hyperinsulinemia and a concomitant defect in the metabolic branch of the insulin signaling pathway (IRS/PI3K/Akt pathway) has been established with both cell culture and animal models (34-36).

Finally, O-GlcNAcase is a nucleocytoplasmic enzyme that catalyzes O-GlcNAc removal from proteins (37-39). O-(2-acetamido-2-deoxy-D-glucopyranosylidene)amino-N-phenylcarbamate (PUGNAc) is a GlcNAc analogue that prevents cycling of O-GlcNAc modification through inhibition of O-GlcNAcase in cells, leading to globally elevated levels of this modification without significantly altering N-linked glycosylation or UDP-GlcNAc levels (40). Inhibition of O-GlcNAcase by PUGNAc in differentiated 3T3-L1 adipocytes leads to insulin resistance (32). In this study, we examine the relationship between elevated O-GlcNAc levels such as both classically induced-insulin resistant (chronic hyperglycemia and hyperinsulinemia) and the pharmacologically induced-insulin resistant (by PUGNAc) conditions and alteration of secretome and glycome in mammalian adipocytes.

1.2. ADIPOCYTES AND ADIPOCYTOKINES

In the last decade, adipocytes have been demonstrated to play a key role in energy homeostasis. Adipocytes possess the largest energy reserve in the animal body and are an endocrine tissue that regulates energy metabolism through paracrine and endocrine mechanisms shown in Figure 1-2 (41-43). In addition to the secretion of free fatty acid by adipocytes, many adipocyte-secreted proteins, collectively termed adipocytokines or adipokines, can act in an autocrine, paracrine or endocrine fashion (44). For instance, adipocytes secrete tumor necrosis factor α (TNF- α), a cytokine that interferes with insulin signaling by blocking phosphorylation of insulin receptor substrate-1 (IRS-1), and leptin, a peptide hormone that regulates energy intake and expenditure (45, 46). In addition, serum retinol binding protein 4 (RBP4) is the adipocyte 'signal' that contributes to systemic insulin resistance and consequently to type 2 diabetes (47). Several adipokines have been implicated in hypertension (angiotensinogen), impaired

fibrinolysis (PAI-1), insulin resistance (ASP, TNF- α , IL-6, resistin and adiponectin) and food intake (leptin) (42, 43, 48, 49).

Adipocytokines identified so far that appear to act as signaling molecules include angiotensin, leptin, adiponectin, adipisin, TNF- α , TGF- β IL-6 and resistin (42). Most of these adipocytokines have been shown to be secreted at higher or lower levels by modulation of nutrient (primarily glucose) levels and/or hormone stimulation (44). For those investigated, it appears the secreted adipocytokine levels are dictated primarily at the level of transcription regulation (50). Many researchers have begun to define the secreted proteome of 3T3-L1 mouse adipocytes, primary rat adipose tissues and primary human adipocytes by gel-based and liquid chromatography-based mass spectrometry (51-59). Several research groups have demonstrated the adipocytokines contributes to insulin resistance, the hallmark of the metabolic syndrome and the preceding complication of type 2 diabetes (42, 60). In at least two cases, for leptin and adiponectin, transcription is regulated by glucose flux through the HBP shown in Figure 1-1 (61-64). UDP-GlcNAc levels are proportional to the amount entering the cell and diabetic animal and diabetic patients have elevated UDP-GlcNAc levels (65). Adipocytokines are now known to secrete humoral factors and some of these (e.g. leptin, adiponectin and resistin) can modulate insulin sensitivity. Thus, the altered production of these adipokines could be involved in predisposition to diabetes (66).

Recent work by our group has expanded the adipocytokine list to over two hundred secreted proteins with 3T3-L1 and 3T3-F442A mouse adipocytes, primary rat adipose tissues and primary human adipocytes respectively (67, 68). From these studies, we have defined not just the proteins but the post-translational modification of these proteins and glycosylation of

adipocytes and discovered regulated proteins upon the induction of insulin resistance in adipocytes.

1.3. QUANTITATIVE PROTEOMICS AND GLYCOMICS

Proteomics is the large-scale study of proteins and built on technologies to analyze a mixture of proteins simultaneously in one experiment. Mass spectrometry (MS) has been used to identify proteins in complex mixtures via largely qualitative analysis. Currently, the most popular method is an automated method for rapid and large-scale shotgun proteomics that is commonly referred to as multidimensional protein identification technology (MudPIT), of which multidimensional liquid chromatography (LC) with electrospray ionization tandem mass spectrometry were used followed by database searching (69-73). Recently developed methodologies offer the opportunity to obtain quantitative proteome between the biological states of an organism. The quantitative proteomic profiling of complex biological samples for the purposes of biomarker discovery is a key challenge in proteomics. Quantitative proteomics has traditionally been performed by two-dimensional (2D) differential in-gel electrophoresis (DIGE) (74, 75). In 2D gel electrophoresis, the relative quantitation is achieved by recording differences in the staining intensity of protein spots derived from two states of differently labeled cell populations or tissues (76, 77). In the past decade, gel-free proteomics techniques have emerged as more sensitive and reproducible methods for quantitatively comparing proteins levels among biological samples. More accurately, relative quantitative proteomics often utilizes isotopic labeling to tag one of the two peptide samples to introduce an isotopically distinguishable mass between peptides from two experimental conditions. Stable isotope labels can be incorporated by chemical approaches (*in vitro*) or through metabolic incorporation (*in*

vivo). Isotope-labeling methods introduce stable isotope tags to proteins via chemical reactions using isotope-coded affinity tags (ICAT) (78-81), or via enzymatic labeling using ^{18}O water for trypsin digestion (82-84), or via metabolic labeling using stable isotope labeling by amino acids in cell culture (SILAC) shown in Table 1-1 (85-87). Among the emerging proteomic technologies, iTRAQ (isobaric tags for relative and absolute quantitation), is a shotgun based tandem mass spectrometric technique (MS/MS) that allows the concurrent identification and relative quantification of hundreds of proteins in different biological samples in a single experiment (88-90). The iTRAQ technology has many advantages over other proteomic techniques, such as being relatively high throughput, increased sensitivity and confidence in both the identification and quantification of the protein. A strategy for the absolute quantification (termed AQUA) exists for technologies that permit the direct quantification of protein and post-translational modification status (91-94). The AQUA peptide strategy requires chemically synthesized isotope-labeled peptides which are spiked into the samples in known quantities before MS analysis.

Label-free MS-based quantitative methods is an attractive alternative to isotopic labeling if they could be used to quantitatively compare protein expression in samples. However, the comparison of multiple LC-MS runs of highly complex biological samples is very challenging. Several laboratories have developed software to assist in analysis of label-free samples, including SpecArray and 2DICAL (95, 96). In addition, a variety of label-free methods have been developed for quantifying relative protein abundance, including peptide counts (97, 98), mass spectral peak intensities and spectral counts that add all the MS/MS spectra observed for peptides derived from a single protein in an LC-MS/MS analysis (99-106). Because proteins that are more abundant in a sample have a higher probability of being identified during data-

dependent MS/MS scanning (100, 106), the number of tandem spectra acquired for individual peptides reflect protein abundance. This has led to the proposal that spectral counting can assess relative protein abundance (100).

Glycosylation is one of the most common post-translational modifications (107, 108). It is common knowledge that approximately 50% of proteins in mammalian cells are glycosylated and virtually all membrane and secreted proteins are glycosylated (108). Glycans play crucial roles in various biological events including cell recognition (107), adhesion (109) and cell-cell interaction (110). A correlation between glycosyltransferase expression and subsequent changes in glycan structures has been reported in several diseases, including inherited diseases (111), the progression of cancer (112) and autoimmune diseases (113-115). Researcher focused on analyzing the glycosylation sites and the alteration of glycan structures on glycoproteins in normal and disease stage(s) are becoming increasingly important in the discovery of diagnostic biomarkers. In the past decade, site-mapping for N-linked glycosylation has become an integral part of proteomic examinations of various congenital and infectious diseases. A common procedure for identifying N-linked glycosylation site(s) involves tryptic digestion of the glycoprotein(s), followed by the conversion of glycosylated asparagine residues into ^{18}O -labeled aspartic acids by PNGase F digestion in ^{18}O water (67, 116-119). The 2.9883 Da mass tag created by this process is readily observable by LC-MS/MS analysis, and is often used to identify the sites of N-linked glycosylation.

The structural diversity of glycans is determined by the expression and regulation of glycosyltransferase activities and by the availability of the appropriate acceptor/donor substrates. To characterize glycan structures, MS fulfills these requirements while providing a rapid and reliable mean to analyze complex mixtures. The fragmentation of methylated glycans is leading

to accurate structural assignment when MS/MS analyses are performed (120-129).

Methodologies for quantitative alteration of glycan expression levels require highly sensitive methods that can distinguish even subtle changes in structure. Current challenges in the field of glycomics are being met by using novel strategies such as the isotopic labeling of oligosaccharides with ^{13}C -labeled iodomethane ($^{13}\text{CH}_3\text{I}$) and isobaric labeling of glycans with $^{13}\text{CH}_3\text{I}$ or $^{12}\text{CH}_2\text{DI}$ (QUIBL, quantitation by isobaric labeling) using standard permethylation procedure shown in Table 1-1 (128, 130, 131). Prevalence ratio from full MS and total ion mapping (TIM) is utilized to determine normalized peak height and area for relative quantification of glycans between different developmental stages (128). A cell culture labeling strategy for glycomics, similar to SILAC for proteomics, was reported for the incorporation of differential mass tags into the glycans of cultured cells named IDAWG: isotopic detection of aminosugars with glutamine (132). In this method, culture media containing amide- ^{15}N -Gln is used to metabolically label cellular aminosugars with heavy nitrogen.

In this study, we identified and quantified the secreted proteome of mammalian adipocytes under insulin responsive and two insulin resistant conditions by using nano LC-MS/MS and normalized peptide and spectral counts from MS/MS runs. We identified N-linked glycosylation sites on secreted proteins from mammalian adipocytes by the conversion of glycosylated asparagine residues into ^{18}O -labeled aspartic acids by PNGase F digestion in ^{18}O water. We also characterized and quantified the N-linked and O-linked glycans of mammalian adipocytes under the conditions using TIM analysis, the isotopic labeling of glycans with ^{13}C -labeled iodomethane and prevalence ratios. With the use of multiple adipocyte cell lines, methods for inducing insulin resistance, and mass spectrometry-based approaches of analysis, this work will provide a more complete insights into adipose tissue physiology and pathology.

REFERENCES

1. American Diabetes Association. Diagnosis and classification of diabetes mellitus. *Diabetes Care* **2006**, *29* (Suppl 1), S43-48.
2. Ford, E. S.; Giles, W. H.; Dietz, W. H. Prevalence of the metabolic syndrome among US adults: findings from the third National Health and Nutrition Examination Survey. *JAMA* **2002**, *287* (3), 356-359.
3. Eckel, R. H.; Grundy, S. M.; Zimmet, P. Z. The metabolic syndrome. *Lancet* **2005**, *365* (9468), 1415-1428.
4. Wilson, P. W.; D'Agostino, R. B.; Parise, H.; Sullivan, L.; Meigs, J. B. Metabolic syndrome as a precursor of cardiovascular disease and type 2 diabetes mellitus. *Circulation* **2005**, *112*, 3066-3072.
5. Brownlee, M. Biochemistry and molecular cell biology of diabetic complications. *Nature* **2001**, *414* (6865), 813-820.
6. Marshall, S.; Bacote, V.; Traxinger, R. R. Complete inhibition of glucose-induced desensitization of the glucose transport system by inhibitors of mRNA synthesis. Evidence for rapid turnover of glutamine:fructose-6-phosphate amidotransferase. *J Biol Chem.* **1991**, *266* (16), 10155-10161.
7. Marshall, S.; Garvey, W. T.; Traxinger, R. R. New insights into the metabolic regulation of insulin action and insulin resistance: role of glucose and amino acids. *FASEB J.* **1991**, *5* (15), 3031-3066.
8. Patti, M. E. Nutrient modulation of cellular insulin action. *Ann N Y Acad Sci.* **1999**, *892*, 187-203.

9. Wells, L.; Vosseller, K.; Hart, G. W. A role for N-acetylglucosamine as a nutrient sensor and mediator of insulin resistance. *Cell. Mol. Life Sci.* **2003**, *60* (2), 222-228.
10. Bosch, R. R.; Pouwels, M. J.; Span, P. N.; Olthaar, A. J.; Tack, C.; Hermus, A. R.; Sweep, C. G. Hexosamines are unlikely to function as a nutrient-sensor in 3T3-L1 adipocytes: a comparison of UDP-hexosamine levels after increased glucose flux and glucosamine treatment. *Endocrine* **2004**, *23* (1), 17-24.
11. Schleicher, E. D.; Weigert, C. Role of the hexosamine biosynthetic pathway in diabetic nephropathy. *Kidney Int Suppl.* **2000**, *77*, S13-18.
12. Kawanaka, K.; Han, D. H.; Gao, J.; Nolte, L.; Holloszy, J. O. Development of glucose-induced insulin resistance in muscle requires protein synthesis. *J Biol Chem.* **2001**, *276* (23), 20101-20107.
13. Comer, F. I.; Hart, G. W. O-GlcNAc and the control of gene expression. *Biochim Biophys Acta.* **1999**, *1473* (1), 161-171.
14. Torres, C. R.; Hart, G. W. Topography and polypeptide distribution of terminal N-acetylglucosamine residues on the surfaces of intact lymphocytes. Evidence for O-linked GlcNAc. *J Biol Chem.* **1984**, *259* (5), 3308-3317.
15. Haltiwanger, R. S.; Holt, G. D.; Hart, G. W. Enzymatic addition of O-GlcNAc to nuclear and cytoplasmic proteins. Identification of a uridine diphospho-N-acetylglucosamine:peptide beta-N-acetylglucosaminyltransferase. *J Biol Chem.* **1990**, *265* (5), 2563-2568.
16. Kreppel, L. K.; Blomberg, M. A.; Hart, G. W. Dynamic glycosylation of nuclear and cytosolic proteins. Cloning and characterization of a unique O-GlcNAc transferase with multiple tetratricopeptide repeats. *J Biol Chem.* **1997**, *272* (14), 9308-9315.

17. Lubas, W. A.; Frank, D. W.; Krause, M.; Hanover, J. A. O-Linked GlcNAc transferase is a conserved nucleocytoplasmic protein containing tetratricopeptide repeats. *J Biol Chem.* **1997**, *272* (14), 9316-9324.
18. Zachara, N. E.; Hart, G. W. O-GlcNAc a sensor of cellular state: the role of nucleocytoplasmic glycosylation in modulating cellular function in response to nutrition and stress. *Biochim. Biophys. Acta* **2004**, *1673*, 13-28.
19. Love, D. C.; Hanover, J. A. The hexosamine signaling pathway: deciphering the “O-GlcNAc code”. *Sci. STKE* **2005**, *312*, re13.
20. Zachara, N. E.; Hart, G. W. Cell signaling, the essential role of O-GlcNAc! *Biochim. Biophys. Acta* **2006**, *1761*, 599-617
21. Hart, G. W.; Greis, K. D.; Dong, D.; Blomberg, M. A.; Chou, T.; Jiang, M.; Roquemore, E. P.; Snow, D. M.; Kreppel, L. K.; Cole, R. N.; *et al.* O-linked N-acetylglucosamine: the "yin-yang" of Ser/Thr phosphorylation? Nuclear and cytoplasmic glycosylation. *Adv. Exp. Med. Biol.* **1995**, *376*, 115-123.
22. Haltiwanger, R. S.; Busby, S.; Grove, K.; Li, S.; Mason, D.; Medina, L.; Moloney, D.; Phillipsberg, G.; Scartozzi, R. O-glycosylation of nuclear and cytoplasmic proteins: regulation analogous to phosphorylation? *Biochem. Biophys. Res. Commun.* **1997**, *231*, 237-242.
23. Vosseller, K.; Wells, L.; Hart, G. W. Nucleocytoplasmic O-glycosylation: O-GlcNAc and functional proteomics. *Biochimie* **2001**, *83*, 575-581.
24. Wells, L.; Vosseller, K.; Hart, G. W. Glycosylation of nucleocytoplasmic proteins: signal transduction and O-GlcNAc. *Science* **2001**, *291*, 2376-2378.

25. Comer, F. I.; Hart, G. W. O-Glycosylation of nuclear and cytosolic proteins. Dynamic interplay between O-GlcNAc and O-phosphate. *J Biol Chem.* **2000**, *275* (38), 29179-29182.
26. Chou, T.; Hart, G. W.; Dang, C. V. c-Myc is glycosylated at threonine 58, a known phosphorylation site and a mutational hot spot in lymphomas. *J. Biol. Chem.* **1995**, *270*, 18961-18965.
27. Kelly, W. G.; Dahmus, M. E.; Hart, G. W. RNA polymerase II is a glycoprotein. Modification of the COOH-terminal domain by O-GlcNAc. *J. Biol. Chem.* **1993**, *268*, 10416-10424.
28. Arnold, C. S.; Johnson, G. V.; Cole, R. N.; Dong, D. L.; Lee, M.; Hart, G. W. The microtubule-associated protein tau is extensively modified with O-linked N-acetylglucosamine. *J. Biol. Chem.* **1996**, *271*, 28741-28744.
29. Comer, F. I.; Hart, G. W. Reciprocity between O-GlcNAc and O-phosphate on the carboxyl terminal domain of RNA polymerase II. *Biochemistry* **2001**, *40*, 7845-7852.
30. Lefebvre, T.; Alonso, C.; Mahboub, S.; Dupire, M. J.; Zanetta, J. P.; Caillet-Boudin, M. L.; Michalski, J. C. Effect of okadaic acid on O-linked N-acetylglucosamine levels in a neuroblastoma cell line. *Biochim. Biophys. Acta* **1999**, *1472*, 71-81.
31. Lima, F. B.; Thies, R. S.; Garvey, W. T. Glucose and insulin regulate insulin sensitivity in primary cultured adipocytes without affecting insulin receptor kinase activity. *Endocrinology* **1991**, *128*, 2415-2426.
32. Vosseller, K.; Wells, L.; Lane M. D.; Hart, G. W. Elevated nucleocytoplasmic glycosylation by O-GlcNAc results in insulin resistance associated with defects in Akt activation in 3T3-L1 adipocytes. *PNAS* **2002**, *99* (8), 5313-5318.

33. Cho, H.; Mu, J.; Kim, J. K.; Thorvaldsen, J. L.; Chu, Q.; Crenshaw, E. B. 3rd.; Kaestner, K. H.; Bartolomei, M. S.; Shulman, G. I.; Birnbaum, M. J. Insulin resistance and a diabetes mellitus-like syndrome in mice lacking the protein kinase Akt2 (PKB beta). *Science* **2001**, *292* (5522), 1728-1731.
34. Heart, E.; Choi, W. S.; Sung, C. K. Glucosamine-induced insulin resistance in 3T3-L1 adipocytes. *Am. J. Physiol. Endocrinol. Metab.* **2000**, *278*, E103-112.
35. Nelson, B. A.; Robinson, K. A.; Buse, M. G. Defective Akt activation is associated with glucose- but not glucosamine-induced insulin resistance. *Am. J. Physiol. Endocrinol. Metab.* **2002**, *282*, E497-506.
36. Singh, L. P.; Gennerette, D.; Simmons, S.; Crook, E. D. Glucose-induced insulin resistance of phosphatidylinositol 3'-OH kinase and AKT/PKB is mediated by the hexosamine biosynthesis pathway. *J. Diabetes Complications* **2001**, *15*, 88-96.
37. Dong, D. L.; Hart, G. W. Purification and characterization of an O-GlcNAc selective N-acetyl-beta-D-glucosaminidase from rat spleen cytosol. *J. Biol. Chem.* **1994**, *269*, 19321-19330.
38. Gao, Y.; Wells, L.; Comer, F. I.; Parker, G. J.; Hart, G. W. Dynamic O-glycosylation of nuclear and cytosolic proteins: cloning and characterization of a neutral, cytosolic beta-N-acetylglucosaminidase from human brain. *J. Biol. Chem.* **2001**, *276*, 9838-9845.
39. Wells, L.; Gao, Y.; Mahoney, J. A.; Vosseller, K.; Chen, C.; Rosen, A.; Hart, G. W. Dynamic O-glycosylation of nuclear and cytosolic proteins: further characterization of the nucleocytoplasmic beta-N-acetylglucosaminidase, O-GlcNAcase. *J. Biol. Chem.* **2002**, *277*, 1755-1761.

40. Haltiwanger, R. S.; Grove, K.; Philipsberg, G. A. Modulation of O-linked N-acetylglucosamine levels on nuclear and cytoplasmic proteins in vivo using the peptide O-GlcNAc-beta-N-acetylglucosaminidase inhibitor O-(2-acetamido-2-deoxy-D-glucopyranosylidene)amino-N-phenylcarbamate. *J. Biol. Chem.* **1998**, *273*, 3611-3617.
41. Cornelius, P.; MacDougald, O. A.; Lane, M. D. Regulation of adipocyte development. *Annu Rev Nutr.* **1994**, *14*, 99-129.
42. Havel, P. J. Update on adipocyte hormones: regulation of energy balance and carbohydrate/lipid metabolism. *Diabetes* **2004**, *53* (Suppl 1), S143-151.
43. Stolar, M. W. Insulin resistance, diabetes, and the adipocyte. *Am J Health Syst Pharm.* **2002**, *59* (Suppl 9), S3-8.
44. Guerre-Millo, M. Adipose tissue and adipokines: for better or worse. *Diabetes Metab* **2004**, *30*, 13-19.
45. Hotamisligil, G. S.; Peraldi, P.; Budavari, A.; Ellis, R.; White, M. F.; Spiegelman, B. M. IRS-1-mediated inhibition of insulin receptor tyrosine kinase activity in TNF-alpha- and obesity-induced insulin resistance. *Science* **1996**, *271* (5249), 665-668.
46. Zhang, Y.; Proenca, R.; Maffei, M.; Barone, M.; Leopold, L.; Friedman, J. M. Positional cloning of the mouse obese gene and its human homologue. *Nature* **1994**, *372* (6505), 425-32. Erratum in: *Nature* **1995**, *374* (6521), 479.
47. Yang, Q.; Graham, T. E.; Mody, N.; Preitner, F.; Peroni, O. D.; Zabolotny, J. M.; Kotani, K.; Quadro, L.; Kahn, B. B. Serum retinol binding protein 4 contributes to insulin resistance in obesity and type 2 diabetes. *Nature* **2005**, *436* (7049), 356-362.
48. Spranger, J.; Verma, S.; Göhring, I.; Bobbert, T.; Seifert, J.; Sindler, A. L.; Pfeiffer, A.; Hileman, S. M.; Tschöp, M.; Banks, W. A. Adiponectin does not cross the blood-brain

- barrier but modifies cytokine expression of brain endothelial cells. *Diabetes* **2006**, *55* (1), 141-147.
49. Ceddia, R. B.; Somwar, R.; Maida, A.; Fang, X.; Bikopoulos, G.; Sweeney, G. Globular adiponectin increases GLUT4 translocation and glucose uptake but reduces glycogen synthesis in rat skeletal muscle cells. *Diabetologia* **2005**, *48*, 132-139.
50. Moore, G. B.; Chapman, H.; Holder, J. C.; Lister, C. A.; Piercy, V.; Smith, S. A.; Clapham, J. C. Differential regulation of adipocytokine mRNAs by rosiglitazone in db/db mice. *Biochem Biophys Res Commun.* **2001**, *286* (4), 735-741.
51. Kristiansen, T. Z.; Bunkenborg, J.; Gronborg, M.; Molina, H.; Thuluvath, P. J.; Argani, P.; Goggins, M. G.; Maitra, A.; Pandey, A. A proteomic analysis of human bile. *Mol Cell Proteomics* **2004**, *3* (7), 715-728.
52. Wang, P.; Mariman, E.; Keijer, J. F.; Bouwman, F.; Noben, J.-P.; Robben J.; Renes, J. Profiling of the secreted proteins during 3T3-L1 adipocyte differentiation leads to the identification of novel adipokines. *Cell. Mol. Life Sci.* **2004**, *61*, 2405-2417.
53. Welsh, G. I.; Griffiths, M. R.; Webster, K. J.; Page, M. J.; Tavaré, J. M. Proteome analysis of adipogenesis. *Proteomics* **2004**, *4* (4), 1042-1051.
54. Chen, X.; Cushman, S. W.; Pannell, L. K.; Hess, S. Quantitative proteomic analysis of the secretory proteins from rat adipose cells using a 2D liquid chromatography-MS/MS approach. *J. Proteome Res.* **2005**, *4*, 570-577.
55. Chiellini, C.; Cochet, O.; Negroni, L.; Samson, M.; Poggi, M.; Ailhaud, G.; Alessi, M. C.; Dani, C.; Amri, E. Z. Characterization of human mesenchymal stem cell secretome at early steps of adipocyte and osteoblast differentiation. *BMC Mol Biol.* **2008**, *9*, 26.

56. Adachi, J.; Kumar, C.; Zhang, Y.; Mann, M. In-depth analysis of the adipocyte proteome by mass spectrometry and bioinformatics. *Mol Cell Proteomics* **2007**, *6* (7), 1257-1273.
57. Alvarez-Llamas, G.; Szalowska, E.; de Vries, M. P.; Weening, D.; Landman, K.; Hoek, A.; Wolffenbuttel, B. H.; Roelofsen, H.; Vonk, R. J. Characterization of the human visceral adipose tissue secretome. *Mol Cell Proteomics* **2007**, *6* (4), 589-600.
58. Zvonic, S.; Lefevre, M.; Kilroy, G.; Floyd, Z. E.; DeLany, J. P.; Kheterpal, I.; Gravois, A.; Dow, R.; White, A.; Wu, X.; Gimble, J. M. Secretome of primary cultures of human adipose-derived stem cells: modulation of serpins by adipogenesis. *Mol Cell Proteomics* **2007**, *6* (1), 18-28.
59. Lee, H. K.; Lee, B. H.; Park S. A.; Kim C. A. The proteomic analysis of an adipocyte differentiated from human mesenchymal stem cells using twodimensional gel electrophoresis. *Proteomics* **2006**, *6*, 1223-1229.
60. Matsuzawa, Y. The metabolic syndrome and adipocytokines. *FEBS Lett.* **2006**, *580* (12), 2917-2921.
61. Considine, R. V.; Cooksey, R. C.; Williams, L. B.; Fawcett, R. L.; Zhang, P.; Ambrosius, W. T.; Whitfield, R. M.; Jones, R.; Inman, M.; Huse, J.; McClain, D. A. Hexosamines regulate leptin production in human subcutaneous adipocytes. *J Clin Endocrinol Metab.* **2000**, *85* (10), 3551-3556.
62. Hazel, M.; Cooksey, R. C.; Jones, D.; Parker, G.; Neidigh, J. L.; Witherbee, B.; Gulve, E. A.; McClain, D. A. Activation of the hexosamine signaling pathway in adipose tissue results in decreased serum adiponectin and skeletal muscle insulin resistance. *Endocrinology* **2004**, *145* (5), 2118-2128.

63. McClain, D. A.; Lubas, W. A.; Cooksey, R. C.; Hazel, M.; Parker, G. J.; Love, D. C.; Hanover, J. A. Altered glycan-dependent signaling induces insulin resistance and hyperleptinemia. *Proc Natl Acad Sci U S A.* **2002**, *99* (16), 10695-10699.
64. Wang, J.; Liu, R.; Hawkins, M.; Barzilai, N.; Rossetti, L. A nutrient-sensing pathway regulates leptin gene expression in muscle and fat. *Nature* **1998**, *393* (6686), 684-688.
65. McClain, D. A. Hexosamines as mediators of nutrient sensing and regulation in diabetes. *J Diabetes Complications* **2002**, *16* (1), 72-80.
66. Trujillo, M. E.; Scherer, P. E. Adipose tissue-derived factors: impact on health and disease. *Endocr. Rev.* **2006**, *27*, 762-778.
67. Lim, J. M.; Sherling, D.; Teo, C. F.; Hausman, D. B.; Lin, D.; Wells, L. Defining the regulated secreted proteome of rodent adipocytes upon the induction of insulin resistance. *J. Proteome Res.* **2008**, *7*, 1251-1263.
68. Lim, J. M.; Teo, C. F.; Hausman, D.; Wells, L. Quantitative secretome and glycome of primary human adipocytes under insulin resistant conditions, **2009**, in progress.
69. Washburn, M. P.; Wolters, D.; Yates, J. R. 3rd. Large-scale analysis of the yeast proteome by multidimensional protein identification technology. *Nat Biotechnol.* **2001**, *19* (3), 242-247.
70. Link, A. J.; Eng, J.; Schieltz, D. M.; Carmack, E.; Mize, G. J.; Morris, D. R.; Garvik, B. M.; Yates J. R. 3rd. Direct analysis of protein complexes using mass spectrometry. *Nat. Biotechnol.* **1999**, *17*, 676-682.
71. Wolters, D. A.; Washburn, M. P.; Yates, J. R. 3rd. An automated multidimensional protein identification technology for shotgun proteomics. *Anal. Chem.* **2001**, *73*, 5683-5690.

72. Washburn, M. P.; Ulaszek, R.; Deciu, C.; Schieltz, D. M.; Yates, J. R. 3rd. Analysis of quantitative proteomic data generated via multidimensional protein identification technology. *Anal. Chem.* **2002**, *74*, 1650-1657.
73. MacCoss, M. J.; McDonald, W. H.; Saraf, A.; Sadygov, R.; Clark, J. M.; Tasto, J. J.; Gould, K. L.; Wolters, D.; Washburn, M.; Weiss, A.; Clark, J. I.; Yates, J. R. 3rd. Shotgun identification of protein modifications from protein complexes and lens tissue. *Proc. Natl. Acad. Sci. U.S.A.* **2002**, *99*, 7900-7905.
74. O'Farrell, P. H. High resolution two-dimensional electrophoresis of proteins. *J. Biol. Chem.* **1975**, *250*, 4007-4021.
75. Klose, J.; Kobalz, U. Two-dimensional electrophoresis of proteins: an updated protocol and implications for a functional analysis of the genome. *Electrophoresis* **1995**, *16*, 1034-1059.
76. Patton, W. F.; Beechem, J. M. Rainbow's end: the quest for multiplexed fluorescence quantitative analysis in proteomics. *Curr. Opin. Chem. Biol.* **2002**, *6*, 63-69.
77. Zhou, G.; Li, H.; DeCamp, D.; Chen, S.; Shu, H.; Gong, Y.; Flaig, M.; Gillespie, J. W.; Hu, N.; Taylor, P. R.; Emmert-Buck, M. R.; Liotta, L. A.; Petricoin, E. F. III.; Zhao, Y. 2D differential in-gel electrophoresis for the identification of esophageal scans cell cancer-specific protein markers. *Mol. Cell. Proteomics* **2005**, *1*, 117-124.
78. Gygi, S. P.; Rist, B.; Gerber, S. A.; Turecek, F.; Gelb, M. H.; Aebersold, R. Quantitative analysis of complex protein mixtures using isotope-coded affinity tags. *Nat Biotechnol* **1999**, *17*, 994-999.
79. Haqqani, A. S.; Nesic, M.; Preston, E.; Baumann, E.; Kelly, J.; Stanimirovic, D. Characterisation of vascular protein expression patterns in cerebral ischemia/reperfusion

- using laser capture microdissection and ICAT-nanoLC-MS/MS. *FASEB J.* **2005**, *19*, 1809-1821.
80. Haqqani, A. S.; Kelly, J.; Baumann, E.; Haseloff, R. F.; Blasig, I. E.; Stanimirovic, D. B. Protein markers of ischemic insult in brain endothelial cells identified using 2D gel electrophoresis and ICAT-based quantitative proteomics. *J Proteome Res.* **2007**, *6*, 226-239.
81. Haqqani, A. S.; Hutchison, J. S.; Ward, R.; Stanimirovic, D. B. Protein biomarkers in serum of pediatric patients with severe traumatic brain injury identified by ICAT-LC-MS/MS. *J Neurotrauma* **2007**, *24*, 54-74.
82. Shevchenko, A.; Chernushevich, I.; Standing, K. G.; Thompson, B.; Wilm, M.; Mann, M. Rapid “*de novo*” peptide sequencing by a combination of nanoelectrospray, isotopic labeling and a quadrupole/time-of-flight mass spectrometer. *Rapid Commun. Mass Spectrom.* **1997**, *11*, 1015-1024.
83. Schnolzer, M.; Jedrzejewski, P.; Lehmann, W. D. Proteasecatalyzed incorporation of ^{18}O into peptide fragments and its application for protein sequencing by electrospray and matrix-assisted laser desorption/ionization mass spectrometry. *Electrophoresis* **1996**, *17*, 945-953.
84. Uttenweiler-Joseph, S.; Neubauer, G.; Christoforidis, S.; Zerial, M.; Wilm, M. Automated *de novo* sequencing of proteins using the differential scanning technique. *Proteomics* **2001**, *1*, 668-682.
85. Ong, S. E.; Mann, M. Mass spectrometry-based proteomics turns quantitative. *Nat Chem Biol.* **2005**, *1* (5), 252-262.

86. Ong, S. E.; Blagoev, B.; Kratchmarova, I.; Kristensen, D. B.; Steen, H.; Pandey, A.; Mann, M. Stable isotope labeling by amino acids in cell culture, SILAC, as a simple and accurate approach to expression proteomics. *Mol Cell Proteomics* **2002**, *1* (5), 376-386.
87. Ong, S. E.; Kratchmarova, I.; Mann, M. Properties of ¹³C-substituted arginine in stable isotope labeling by amino acids in cell culture (SILAC). *J Proteome Res.* **2003**, *2* (2), 173-181.
88. Ross, P. L.; Huang, Y. N.; Marchese, J. N.; Williamson, B.; Parker, K.; Hattan, S.; Khainovski, N.; Pillai, S.; Dey, S.; Daniels, S.; Purkayastha, S.; Juhasz, P.; Martin, S.; Bartlett-Jones, M.; He, F.; Jacobson, A.; Pappin, D. J. Multiplexed protein quantitation in *Saccharomyces cerevisiae* using amine-reactive isobaric tagging reagents. *Mol. Cell. Proteomics* **2004**, *3*, 1154-1156.
89. Zieske, L. R. A perspective on the use of iTRAQ reagent technology for protein complex and profiling studies. *J. Exp. Bot.* **2006**, *57*, 1501-1508.
90. Glen, A.; Gan, C. S.; Hamdy, F. C.; Eaton, C. L.; Cross, S. S.; Catto, J. W. F.; Wright, P. C.; Rehman, I. iTRAQ-Facilitated Proteomic Analysis of Human Prostate Cancer Cells Identifies Proteins Associated with Progression. *J. Proteome Res.* **2008**, *7* (3), 897-907.
91. Gerber, S. A.; Rush, J.; Stemman, O.; Kirschner, M. W.; Gygi, S. P. Absolute quantification of proteins and phosphoproteins from cell lysates by tandem MS. *Proc. Natl. Acad. Sci. U. S. A.* **2003**, *100*, 6940-6945.
92. Kirkpatrick, D. S.; Gerber, S. A.; Gygi, S. P. The absolute quantification strategy: a general procedure for the quantification of proteins and post-translational modifications. *Methods* **2005**, *35*, 265-273.

93. Stemmann, O.; Zou, H.; Gerber, S. A.; Gygi, S. P.; Kirschner, M. W. Dual inhibition of sister chromatid separation at metaphase. *Cell* **2001**, *107*, 715-726.
94. Barr, J. R.; Maggio, V. L.; Patterson, D. G. Jr.; Cooper, G. R.; Henderson, L. O.; Turner, W. E.; Smith, S. J.; Hannon, W. H.; Needham, L. L.; Sampson, E. J. Isotope dilution–mass spectrometric quantification of specific proteins: model application with apolipoprotein A-I. *Clin. Chem.* **1996**, *42*, 1676-1682.
95. Li, X. J.; Yi, E. C.; Kemp, C. J.; Zhang, H.; Aebersold, R. A software suite for the generation and comparison of peptide arrays from sets of data collected by liquid chromatography-mass spectrometry. *Mol Cell Proteomics* **2005**, *4*, 1328-1340.
96. Ono, M.; Shitashige, M.; Honda, K.; Isobe, T.; Kuwabara, H.; Matsuzuki, H.; Hirohashi, S.; Yamada, T. Label-free quantitative proteomics using large peptide data sets generated by nanoflow liquid chromatography and mass spectrometry. *Mol Cell Proteomics* **2006**, *5*, 1338-1347.
97. Lu, P.; Vogel, C.; Wang, R.; Yao, X.; Marcotte, E. M. Absolute protein expression profiling estimates the relative contributions of transcriptional and translational regulation. *Nat. Biotechnol.* **2007**, *25*, 117-124.
98. Mallick, P.; Schirle, M.; Chen, S. S.; Flory, M. R.; Lee, H.; Martin, D.; Ranish, J.; Raught, B.; Schmitt, R.; Werner, T.; Kuster, B.; Aebersold, R. Computational prediction of proteotypic peptides for quantitative proteomics. *Nat. Biotechnol.* **2007**, *25*, 125-131.
99. Wiener, M. C.; Sachs, J. R.; Deyanova, E. G.; Yates, N. A. Differential mass spectrometry: a label-free LC-MS method for finding significant differences in complex peptide and protein mixtures. *Anal. Chem.* **2004**, *76*, 6085-6096.

100. Liu, H.; Sadygov, R. G.; Yates, J. R. III. A model for random sampling and estimation of relative protein abundance in shotgun proteomics. *Anal. Chem.* **2004**, *76*, 4193-4201.
101. Bondarenko, P. V.; Chelius, D.; Shaler, T. A. Identification and relative quantitation of protein mixtures by enzymatic digestion followed by capillary reversed-phase liquid chromatography tandem mass spectrometry. *Anal. Chem.* **2002**, *74*, 4741-4749.
102. Chelius, D.; Bondarenko, P. V. Quantitative profiling of proteins in complex mixtures using liquid chromatography and mass spectrometry. *J. Proteome Res.* **2002**, *1*, 317-323.
103. Old, W. M.; Meyer-Arendt, K.; Aveline-Wolf, L.; Pierce, K. G.; Mendoza, A.; Sevinsky, J. R.; Resing, K. A.; Ahn, N. G. Comparison of label-free methods for quantifying human proteins by shotgun proteomics. *Mol. Cell. Proteomics* **2005**, *4*, 1487-1502.
104. Higgs, R. E.; Knierman, M. D.; Gelfanova, V.; Butler, J. P.; Hale, J. E. Comprehensive label-free method for the relative quantification of proteins from biological samples. *J. Proteome Res.* **2005**, *4*, 1442-1450.
105. Andreev, V. P.; Li, L.; Cao, L.; Gu, Y.; Rejtar, T.; Wu, S. L.; Karger, B. L. A New Algorithm Using Cross-Assignment for Label-Free Quantitation with LC-LTQ-FT MS. *J. Proteome Res.* **2007**, *6*, 2186-2194.
106. Nesvizhskii, A. I.; Keller, A.; Kolker, E.; Aebersold, R. A statistical model for identifying proteins by tandem mass spectrometry. *Anal. Chem.* **2003**, *75*, 4646-4658.
107. Varki, A. Biological roles of oligosaccharides: all of the theories are correct. *Glycobiology* **1993**, *3* (2), 97-130.
108. Krueger, K. E.; Srivastava, S. Posttranslational Protein Modifications: Current Implications for Cancer Detection, Prevention, and Therapeutics. *Mol. Cell. Proteomics* **2006**, *5* (10), 1799-1810.

109. Isaji, T.; Gu, J.; Nishiuchi, R.; Zhao, Y.; Takahashi, M.; Miyoshi, E.; Honke, K.; Sekiguchi, K.; Taniguchi, N. Introduction of bisecting GlcNAc into integrin alpha5 beta1 reduces ligand binding and down-regulates cell adhesion and cell migration. *J. Biol. Chem.* **2004**, *279*, 19747-19754.
110. Stanley, P. Biological consequences of overexpressing or eliminating N-acetylglucosaminyltransferase-TIII in the mouse. *Biochim. Biophys. Acta* **2002**, *1573*, 363-368.
111. Schachter, H. Congenital disorders involving defective N-glycosylation of proteins. *Cell Mol. Life Sci.* **2001**, *58*, 1085-1104.
112. Dennis, J. W.; Granovsky, M.; Warren, C.E. Glycoprotein glycosylation and cancer progression. *Biochim. Biophys. Acta* **1999**, *1473*, 21-34.
113. Delves, P. J. The role of glycosylation in autoimmune disease. *Autoimmunity* **1998**, *27*, 239-253.
114. Gleeson, P. A. Glycoconjugates in autoimmunity. *Biochim. Biophys. Acta* **1994**, *1197*, 237-255.
115. Chui, D.; Sellakumar, G.; Green, R.; Sutton-Smith, M.; McQuistan, T.; Marek, K.; Morris, H.; Dell, A.; Marth, J. Genetic remodeling of protein glycosylation in vivo induces autoimmune disease. *Proc. Natl. Acad. Sci. USA* **2001**, *98*, 1142-1147.
116. Kristiansen, T. Z.; Bunkenborg, J.; Gronborg, M.; Molina, H.; Thuluvath, P. J.; Argani, P.; Goggins, M. G.; Maitra, A.; Pandey, A. A proteomic analysis of human bile. *Mol Cell Proteomics* **2004**, *3* (7), 715-728.

117. Angel, P.; Lim, J. M.; Wells, L.; Bergmann, C.; Orlando, R. A potential pitfall in 18-O based N-linked glycosylation site mapping. *Rapid Commun. Mass Spectrom.* **2007**, *21*, 674-682.
118. Koles, K.; Lim, J. M.; Aoki, K.; Porterfield, M.; Tiemeyer, M.; Wells, L.; Panin, V. Identification of N-glycosylated proteins from the central nervous system of *Drosophila melanogaster*. *Glycobiology* **2007**, *17* (12), 1388-1403.
119. Lim, J. M.; Aoki, K.; Angel, P.; Garrison, D.; King, D.; Tiemeyer, M.; Bergmann, C.; Wells, L. Mapping glycans onto specific N-linked glycosylation sites of *Pyrus communis* PGIP redefines the interface for EPG-PGIP interactions. *J Proteome Res.* **2009**, *8* (2), 673-680.
120. Dell, A.; Reason, A. J.; Khoo, K. H.; Panico, M.; McDowell, R. A.; Morris, H. R. Mass spectrometry of carbohydrate-containing biopolymers. *Methods Enzymol.* **1994**, *230*, 108-132.
121. Wührer, M.; Deelder, A. M.; Hokke, C. H. Protein glycosylation analysis by liquid chromatography-mass spectrometry. *J Chromatogr B Analyt Technol Biomed Life Sci.* **2005**, *825* (2), 124-133.
122. Morelle, W.; Faid, V.; Michalski, J. C. Structural analysis of permethylated oligosaccharides using electrospray ionization quadrupole time-of-flight tandem mass spectrometry and deuteroreduction. *Rapid Commun. Mass Spectrom.* **2004**, *18* (20), 2451-2464.
123. Reinhold, V. N.; Sheeley, D. M. Detailed characterization of carbohydrate linkage and sequence in an ion trap mass spectrometer: glycosphingolipids. *Anal. Biochem.* **1998**, *259* (1), 28-33.

124. Sheeley, D. M.; Reinhold, V. N. Structural characterization of carbohydrate sequence, linkage, and branching in a quadrupole Ion trap mass spectrometer: neutral oligosaccharides and N-linked glycans. *Anal. Chem.* **1998**, *70* (14), 3053-3059.
125. Viseux, N.; de Hoffmann, E.; Domon, B. Structural analysis of permethylated oligosaccharides by electrospray tandem mass spectrometry. *Anal. Chem.* **1997**, *69* (16), 3193-3198.
126. Prien, J. M.; Huysentruyt, L. C.; Ashline, D. J.; Lapadula, A. J.; Seyfried, T. N.; Reinhold, V. N. Differentiating N-linked glycan structural isomers in metastatic and nonmetastatic tumor cells using sequential mass spectrometry. *Glycobiology* **2008**, *18* (5), 353-366.
127. Aoki, K.; Porterfield, M.; Lee, S. S.; Dong, B.; Nguyen, K.; McGlamry, K. H.; Tiemeyer, M. The diversity of O-linked glycans expressed during *Drosophila melanogaster* development reflects stage- and tissue-specific requirements for cell signaling. *J Biol Chem.* **2008**, *283* (44), 30385-30400.
128. Aoki, K.; Perlman, M.; Lim, J. M.; Cantu, R.; Wells, L.; Tiemeyer, M. Dynamic developmental elaboration of N-linked glycan complexity in the *Drosophila melanogaster* embryo. *J Biol Chem.* **2007**, *282* (12), 9127-9142.
129. Abbott, K. L.; Aoki, K.; Lim, J. M.; Porterfield, M.; Johnson, R.; O'Regan, R. M.; Wells, L.; Tiemeyer, M.; Pierce, M. Targeted glycoproteomic identification of biomarkers for human breast carcinoma. *J Proteome Res.* **2008**, *7* (4), 1470-1480.
130. Alvarez-Manilla, G.; Warren, N. L.; Abney, T.; Atwood, J., III; Azadi, P.; York, W. S.; Pierce, M.; Orlando, R. Tools for glycomics: relative quantitation of glycans by isotopic permethylation using $^{13}\text{CH}_3\text{I}$. *Glycobiology* **2007**, *17* (7), 677-687.

131. Atwood III, J. A.; Cheng, L.; Alvarez-Manilla, G.; Warren, N. L.; York, W. S.; Orlando, R. Quantitation by Isobaric Labeling: Applications to Glycomics *J. Proteome Res.*, **2008**, *7* (01), 367-374.
132. Orlando, R.; Lim, J. M.; Atwood, J.; Angel, P.; Fang, M.; Aoki, K.; Alvarez-Manilla, G.; Moremen, K.; York, W.; Tiemeyer, M.; Pierce, M.; Dalton, S.; Wells, L. IDAWG: Metabolic incorporation of stable isotope labels for quantitative glycomics of cultured cells. *J. Proteome Res.* **2009**, in press.

Table 1-1. Summary of the quantification technologies for proteomics and glycomics

experiments

Labeling	Proteomics	Glycomics
Label-free	Spectral count Protein coverage DIGE	Prevalence
<i>In vitro</i> isotopic and isobaric labeling	ICAT iTRAQ ¹⁸ O-H ₂ O AQUA	¹³ C-CH ₃ I QUIBL
<i>In vivo</i> isotopic labeling	SILAC	IDAWG

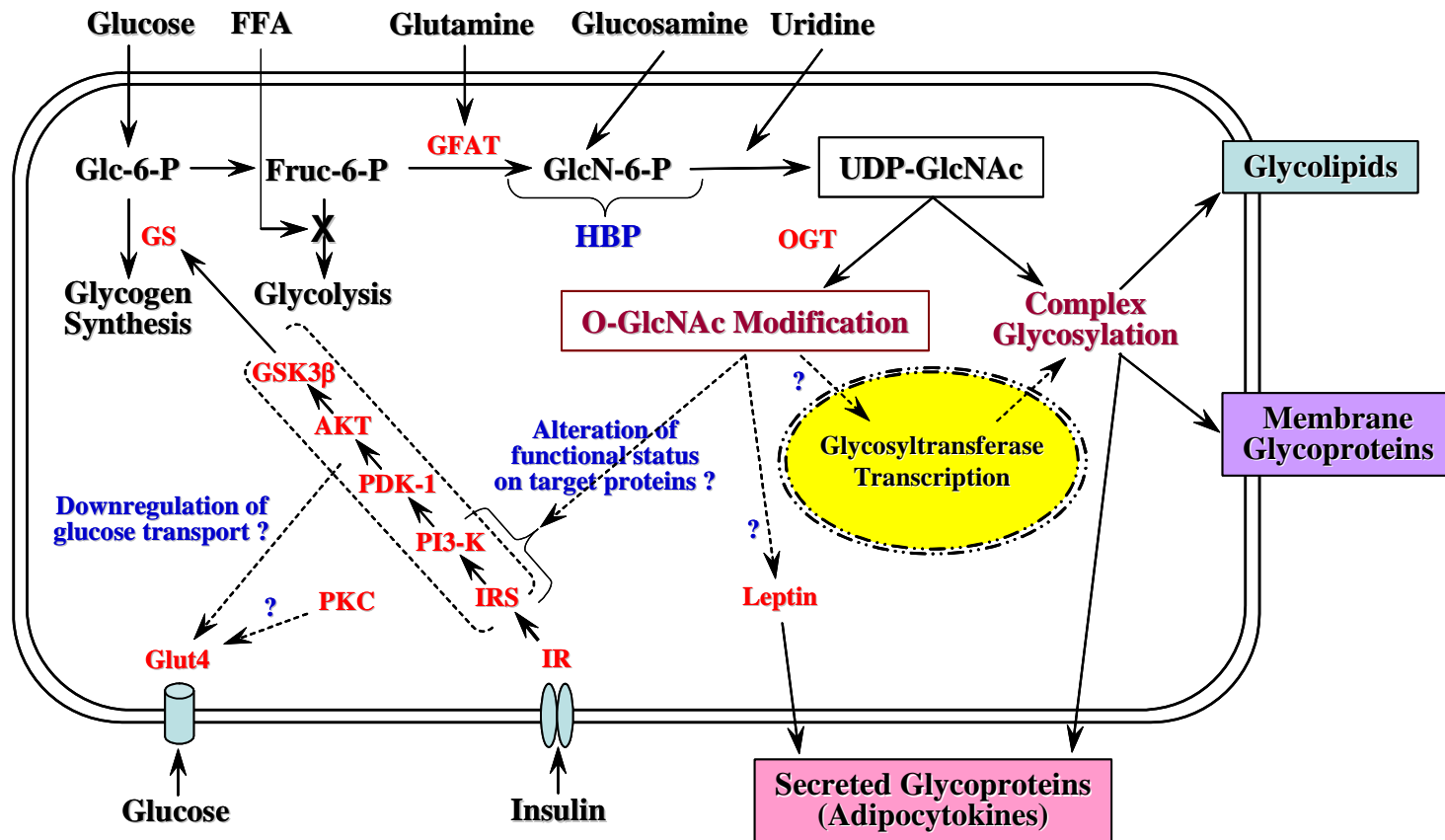
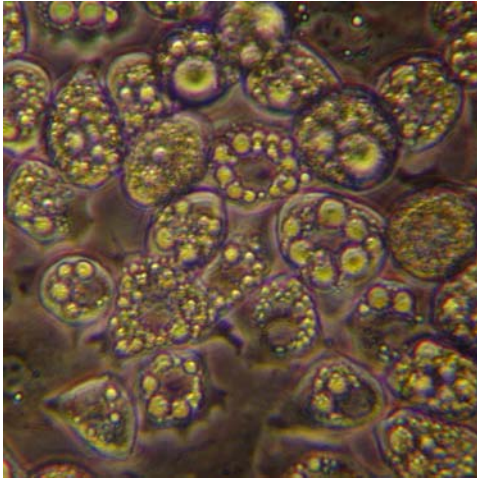
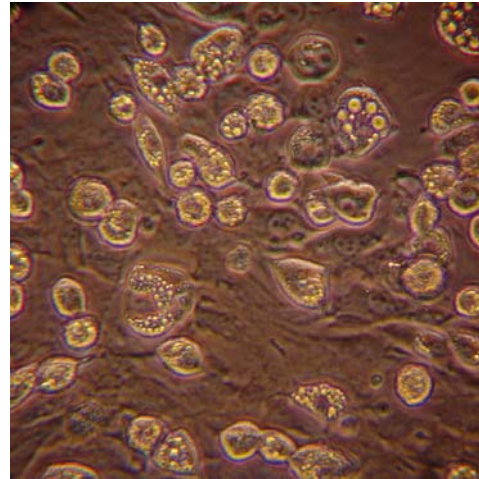


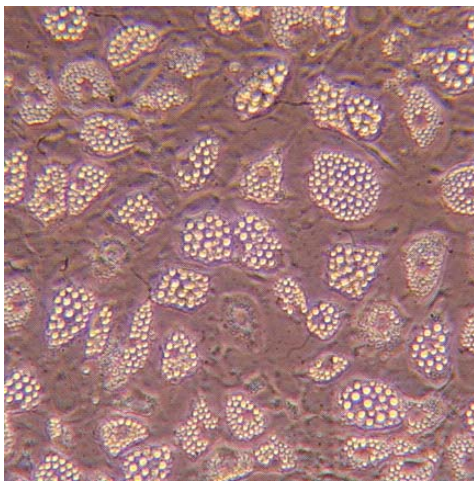
Figure 1-1. Glucose metabolism and insulin transduction in adipocytes. Increased flux through the HBP results in O-GlcNAc modification of nucleocytoplasmic proteins and alteration of secreted proteome and glycome. Adapted and modified from Wells, L.; Vosseller, K.; Hart, G. W.; *Cell. Mol. Life Sci.*, **2003**, 60, 222-228 (9).



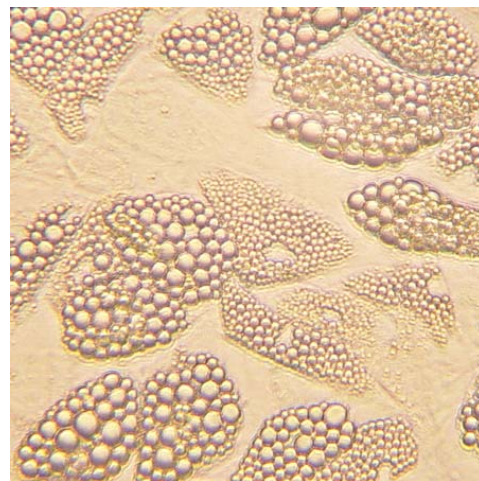
3T3-L1



3T3-F442A



Primary Rat Adipocytes



Primary Human Adipocytes

Figure 1-2. Images of fat droplets in mammalian adipocytes.

CHAPTER 2

DEFINING THE REGULATED SECRETED PROTEOME OF RODENT ADIPOCYTES UPON THE INDUCTION OF INSULIN RESISTANCE

Reproduced with permission from Jae-Min Lim, Dan Sherling, Chin Fen Teo, Dorothy B.

Hausman, Dawei Lin and Lance Wells, *Journal of Proteome Research* **2008**, 7 (3), 1251-1263.

Copyright 2009 American Chemical Society

ABSTRACT

Insulin resistance defines the metabolic syndrome and precedes, as well is the hallmark of, type 2 diabetes. Adipocytes, besides being a major site for energy storage, are endocrine in nature and secrete a variety of proteins, adipocytokines (adipokines), that can modulate insulin sensitivity, inflammation, obesity, hypertension, food intake (anorexigenic and orexigenic), and general energy homeostasis. Recent data demonstrates that increased intracellular glycosylation of proteins via O-GlcNAc can induce insulin resistance and that a rodent model with genetically elevated O-GlcNAc levels in muscle and fat displays hyperleptinemia. The link between O-GlcNAc levels, insulin resistance, and adipocytokine secretion is further explored here. First, with the use of immortalized and primary rodent adipocytes, the secreted proteome of differentiated adipocytes is more fully elucidated by the identification of 97 and 203 secreted proteins, respectively. Mapping of more than 80 N-linked glycosylation sites on adipocytokines from the cell lines further defines this proteome. Importantly, adipocytokines that are modulated when cells are shifted from insulin responsive to insulin resistant conditions are determined. By the use of two protocols for inducing insulin resistance, classical hyperglycemia with chronic insulin exposure and pharmacological elevation of O-GlcNAc levels, several proteins are identified that are regulated in a similar fashion under both conditions including HCNP, Quiescin Q6, Angiotensin, lipoprotein lipase, matrix metalloproteinase 2, and slit homologue 3. Detection of these potential prognostic/diagnostic biomarkers for metabolic syndrome, type 2 diabetes, and the resulting complications of both diseases further establish the central role of the O-GlcNAc modification of intracellular proteins in the pathophysiology of these conditions.

Keywords: O-GlcNAc, insulin resistance, tandem mass spectrometry, shotgun proteomics,

type 2 diabetes, metabolic syndrome, glycosylation, adipocytokine

2.1. INTRODUCTION

Type 2 diabetes affects more than 7% of the American adult population. Chronic hyperglycemia is the hallmark of all types of diabetes. In type 2 diabetes, insulin resistance is a primary, early feature and, along with “glucose toxicity”, is likely responsible for the plethora of observed patient complications such as cardiovascular disease, blindness, and kidney disease (1). Insulin resistance results in defects in a multitude of systems including pancreatic β -cells, the liver, and peripheral insulinresponsive tissues (adipocytes and skeletal muscle) (2). Insulin normally regulates a variety of processes such as glucose uptake, glycogen synthesis, triglyceride synthesis, lipolysis, gluconeogenesis, apoptosis, cell growth, differentiation, and adipocytokine (adipokine) secretion (3).

It has been suggested that insulin resistance is an adaptation to nutrient excess and lack of energy expenditure (4). Increased flux through the hexosamine biosynthetic pathway that converts fructose-6-phosphate (a glycolysis intermediate) to UDP-GlcNAc (a donor sugar nucleotide) has been heavily implicated in the induction of insulin resistance (5, 6). UDP-GlcNAc serves as a donor for glycosylation of macromolecules including the O-linked β -N-acetylglucosamine (O-GlcNAc) modification of nuclear and cytosolic proteins (7). Elevation in global O-GlcNAc modification of proteins has been directly demonstrated to generate insulin resistance and glucose disposal defects in adipocytes and muscle cells in culture as well as in rodent models (8-11).

In the past decade, it has become apparent that adipose tissue, in addition to being an energy storage depot, is an endocrine tissue (12, 13). In addition to the free fatty acids secreted

by adipocytes, a number of adipocyte-secreted proteins, adipocytokines (adipokines), can act in an autocrine, paracrine, or endocrine fashion to modulate a variety of processes including insulin sensitivity, inflammation, obesity, hypertension, food intake (anorexigenic and orexigenic), and general energy homeostasis (12-14). Adipocytokine secretion has been implicated in a variety of the complications associated with type 2 diabetes (15, 16).

A few groups have sought to define the secreted proteome of adipocytes by a variety of approaches (17-21). Most of these studies focused on differential protein expression during adipocyte differentiation. Secretion of many adipocytokines in mature adipocytes appears to be regulated by insulin stimulation and glucose levels (22). In at least two cases, for leptin and adiponectin, transcriptional regulation of the adipocytokines is regulated by the hexosamine biosynthetic pathway (23, 24). Furthermore, mice with elevated O-GlcNAc levels display hyperleptinemia (9).

To more completely define the repertoire of adipocytokines, we report here a detailed proteomic analysis of the secreted proteome of rodent adipocytes (both immortalized mouse and primary rodent-derived) using a combination of shotgun proteomics, N-linked glycosylation site mapping, and 2D-reverse phase separations that allowed us to assign more than 200 secreted polypeptides with high confidence. We also demonstrate via quantitative proteomics that multiple secreted proteins are regulated by classical induction of insulin resistance (hyperglycemia and chronic insulin exposure) as well as elevated O-GlcNAc level-induced insulin resistance. With the use of multiple adipocyte cell lines, methods for inducing insulin resistance, and mass spectrometry-based approaches of analysis, we are able to establish a more complete repertoire of those proteins that are likely candidates as prognostic/

diagnostic/therapeutic targets in metabolic syndrome, type 2 diabetes, and the resulting complications.

2.2. EXPERIMENTAL PROCEDURES

Tissue Culture. 3T3s Cell Lines: 3T3-L1 and -F442A fibroblasts were maintained and differentiated on 10 cm plates essentially as previously described (11, 25). Briefly, 2 days after the cells reached confluence, cells were induced to differentiate with high (4.5 g/L, 3T3-L1) or low (1.0 g/L, 3T3-F442A) glucose DMEM containing 10% fetal bovine serum (3T3-L1) or 10% calf serum (3T3-F442A) via addition of 0.5 mM (115 $\mu\text{g}/\text{mL}$) 3-isobutyl-1-methylxanthine (MIX, Sigma), 1 μM (390 ng/mL) dexamethasone (Sigma), and 175 nM (1 $\mu\text{g}/\text{mL}$) recombinant insulin (human, Roche). After 48 h (day 2), the medium was replaced with high (3T3-L1) or low (3T3-F442A) glucose DMEM plus 10% FBS and supplemented with 1 $\mu\text{g}/\text{mL}$ insulin for an additional 48 h. After 96 h (day 4), cells were maintained in appropriate medium depending on the condition being examined.

Rat Primary Cell Culture: inguinal and retroperitoneal fat pads were removed aseptically from male Sprague–Dawley rats (Harlan Industries, Indianapolis, IN), and primary preadipocytes were isolated as described in detail previously (26, 27). After additional washing and centrifugation steps, the preadipocyte pellet was resuspended in plating medium (high glucose DMEM, antibiotics: PS, 10% FBS) and seeded at an average density of 1.35×10^4 cells/cm² for inguinal and 1.63×10^3 cells/cm² for retroperitoneal on 10 cm dishes for the differentiation. Primary cells were maintained in a humidified atmosphere containing 5% CO₂ in air at 37 °C and cultured to confluence, changing the plating medium every 2 days. After 2 days of confluence, referred to as day 0, the medium was replaced with differentiation medium (high

glucose DMEM containing antibiotics and 10% FBS, 0.25 mM MIX, 0.1 μ M dexamethasone, and 17 nM insulin), and at day 2, an additional 17 nM of insulin was administered with the plating medium for an additional 48 h incubation. The cells were maintained in low glucose DMEM containing 10% FBS and treatments (see below) until harvest.

Cell Treatments and Sample Preparation. On the designated days (day 4 for 3T3-L1, day 5 for 3T3-F442A, and day 9 for rat primary adipocytes), adipocytes were induced with a combined treatment of low or high glucose containing 10% FBS, with or without insulin (100 nM) and PUGNAc (100 μ M, TRC Inc.) according to the experimental conditions described in the results. After 24 h incubation, the medium was removed and the cells were washed five times with low or high glucose serum-free DMEM without antibiotics and vitamins and incubated with the last rinse for 15 min. After the final wash was removed, serum-free media supplemented with insulin (1 nM) or PUGNAc (100 μ M) was added, and cells were incubated for 16 h.

After incubation, the conditioned media were harvested with extreme care and then centrifuged once at 1800 rpm at 4 °C for 7 min. The supernatants were filtered using 1 μ m syringe filters (PALL). The samples were then collected in centrifuge tubes and centrifuged again at 30 000g at 4 °C for 30 min. The samples were then transferred to an equilibrated spin column (Centriprep YM-3, Amicon, Millipore) and buffer-exchanged at 2800 g and 4 °C into 40 mM ammonium bicarbonate (NH_4HCO_3) plus 1 mM DTT and concentrated. The concentrated samples were denatured with 1 M urea, reduced with 10mM DTT for 1 h at 56 °C, carboxyamidomethylated with 55 mM iodoacetamide in the dark for 45 min, and then digested with 5 μ g of trypsin (Promega) in 40 mM NH_4HCO_3 overnight at 37 °C. After digestion, the peptides were acidified with 200 μ L of 1% trifluoroacetic acid (TFA). Desalting was

subsequently performed with C18 spin columns (Vydac Silica C18, The Nest Group, Inc.), and the resulting peptides were dried down in a Speed Vac and stored at -20 °C until analyzed. For the subset of samples to be analyzed for N-linked glycosylation, peptides were resuspended in 19 μL of ^{18}O -water and 1 μL of N-glycanase (PNGase F, Prozyme) and allowed to incubate for 18 h at 37 °C. Peptides were dried back down and resuspended in 50 μL of 40 mM NH_4HCO_3 , with 1 μg of trypsin, to remove any possible C-terminal incorporation of ^{18}O from residual trypsin activity (28) for 4 h and then dried down and stored at -20 °C until analyzed.

Whole Cell Extracts and Western Blots. Whole cell extracts were prepared and Western blots performed on equal amounts of SDS-PAGE separated proteins using the anti-O-GlcNAc antibody RL-2 and ERK-2 (as a positive control for loading) essentially as previously described (29).

Analysis of Secreted Proteins by RP and RP/RP-LC-MS/MS. The peptides were resuspended with 78 μL of mobile phase A (0.1% formic acid, FA, in water) and 2 μL of mobile phase B (80% acetonitrile, ACN, and 0.1% formic acid in water) and filtered with 0.2 μm filters (Nanosep, PALL). The samples were loaded off-line onto a nanospray tapered capillary column/emitter (360 \times 75 \times 15 μm , PicoFrit, New Objective) self-packed with C18 reverse-phase (RP) resin (8.5 cm, Waters) in a Nitrogen pressure bomb for 10 min at 1000 psi (\sim 5 μL load) and then separated via a 160-min linear gradient of increasing mobile phase B at a flow rate of \sim 200 nL/min directly into the mass spectrometer. One-dimensional (RP separation) LC-MS/MS analysis was performed on a Finnigan LTQ mass spectrometer (ThermoFisher, San Jose, CA) equipped with a nanoelectrospray ion source. A full MS spectrum was collected (m/z 350–2000)

followed by 8 MS/MS spectra following CID (34% normalized collision energy) of the most intense peaks. Dynamic exclusion was set at 2 for 30 s exclusion.

Two-dimensional RP/RP-HPLC separation of peptides using an off-line mode was investigated recently and provides increased practical peak capacity and flexibility (30, 31). For offline separations, an Agilent 1100 series with a quaternary pump and variable wavelength detector (Semimicro flow cell) was used. A volume of 45 μL of the resuspended peptide mixture was loaded onto a reverse-phase column (C18, 2.1×150 mm, 5 μm , GraceVydac) using 5% of mobile phase C (0.1% trifluoroacetic acid, TFA, in water) at a 100 $\mu\text{L}/\text{min}$ flow rate for fraction collection. The peptides were eluted in a 55 min linear gradient from 5 to 60% of mobile phase D (80% ACN and 0.085% TFA in water), followed by a 10 min linear gradient from 60 to 95% of mobile phase B and a 5 min hold to flush the column. The eluent was monitored by UV absorbance detection at 210 nm, and the fractions were collected every 4 min. Five aliquots (F1, 15–32%; F2, 32–40%; F3, 40–45%; F4, 45–55%; and F5, 55–85% of mobile phase D) of pooled fractions were dried under vacuum. For LC-MS/MS analysis, the peptides were resuspended with 39 μL of mobile phase A and 1 μL of mobile phase B and loaded onto the capillary C18 column in the pressure bomb for 10 min. Resulting peptides were analyzed as described above via LC-MS/MS except that the slope of the gradients were reduced over a 70 min period in the appropriate region corresponding to the fraction (F1, 4-30%; F2, 9-35%; F3, 15-42%; F4, 20-55%; and F5, 28-85%).

Data Analysis. The resulting data was searched against the nonredundant mouse (*Mus musculus*, 11-7-04), rat (*Rattus norvegicus*, 7-13-05), and combined human (*Homo sapiens*), mouse, and rat (HMR, released on 7-13-05) database, respectively, obtained from the National Center for

Biotechnology Information (NCBI) using the TurboSequest algorithm (BioWorks 3.1, Thermo Finnigan) (32, 33), as well as the reverse mouse, rat, and HMR database to estimate the false-positive rate (FPR) and the false-discovery rate (FDR) of peptide identification (see Table 2-1). DTA files were generated for spectra with a threshold of 15 ions and a TIC of $3e^3$. ZSA, correct ion, combion, and ionquest were all applied over a range of $[MH]^+$ 600-4000. The SEQUEST parameters were set to allow 2.2 Da of precursor ion mass tolerance and 0.1 Da of fragment ion tolerance with monoisotopic mass. Only strict tryptic peptides were allowed with up to three missed internal cleavage sites. Dynamic mass increases of 15.99 and 57.02 Da were allowed for oxidized methionine and alkylated cysteine, respectively. In the cases where sites of N-linked glycosylation were investigated with PNGase F and ^{18}O -water, a dynamic mass increase of 3 Da was allowed for Asn residues (34). The results of the SEQUEST search were filtered to establish the FPR and the FDR as summarized in Table 2-1. The SEQUEST criteria were determined with FDR of less than 0.1% with the mouse database and 0.2% with the rat database for proteins identified by 2 unique peptides. More stringent SEQUEST criteria were established for one peptide assignments with FDR of below 1% with both databases. For the RP-RP analysis, the five SEQUEST directories were combined and then filtered after redundant peptides were removed manually. iProtein was used to inspect mouse data in terms of secretion signals and localization [a program written by Dawei Lin (web-interface in process) that queries and stores localization information for an entire user-defined database by both SignalP (www.cbs.dtu.dk/services/SignalP) and PsortII (<http://psort.ims.u-tokyo.ac.jp/form2.html>) and then allows filtered Sequest output files to be screened in a single step and exports the localization data with the sequest data in an excel compatible format.

2.3. RESULTS

Elevation of the O-GlcNAc Modification via the Induction of Insulin Resistance. Elevation in O-GlcNAc levels has previously been correlated with insulin resistance and the diabetic condition (5, 8, 9, 35-40). Furthermore, induction of insulin resistance in 3T3-L1 adipocytes by hyperglycemia and chronic insulin exposure elevates O-GlcNAc levels (11). We have previously shown that elevation of O-GlcNAc levels with the O-GlcNAcase inhibitor PUGNAc induces insulin resistance (11). Both insulin resistant conditions (classical hyperglycemia combined with chronic insulin exposure and PUGNAc treatment) elevate O-GlcNAc levels significantly in mouse immortalized and rat primary adipocytes (Figure 2-1). The induction of classical insulin resistance has been shown to modulate multiple adipocytokines and O-GlcNAc has been implicated in regulating leptin and adiponectin (9, 16, 23, 24, 41). The present results illustrate that the induction of either insulin resistant condition elevates O-GlcNAc levels in both immortalized and primary rodent adipocytes.

Analysis of the Secreted Proteome from Differentiated 3T3-L1 and 3T3-F442A Adipocytes. Two immortalized mouse preadipocyte cell lines (3T3-L1 and 3T3-F442A) were differentiated into adipocytes using standard methodologies. Adipocytes were then maintained with serum in either physiological glucose (LG, low glucose) in the presence or absence of PUGNAc (PUG) or shifted to hyperglycemic (HG, high glucose) conditions with or without chronic insulin (I/Ins) exposure for 24 h (Figure 2-2). The resulting cells were washed extensively with PBS, identical serum-free medium was replaced onto the cells, and cells were maintained for an additional 16 h. The proteins secreted into the medium during this 16 h period were collected and processed for analysis by LC-MS/MS. The mass spectra acquired from equivalent normalized aliquots, for

quantification by protein coverage, were searched against a mouse nonredundant database using SEQUEST. False-discovery rates were calculated using a reversed database (Table 2-1) and all analysis was performed in at least quintuplicate with a new set of cells each time. Each protein identified was assigned a cellular location using PSORT II and SignalP (42). Because of the large data set (a total of 50 LC-MS/MS experiments) and the secreted proteome being contaminated by abundant intracellular proteins due presumably to cell lysis, we designed a bioinformatics tool named iProtein that uses precalculated databases generated from PSORT II and SignalP for assigning localization (manuscript in preparation). We also validated the secreted proteins using Bioinformatic Harvester (<http://harvester.embl.de/>), the Human Protein Reference Database (using the equivalent human protein when available, <http://www.hprd.org/>), and the literature (8-20). More than half of all the proteins identified appeared to be abundant intracellular proteins suggesting cell lyses during the incubation period. Thus, we performed a shotgun proteomics experiment on cells purposely lysed by scraping in ammonium bicarbonate to identify and easily remove from the secreted proteome list abundant intracellular proteins (data not shown). In total, under all conditions, we assigned 97 proteins as being secreted from 3T3 derived adipocytes (Table 2-S1 in Supporting Information). Forty-three of these proteins had been previously described in other proteomic studies (18-20) while 54 proteins were novel in terms of being defined as being secreted from 3T3-derived adipocytes (Table 2-2).

Multiple methodologies exist for protein quantification including isotopic and nonisotopic methods (43-46). To identify proteins that were significantly altered in expression, we identified the total number of unique peptides assigned to each protein in each experiment. An average number of unique peptides were calculated for each protein assigned under the different growth conditions based on the 5 independent experiments under identical conditions.

Shown in Table 2-3 are the 8 proteins whose average number of unique peptides changed by at least 2.5-fold between the insulin responsive (LG) versus both of the two different insulin resistance conditions (HG+I and PUG). We also identified proteins whose abundance only changed under one of the insulin resistant conditions as well as comparisons induced by insulin in low glucose and high glucose alone compared to low glucose conditions (Tables 2-S2 and tables S3 in Supporting Information).

Quantitative Analysis of the Secreted Proteome from Differentiated Primary Rat Adipocytes by LC-MS/MS and 2D-LC-MS/MS. Given that the 3T3 cell lines are an immortalized cell line, have been cultured under high glucose conditions for multiple passages through the years, and that cell lysis was relatively high in these cells, we decided to investigate the secreted proteome of primary rat adipocytes. The secreted proteomes of primary rat adipocytes were harvested under three conditions; two insulin resistance conditions (HG+I and PUG) and one insulin responsive (LG) condition were used. All analysis was carried out on three independently grown and harvested populations for each condition. Once tryptic peptides were generated, a fraction of each sample was analyzed by LC-MS/MS essentially as described for the 3T3-derived proteome. The remaining peptides were separated off-line by reverse-phase chromatography and combined into 5 fractions. Each fraction was analyzed by LC-MS/MS with a shallow gradient corresponding to where the peptides eluted in the offline chromatography. Thus, for each independent sample, 6 LC-MS/MS experiments were performed (Figures 2-3 and 2-4). For each condition performed in triplicate, there were 18 LC-MS/MS experiments conducted for a total of 54 LC-MS/MS experiments in the complete set. Combining LC-MS/MS and 2D-LC-MS/MS analyses for all conditions following stringent filtering (see Table 2-1) allowed us to assign 203

proteins to the secreted proteome of rat primary adipocytes (Table 2-S4 in Supporting Information). Importantly, approximately 75% of the identified proteins in the secreted proteome could be clearly defined as being secreted and not contaminants from cell lysis (compared to 30–35% of the proteins identified in the 3T3-based experiments). Two dimensional analysis increased the total number of unique peptides by slightly more than 2-fold that greatly aided in confident assignments. A total of 132 of these secreted proteins were not identified in previous proteomic screens for secreted proteins from rat primary adipocytes (Table 2-4) (18). Next, we wanted to compare the secreted proteomes from the two insulin resistant conditions to the insulin responsive conditions. For LC-MS/MS quantitative analysis, we used the number of unique peptides assigned to a protein and area under the peak for normalized reconstructed ion chromatograms of individual peptides that were identified in both conditions (Figure 2-4). Since we used two different methods for relative quantifications, we set our threshold for reporting differences at 150%. For most proteins observed, both methods showed similar trends once the threshold of 1.5-fold change was used (Table 2-S5 in Supporting information). For the two-dimensional analysis, the combined data sets were compared at the level of unique peptides alone to determine proteins showing a change of at least 150% (Table 2-S6 in Supporting Information). Reported in Table 2-5 are the 20 proteins that changed secretion levels by at least 1.5-fold under both insulin resistant conditions using both LC-MS/MS shotgun data and the two-dimensional data or at least 2-fold change for both conditions under one of the experimental approaches when compared to the insulin responsive condition. Because of the difficulty of assigning unique peptides to specific collagen isoforms (that share high amino acid identity), these proteins are not reported in Table 2-5 but are shown in Tables 2-S5 and 2-S6 in Supporting Information.

N-Glycan Site Mapping of the Secreted Proteome of Rodent Adipocytes. Since the majority of secreted proteins are glycoproteins, one sample from each condition for both mouse and rat adipocytes was treated with PNGase F in ^{18}O -water to convert the glycan-modified Asn to an ^{18}O -Asp residue (mass shift of 3 Da). These experiments were performed to increase coverage (unique proteins identified in this manner are included in the previous data shown in terms of performing relative quantification) and serve as the first step toward identifying possibly unique glycoforms of these potential biomarkers. In mouse immortalized adipocyte and rat primary adipocyte secreted proteomes, without enrichment, we were able to identify 37 sites on 21 proteins and 48 sites on 30 proteins of N-linked glycosylation, respectively (Table 2-6). Care was taken to avoid ^{18}O incorporation into the C-terminus of peptides by residual trypsin as previously described (28). All modified asparagine residues were in the consensus sequence, N-X-S/T, for N-linked glycosylation, adding further proof that our filtering of assignments was sufficiently strict to properly assign peptides and sites of modification.

2.4. DISCUSSION

Using a combination of cell lines and growth conditions, we have more completely defined the secreted proteome of rodent adipocytes. More complete characterization of this secretome should facilitate understanding the central role that adipocytokines play in regulating a variety of processes including energy homeostasis, host defense mechanisms, and insulin sensitivity. Furthermore, this work may aid in the detection and treatment of multiple disease states such as metabolic syndrome, cardiovascular disease, and type 2 diabetes. Mouse models, especially the adipose-specific Glut4 ablation and overexpression animals, clearly highlight the importance of adipose tissue not only in glucose uptake in that tissue but in whole body insulin

action and resistance (47-50). The ability of adipose tissue to alter insulin sensitivity in other tissues is likely explained by the endocrine nature of adipocytes. Thus, in an effort to identify potential key signaling molecules, we have begun to explore changes in the secreted proteome of adipocytes when the cells are shifted from being insulin responsive to insulin resistant. Also, given that sugar metabolism is central to diabetes and because we are studying secreted proteins, we have reported preliminary efforts to map some of the N-glycosylation sites, but this will need to be focused on in more detail in efforts beyond the scope of this paper to determine if complex glycosylation is being modulated by intracellular glycosylation and/or insulin responsiveness.

Multiple hypotheses have been put forth for the generation of insulin resistance in cells. One model is that cells detect high glucose levels indirectly through generation of UDP-GlcNAc via the hexosamine biosynthetic pathway and downregulate their sensitivity to insulin (4, 39, 51, 52). Recent work by our group and others has demonstrated that the mechanism by which UDP-GlcNAc levels impinge on insulin signaling is likely controlled via O-GlcNAc modification of nuclear and cytosolic proteins (9, 11, 53). Given that elevation of O-GlcNAc levels on intracellular proteins via pharmacological inhibition of O-GlcNAcase with PUGNAc alone is sufficient to induce insulin resistance (11), this has provided us with two different means of inducing insulin resistance in rodent adipocytes in culture. Furthermore, leptin and adiponectin have previously been shown to be regulated at the transcriptional level by hexosamine flux, and mice overexpressing the O-GlcNAc transferase in skeletal muscle and adipose tissue display hyperleptinemia (9, 23, 24). Therefore, we decided to focus on secreted proteins that were regulated in a like manner when insulin resistance was produced by either PUGNAc treatment or a combination of hyperglycemia and hyperinsulinemia. Defining this subset of proteins lays the initial groundwork for testing whether any or all of these proteins are potential

diagnostic/therapeutic biomarkers for multiple metabolic diseases such as cardiovascular disease and type 2 diabetes. In fact, several of the proteins we have identified have already been implicated in complications associated with metabolic disease. This data also serves to further illustrate that multiple changes that occur under classical insulin resistance can be recapitulated simply by elevating intracellular glycosylation. Given that elevated O-GlcNAc levels impinge on insulin-dependent glucose uptake and modulate adipocytokine secretion combined with the recent finding that a SNP in OGA (O-GlcNAcase), the neutral, nuclear, and cytoplasmic N-acetylglucosaminidase responsible for removing O-GlcNAc from intracellular proteins, correlates strongly with diabetes in Mexican Americans (54) highlights the importance of understanding this modification as it relates to diabetes. It further demonstrates the potential for modulation of O-GlcNAc levels as a possible therapeutic target in the treatment of insulin resistance-associated diseases such as metabolic syndrome and type 2 diabetes and their resulting complications.

In the 3T3 system, we identified nine proteins whose steady state levels in the secreted media changed, compared to low glucose, when cells were shifted to either of the insulin resistant conditions. Several of these proteins have previously been associated with type 2 diabetes or known complications arising from the induction of insulin resistance. For example, hippocampal cholinergic neurostimulating protein (HCNP), that is upregulated (Table 2-3), has been shown to play a cardioinhibitory role and cardiovascular disease is the leading cause of death in type 2 diabetics (55). Furthermore, HCNP in the CSF has been associated with Alzheimer's disease and insulin resistance increases the risk of Alzheimer's disease (56). Further, HCNP has been linked with depression which is a disorder increased in obese and diabetic individuals (57). Also, angiotensin, that is upregulated (Table 2-3), and matrix

metalloproteinase 2 (MMP-2) (that is downregulated) have been extensively linked to macro- and microvascular diseases commonly seen in diabetic patients (58). Further, angiotensin itself has been shown to regulate certain adipocytokines as well as being linked to diabetic retinopathy and nephropathy (59). Laminins, such as B1 seen in Table 2-3, have been implicated in diabetic nephropathy (60). In the 3T3 system, as well as the primary adipocytes, an increase in adiponectin was detected. This is consistent with the findings of Hess and colleagues¹⁸ and may indicate that adiponectin, that is known to be suppressed in rodent models of chronic insulin resistance (61) is upregulated initially upon insulin resistance (in an attempt to improve insulin sensitivity?) and later downregulated. Finally, cyclophilin A overexpression, as seen in Table 2-3, has been linked to pancreatic cancer (62), and type 2 diabetes, obesity, and insulin resistance increase the incidence rate of this malignancy (63).

Due mainly to the decrease in intracellular contamination and the increased depth of analysis afforded by multidimensional chromatography, we were able to explore the secreted proteome of primary adipocytes in more detail. This is ideal, as unlike 3T3-derived adipocytes, these cells more closely resemble *in vivo* conditions in that they are not immortal nor have they been passaged under hyperglycemic conditions for long periods of time. Several more insulin resistance-regulated proteins were detected in the rat primary adipocyte secretome. Interestingly, in general, detected protease inhibitors appeared to be upregulated, while proteases were downregulated. Similar to the 3T3 cells, we noted several proteins (Table 2-5) that were regulated in a similar fashion via the induction of insulin resistance using classical methods (hyperglycemia and chronic insulin) and through the elevation of intracellular glycosylation (PUGNAc treatment). Included on this list of regulated proteins were slit homologue 3 and fibulin-2, both of which were downregulated and have been associated with angiogenesis (64,

65). We also saw upregulation of lipoprotein lipase which is involved in breaking down bloodstream fat (66). Multiple proteins involved in oxidative stress and the immune response were also regulated including C6, gelsolin, MASP-3, secretory superoxide dismutates, and thioredoxin. Furthermore, upregulation of proteins involved in extracellular and tissue remodeling such as GP-39, spondin, and protein-S was observed. Interestingly, the cholesterol-binding protein NPC2 was upregulated under both insulin resistance conditions. Finally, upregulation was observed for ceruloplasmin and it has previously been observed that mutations in this gene lead to a diabetic phenotype (67).

These experiments serve to identify possible prognostic/diagnostic markers for metabolic syndrome (insulin-resistance syndrome), type 2 diabetes, and complications such as cardiovascular disease resulting from these conditions. Future work is aimed at determining whether steady-state levels of these proteins are altered in the serum of rodent models of diabetes and patients diagnosed with metabolic syndrome, type I diabetes, or resulting complications. Furthermore, given that intracellular elevation of O-GlcNAc levels is modulating the secretion of many of these proteins, the mechanism of action is being investigated. The majority of adipocytokines studied to date are regulated at the level of transcription, and O-GlcNAc is known to modify and modulate the activity of a number of transcription factors (68). Alternatively, O-GlcNAc has been shown to regulate the insulin pathway upstream of AKT, and therefore, an indirect mode of action may be occurring (11). Understanding how perturbations in O-GlcNAc levels, that appear to play a major role in several key aspects of insulin-resistance, are altering the normal processes of adipocytes may provide novel insights into prognostics, diagnostics, and therapeutics for metabolic syndrome, type 2 diabetes, and the associated complications of these debilitating diseases.

REFERENCES

1. Brownlee, M. The pathobiology of diabetic complications: a unifying mechanism. *Diabetes* **2005**, *54* (6), 1615-1625.
2. Brownlee, M. Biochemistry and molecular cell biology of diabetic complications. *Nature* **2001**, *414* (6865), 813-820.
3. Obici, S.; Rossetti, L. Minireview: nutrient sensing and the regulation of insulin action and energy balance. *Endocrinology* **2003**, *144* (12), 5172-5178.
4. Patti, M. E. Nutrient modulation of cellular insulin action. *Ann. N.Y. Acad. Sci.* **1999**, *892*, 187-203.
5. McClain, D. A.; Crook, E. D. Hexosamines and insulin resistance. *Diabetes* **1996**, *45* (8), 1003-1009.
6. Rossetti, L. Perspective: Hexosamines and nutrient sensing. *Endocrinology* **2000**, *141* (6), 1922-1925.
7. Hart, G. W.; Housley, M. P.; Slawson, C. Cycling of O-linked beta-N-acetylglucosamine on nucleocytoplasmic proteins. *Nature* **2007**, *446* (7139), 1017-1022.
8. Arias, E. B.; Kim, J.; Cartee, G. D. Prolonged incubation in PUGNAc results in increased protein O-Linked glycosylation and insulin resistance in rat skeletal muscle. *Diabetes* **2004**, *53* (4), 921-930.
9. McClain, D. A.; Lubas, W. A.; Cooksey, R. C.; Hazel, M.; Parker, G. J.; Love, D. C.; Hanover, J. A. Altered glycan-dependent signaling induces insulin resistance and hyperleptinemia. *Proc Natl Acad Sci U S A* **2002**, *99* (16), 10695-10699.

10. Parker, G. J.; Lund, K. C.; Taylor, R. P.; McClain, D. A. Insulin resistance of glycogen synthase mediated by O-linked N-acetylglucosamine. *J. Biol. Chem.* **2003**, *278* (12), 10022-10027.
11. Vosseller, K.; Wells, L.; Lane, M. D.; Hart, G. W. Elevated nucleocytoplasmic glycosylation by O-GlcNAc results in insulin resistance associated with defects in Akt activation in 3T3-L1 adipocytes. *Proc. Natl. Acad. Sci. U.S.A.* **2002**, *99* (8), 5313-5318.
12. Havel, P. J. Update on adipocyte hormones: regulation of energy balance and carbohydrate/lipid metabolism. *Diabetes* **2004**, *53* (1), S143-151.
13. Stolar, M. W. Insulin resistance, diabetes, and the adipocyte. *Am. J. Health Syst. Pharm.* **2002**, *59* (9), S3-8.
14. Guerre-Millo, M. Adipose tissue hormones. *J. Endocrinol. Invest.* **2002**, *25* (10), 855-861.
15. Guzik, T. J.; Mangalat, D.; Korbut, R. Adipocytokines-novel link between inflammation and vascular function. *J. Physiol. Pharmacol.* **2006**, *57* (4), 505-528.
16. Matsuzawa, Y. The metabolic syndrome and adipocytokines. *FEBS Lett.* **2006**, *580* (12), 2917-2921.
17. Alvarez-Llamas, G.; Szalowska, E.; de Vries, M. P.; Weening, D.; Landman, K.; Hoek, A.; Wolffenbuttel, B. H.; Roelofsen, H.; Vonk, R. J. Characterization of the human visceral adipose tissue secretome. *Mol. Cell. Proteomics* **2007**, *6* (4), 589-600.
18. Chen, X.; Cushman, S. W.; Pannell, L. K.; Hess, S. Quantitative proteomic analysis of the secretory proteins from rat adipose cells using a 2D liquid chromatography-MS/MS approach. *J. Proteome Res.* **2005**, *4* (2), 570-577.
19. Kratchmarova, I.; Kalume, D. E.; Blagoev, B.; Scherer, P. E.; Podtelejnikov, A. V.; Molina, H.; Bickel, P. E.; Andersen, J. S.; Fernandez, M. M.; Bunkenborg, J.; Roepstorff,

- P.; Kristiansen, K.; Lodish, H. F.; Mann, M.; Pandey, A. A proteomic approach for identification of secreted proteins during the differentiation of 3T3-L1 preadipocytes to adipocytes. *Mol. Cell. Proteomics* **2002**, *1* (3), 213-222.
20. Wang, P.; Mariman, E.; Keijer, J.; Bouwman, F.; Noben, J. P.; Robben, J.; Renes, J. Profiling of the secreted proteins during 3T3-L1 adipocyte differentiation leads to the identification of novel adipokines. *Cell. Mol. Life Sci.* **2004**, *61* (18), 2405-2417.
21. Zvonic, S.; Lefevre, M.; Kilroy, G.; Floyd, Z. E.; DeLany, J. P.; Kheterpal, I.; Gravois, A.; Dow, R.; White, A.; Wu, X.; Gimble, J. M. Secretome of primary cultures of human adipose-derived stem cells: modulation of serpins by adipogenesis. *Mol. Cell. Proteomics* **2007**, *6* (1), 18-28.
22. Moore, G. B.; Chapman, H.; Holder, J. C.; Lister, C. A.; Piercy, V.; Smith, S. A.; Clapham, J. C. Differential regulation of adipocytokine mRNAs by rosiglitazone in db/db mice. *Biochem. Biophys. Res. Commun.* **2001**, *286* (4), 735-741.
23. Hazel, M.; Cooksey, R. C.; Jones, D.; Parker, G.; Neidigh, J. L.; Witherbee, B.; Gulve, E. A.; McClain, D. A. Activation of the hexosamine signaling pathway in adipose tissue results in decreased serum adiponectin and skeletal muscle insulin resistance. *Endocrinology* **2004**, *145* (5), 2118-2128.
24. Wang, J.; Liu, R.; Hawkins, M.; Barzilai, N.; Rossetti, L. A nutrientsensing pathway regulates leptin gene expression in muscle and fat. *Nature* **1998**, *393* (6686), 684-688.
25. Student, A. K.; Hsu, R. Y.; Lane, M. D. Induction of fatty acid synthetase synthesis in differentiating 3T3-L1 preadipocytes. *J. Biol. Chem.* **1980**, *255* (10), 4745-4750.

26. Ramsay, T. G.; Hausman, G. J.; Martin, R. J. Pre-adipocyte proliferation and differentiation in response to hormone supplementation of decapitated fetal pig sera. *J. Anim. Sci.* **1987**, *64* (3), 735-744.
27. Wagoner, B.; Hausman, D. B.; Harris, R. B. Direct and indirect effects of leptin on preadipocyte proliferation and differentiation. *Am. J. Physiol.: Regul. Integr. Comp. Physiol.* **2006**, *290* (6), R1557-1564.
28. Angel, P. M.; Lim, J.; Wells, L.; Bergmann, C.; Orlando, R. A potential pitfall in 18-O based N-linked glycosylation site mapping. *Rapid Commun. Mass Spectrom.* **2007**, *21*, 674-682.
29. Comer, F. I.; Vosseller, K.; Wells, L.; Accavitti, M. A.; Hart, G. W. Characterization of a mouse monoclonal antibody specific for O-linked N-acetylglucosamine. *Anal. Biochem.* **2001**, *293* (2), 169-177.
30. Gilar, M.; Olivova, P.; Daly, A. E.; Gebler, J. C. Orthogonality of separation in two-dimensional liquid chromatography. *Anal. Chem.* **2005**, *77* (19), 6426-6434.
31. Weatherly, D. B.; Astwood, J. A.; Minning, T. A.; Cavola, C.; Tarleton, R. L.; Orlando, R. A Heuristic method for assigning a false-discovery rate for protein identifications from Mascot database search results. *Mol. Cell. Proteomics* **2005**, *4* (6), 762-772.
32. Peng, J.; Elias, J. E.; Thoreen, C. C.; Licklider, L. J.; Gygi, S. P. Evaluation of multidimensional chromatography coupled with tandem mass spectrometry (LC/LC-MS/MS) for large-scale protein analysis: the yeast proteome. *J. Proteome Res.* **2003**, *2* (1), 43-50.
33. Yates, J. R.; McCormack, A. L.; Eng, J. Mining genomes with MS. *Anal. Chem.* **1996**, *68* (17), 534A-540A.

34. Kristiansen, T. Z.; Bunkenborg, J.; Gronborg, M.; Molina, H.; Thuluvath, P. J.; Argani, P.; Goggins, M. G.; Maitra, A.; Pandey, A. A proteomic analysis of human bile. *Mol Cell Proteomics* **2004**, *3* (7), 715-728.
35. Kudlow, J. E. The O-GlcNAcase theory of diabetes: commentary on a candidate gene for diabetes. *Mol. Genet. Metab.* **2002**, *77* (1-2), 1-2.
36. Buse, M. G.; Robinson, K. A.; Marshall, B. A.; Hresko, R. C.; Mueckler, M. M. Enhanced O-GlcNAc protein modification is associated with insulin resistance in GLUT1-overexpressing muscles. *Am. J. Physiol.: Endocrinol. Metab.* **2002**, *283* (2), E241-250.
37. Parker, G.; Taylor, R.; Jones, D.; McClain, D. Hyperglycemia and inhibition of glycogen synthase in streptozotocin-treated mice: role of O-linked N-acetylglucosamine. *J. Biol. Chem.* **2004**, *279* (20), 20636-20642.
38. Vosseller, K.; Sakabe, K.; Wells, L.; Hart, G. W. Diverse regulation of protein function by O-GlcNAc: a nuclear and cytoplasmic carbohydrate post-translational modification. *Curr. Opin. Chem. Biol.* **2002**, *6* (6), 851-857.
39. Wells, L.; Vosseller, K.; Hart, G. W. A role for N-acetylglucosamine as a nutrient sensor and mediator of insulin resistance. *Cell. Mol. Life Sci.* **2003**, *60* (2), 222-228.
40. Yki-Jarvinen, H.; Virkamaki, A.; Daniels, M. C.; McClain, D.; Gottschalk, W. K. Insulin and glucosamine infusions increase O-linked N-acetyl-glucosamine in skeletal muscle proteins in vivo. *Metabolism* **1998**, *47* (4), 449-455.
41. McClain, D. A.; Alexander, T.; Cooksey, R. C.; Considine, R. V. Hexosamines stimulate leptin production in transgenic mice. *Endocrinology* **2000**, *141* (6), 1999-2002.
42. Chen, Y.; Yu, P.; Luo, J.; Jiang, Y. Secreted protein prediction system combining CJ-SPHMM, TMHMM, and PSORT. *Mamm. Genome* **2003**, *14* (12), 859-865.

43. Aebersold, R.; Mann, M. Mass spectrometry-based proteomics. *Nature* **2003**, *422* (6928), 198-207.
44. Gygi, S. P.; Rist, B.; Aebersold, R. Measuring gene expression by quantitative proteome analysis. *Curr. Opin. Biotechnol.* **2000**, *11* (4), 396-401.
45. Old, W. M.; Meyer-Arendt, K.; Aveline-Wolf, L.; Pierce, K. G.; Mendoza, A.; Sevinsky, J. R.; Resing, K. A.; Ahn, N. G. Comparison of label-free methods for quantifying human proteins by shotgun proteomics. *Mol. Cell. Proteomics* **2005**, *4* (10), 1487-1502.
46. Ong, S. E.; Foster, L. J.; Mann, M. Mass spectrometric-based approaches in quantitative proteomics. *Methods* **2003**, *29* (2), 124-130.
47. Abel, E. D.; Peroni, O.; Kim, J. K.; Kim, Y. B.; Boss, O.; Hadro, E.; Minnemann, T.; Shulman, G. I.; Kahn, B. B. Adipose-selective targeting of the GLUT4 gene impairs insulin action in muscle and liver. *Nature* **2001**, *409* (6821), 729-733.
48. Carvalho, E.; Kotani, K.; Peroni, O. D.; Kahn, B. B. Adipose-specific overexpression of GLUT4 reverses insulin resistance and diabetes in mice lacking GLUT4 selectively in muscle. *Am. J. Physiol.: Endocrinol. Metab.* **2005**, *289* (4), E551-561.
49. Postic, C.; Mauvais-Jarvis, F.; Girard, J. Mouse models of insulin resistance and type 2 diabetes. *Ann. Endocrinol.* **2004**, *65* (1), 51-59.
50. Wallberg-Henriksson, H.; Zierath, J. R. GLUT4: a key player regulating glucose homeostasis? Insights from transgenic and knockout mice (review). *Mol. Membr. Biol.* **2001**, *18* (3), 205-211.
51. Marshall, S.; Bacote, V.; Traxinger, R. R. Discovery of a metabolic pathway mediating glucose-induced desensitization of the glucose transport system. Role of hexosamine biosynthesis in the induction of insulin resistance. *J. Biol. Chem.* **1991**, *266* (8), 4706-4712.

52. McClain, D. A. Hexosamines as mediators of nutrient sensing and regulation in diabetes. *J Diabetes Complications* **2002**, *16* (1), 72-80.
53. Dias, W. B.; Hart, G. W. O-GlcNAc modification in diabetes and Alzheimer's disease. *Mol. Biosyst.* **2007**, *3* (11), 766-772.
54. Lehman, D. M.; Fu, D. J.; Freeman, A. B.; Hunt, K. J.; Leach, R. J.; Johnson-Pais, T.; Hamlington, J.; Dyer, T. D.; Arya, R.; Abboud, H.; Goring, H. H.; Duggirala, R.; Blangero, J.; Konrad, R. J.; Stern, M. P. A single nucleotide polymorphism in MGEA5 encoding O-GlcNAc-selective N-acetyl-beta-D glucosaminidase is associated with type 2 diabetes in Mexican Americans. *Diabetes* **2005**, *54* (4), 1214-1221.
55. Angelone, T.; Goumon, Y.; Cerra, M. C.; Metz-Boutigue, M. H.; Aunis, D.; Tota, B. The emerging cardioinhibitory role of the hippocampal cholinergic neurostimulating peptide. *J. Pharmacol. Exp. Ther.* **2006**, *318* (1), 336-344.
56. Tsugu, Y.; Ojika, K.; Matsukawa, N.; Iwase, T.; Otsuka, Y.; Katada, E.; Mitake, S. High levels of hippocampal cholinergic neurostimulating peptide (HCNP) in the CSF of some patients with Alzheimer's disease. *Eur. J. Neurol.* **1998**, *5* (6), 561-569.
57. Khawaja, X.; Xu, J.; Liang, J. J.; Barrett, J. E. Proteomic analysis of protein changes developing in rat hippocampus after chronic antidepressant treatment: Implications for depressive disorders and future therapies. *J. Neurosci. Res.* **2004**, *75* (4), 451-460.
58. Zaoui, P.; Cantin, J. F.; Alimardani-Bessette, M.; Monier, F.; Halimi, S.; Morel, F.; Cordonnier, D. Role of metalloproteases and inhibitors in the occurrence and progression of diabetic renal lesions. *Diabetes Metab.* **2000**, *26* (4), 25-29.

59. Chaldakov, G. N.; Stankulov, I. S.; Hristova, M.; Ghenev, P. I. Adipobiology of disease: adipokines and adipokine-targeted pharmacology. *Curr. Pharm. Des.* **2003**, *9* (12), 1023-1031.
60. Schleicher, E.; Nerlich, A.; Gerbitz, K. D. Pathobiochemical aspects of diabetic nephropathy. *Klin Wochenschr.* **1988**, *66* (18), 873-882.
61. Hug, C.; Lodish, H. F. Diabetes, obesity, and Acrp30/adiponectin. *BioTechniques* **2002**, *33* (3), 654, 656, 658 passim.
62. Li, M.; Wang, H.; Li, F.; Fisher, W. E.; Chen, C.; Yao, Q. Effect of cyclophilin A on gene expression in human pancreatic cancer cells. *Am. J. Surg.* **2005**, *190* (5), 739-745.
63. Friedman, G. D.; van den Eeden, S. K. Risk factors for pancreatic cancer: an exploratory study. *Int. J. Epidemiol.* **1993**, *22* (1), 30-37.
64. Fujiwara, M.; Ghazizadeh, M.; Kawanami, O. Potential role of the Slit/Robo signal pathway in angiogenesis. *Vasc. Med.* **2006**, *11* (2), 115-121.
65. Tsuda, T.; Wang, H.; Timpl, R.; Chu, M. L. Fibulin-2 expression marks transformed mesenchymal cells in developing cardiac valves, aortic arch vessels, and coronary vessels. *Dev. Dyn.* **2001**, *222* (1), 89-100.
66. Franks, P. W.; Mesa, J. L.; Harding, A. H.; Wareham, N. J. Genelifestyle interaction on risk of type 2 diabetes. *Nutr. Metab. Cardiovasc. Dis.* **2007**, *17* (2), 104-124.
67. Shang, H. F.; Jiang, X. F.; Burgunder, J. M.; Chen, Q.; Zhou, D. Novel mutation in the ceruloplasmin gene causing a cognitive and movement disorder with diabetes mellitus. *Mov. Disord.* **2006**, *21* (12), 2217-2220.
68. Wells, L.; Whalen, S. A.; Hart, G. W. O-GlcNAc: a regulatory posttranslational modification. *Biochem. Biophys. Res. Commun.* **2003**, *302* (3), 435-441.

Table 2-1. Calculation of false-discovery rates

Database	Group	SEQUEST criteria*	FPR(%)	FDR(%)
Mouse	Protein	Xcorr>2.0/2.5/3.0, GBU>-1 or dCn>0.1	0.0300 ± 0.0003	0.070 ± 0.003
	Peptide	Xcorr>2.4/3.0/3.8, GBU>-1, dCn>0.16, Sp>600 or RSp<6	0.0700 ± 0.0005	0.630 ± 0.004
Rat	Protein	Xcorr>2.0/2.5/3.0, GBU>-1 or dCn>0.1	0.0323 ± 0.0001	0.190 ± 0.005
	Peptide	Xcorr>2.4/3.0/3.8, GBU>-1, dCn>0.16, Sp>600 or RSp<6	0.1033 ± 0.0005	0.880 ± 0.004

* Xcorr (cross correlation with charge states of +1/+2/+3), GBU (the good, the bad, and the ugly), dCn (delta correlation), Sp (preliminary score), and RSp (the ranking of the primary score).

Table 2-2. Novel secreted proteins from immortalized mouse adipocytes

No.	Gene ID	PSORT Prediction	Signal Peptide	Identified Proteins	Detection	
					3T3-L1	3T3-F442A
1	34328185	exc	Y	(pro)saposin	+	+
2	33859506	exc	Y	albumin 1	+	+
3	21553309	mit	Y	apolipoprotein A-I binding protein	+	+
4	47271511	end	N	betaglycan; transforming growth factor (TGF), beta receptor 3	+	+
5	20137008	exc	Y	biglycan	+	+
6	21450325	exc	N	biliverdin reductase B	+	+
7	12963529	cyt	Y	complement component 1, r subcomponent	+	+
8	6681143	exc	Y	decorin	+	+
9	46849812	nuc	N	fibronectin 1	+	+
10	6679757	nuc	N	fibulin 2 (Fbln 2)	+	+
11	31560699	exc	Y	follistatin-like 1	+	+
12	6680107	exc	Y	granulin (Grn protein, Epithelin 1 & 2)	+	+
13	6981086	exc	Y	insulin-like growth factor binding protein 4	+	+
14	33859490	nuc	N	laminin B1 subunit 1	+	+
15	6755144	exc	Y	lectin, galactoside-binding, soluble, 3 binding protein (galectin 3)	+	+
16	34328049	exc	Y	lipocalin 2	+	+
17	6679182	exc	Y	orosomuroid 1	+	+
18	6754950	exc	Y	orosomuroid 2	+	+
19	6755112	exc	Y	phospholipid transfer protein	+	+
20	9903607	end	Y	putative secreted protein ZSIG9	+	+
21	12963609	end	Y	quiescin Q6	+	+
22	31981237	cyt	N	thimet oligopeptidase 1	+	+
23	33468851	exc	N	(pro)collagen, type IV, alpha 5	+	-
24	13937349	mit	N	(pro)collagen, type XV	+	-
25	6754570	nuc	N	annexin A1 (Annexin I, lipocortin I)	+	-
26	19526463	mit	Y	endoplasmic reticulum protein ERp29	+	-
27	6680397	nuc	Y	interleukin 12b; IL-12 p40	+	-
28	18250288	end	Y	interleukin 25	+	-

Table 2-2. Continued.

No.	Gene ID	PSORT Prediction	Signal Peptide	Identified Proteins	Detection	
					3T3-L1	3T3-F442A
29	19527008	mit	Y	lysophospholipase 3	+	-
30	7305295	nuc	N	myosin heavy chain 11, smooth muscle	+	-
31	6679166	nuc	Y	osteoglycin	+	-
32	8393173	exc	N	(pro)collagen, type V, alpha 3	-	+
33	47059082	nuc	N	ADAMTS-1; a disintegrin-like and metalloprotease (reprolysin type) with thrombospondin type 1 motif, 1	-	+
34	22203763	exc	Y	carboxypeptidase E	-	+
35	6753558	exc	Y	cathepsin L	-	+
36	11968166	exc	Y	cathepsin X	-	+
37	6680816	mit	N	complement component 1, q subcomponent	-	+
38	6755142	end	Y	cyclophilin B (peptidylprolyl isomerase B)	-	+
39	6753642	exc	Y	delta-like 1 homolog	-	+
40	33859532	nuc	Y	dystroglycan 1	-	+
41	31982690	exc	Y	epidermal growth factor (EGF)-containing fibulin-like extracellular matrix protein 2 (Efemp2, fibulin 4)	-	+
42	7657067	exc	Y	ERO1-like (Endoplasmic Reticulum oxidoreductin-1)	-	+
43	6681257	exc	Y	extracellular matrix protein 1 (ECM1)	-	+
44	6806917	end	Y	GM2 ganglioside activator protein	-	+
45	31560691	nuc	N	hepatoma-derived growth factor	-	+
46	6678740	exc	Y	lumican	-	+
47	6678680	exc	Y	lunatic fringe gene homolog	-	+
48	6678792	mit	Y	mannosidase alpha class 2B member 2	-	+
49	21313658	exc	Y	retinoic acid receptor responder (tazarotene induced) 2	-	+
50	38075893	end	N	semaphorin sem2	-	+
51	6755600	end	Y	superoxide dismutase 3, extracellular	-	+
52	6755779	nuc	N	thrombospondin 2	-	+
53	31543867	exc	Y	tissue inhibitor of metalloproteinase 2	-	+
54	7657639	end	Y	transcobalamin 2	-	+

Table 2-3. Mouse adipocytokines regulated by insulin resistance^a

Gene ID	Identified proteins	(HG+I)/LG	PUG/LG
31982423	Adiponectin (Acrp30)	5.8(L), 4.0(F)	4.0(L), 2.7(F)
51765519	Hippocampal cholinergic neurostimulating protein	2.6(L)	3.0(L), 2.6(F)
12963609	Quiescin Q6	7.0(L), 6.0(F)	2.9(F)
19705566	Angiotensinogen	3.8(F)	3.1(F)
6679439	Cyclophilin A	[9/0](F)	[20/0](F)
33859490	Laminin B1 subunit 1	10.0(L)	12.0(L)
Gene ID	Identified protein	LG/(HG+I)	LG/PUG
6678902	Matrix metalloproteinase 2 (collagenase, type IV)	9.0(L), 7.0(F)	7.0(F)
10181164	Fibrinogen/angiopoietin-related protein	[9/0](F)	[9/0](F)

^a Shown in (HG+I)/LG and PUG/LG are the ratios of the average unique peptides from each secreted proteome for a particular sample. (L) refers to 3T3-L1, (F) refers to 3T3-F442A; when no peptides were detected under a given condition, the total number of unique peptides assigned to the protein are shown in brackets [].

Table 2-4. Novel secreted proteins from primary rat adipocytes

No.	Gene ID	Identified proteins	No.	Gene ID	Identified proteins
1	4102819	(pro)collagen C-proteinase enhancer protein	67	13928880	plasma glutamate carboxypeptidase
2	28557685	(pro)collagen lysine, 2-oxoglutarate 5-dioxygenase 2	68	62649105	pregnancy-associated plasma protein-A
3	62644224	(pro)collagen type XI alpha 1	69	51859442	Protease, serine, 11
4	6978677	(pro)collagen, type II, alpha 1	70	1041904	protein S
5	62654019	(pro)collagen, type XII, alpha 1	71	62339361	retinoic acid receptor responder (tazarotene induced) 1
6	16758678	(pro)collagen-lysine, 2-oxoglutarate 5-dioxygenase 1	72	47477890	Ribonuclease, RNase A family 4
7	28400779	(pro)collagen-lysine, 2-oxoglutarate 5-dioxygenase 3	73	40018558	serine (or cysteine) proteinase inhibitor, clade G (C1 inhibitor), member 1, (angioedema, hereditary)
8	53850608	acid sphingomyelinase-like phosphodiesterase 3A	74	19173736	serine carboxypeptidase 1 (Retinoid-inducible serine carboxypeptidase)
9	62660765	AE binding protein 1	75	30027645	short isoform growth hormone receptor
10	11990616	aggrecan 1	76	13786142	slit homologue 3
11	28932816	alpha-2 antiplasmin; serine (or cysteine) proteinase inhibitor, clade F, member 1	77	62640996 (25453372)	spondin 1
12	27436861 (930262)	amyloid beta (A4) protein; Beta-amyloid peptide	78	34880777	tenascin-N
13	40018598	angiopoietin-like protein 4	79	8394446	betaglycan; transforming growth factor (TGF), beta receptor 3
14	2143593	annexin II (calpactin 1)	80	57472 (58476812)	Vascular cell adhesion molecule 1
15	20301954 (37805241)	apolipoprotein E	81	3309591	versican V3 isoform
16	58476724	Biotinidase (predicted)	82	38649303	Wfdc1 protein (WAP four-disulfide core domain 1); Prostate stromal protein ps20
17	62661703	bone morphogenetic protein 1 (procollagen C-proteinase)	83	4519515	(pro)collagen C-proteinase 3
18	20302073	cadherin 13	84	62900635	(Pro)collagen-lysine,2-oxoglutarate 5-dioxygenase 2 (Lysyl hydroxylase 2) (LH2)
19	62645871	Carboxypeptidase X 1 (M14 family); Metalloproteinase CPX-1	85	37048700	ADAMTS-5; a disintegrin-like and metalloproteinase (reprolysin type) with thrombospondin type 1 motif 5 (aggrecanase-2)
20	4558458	Chitinase 3 like 1; glycoprotein-39	86	3776238	aminopeptidase N (CD13)
21	62653824	Cilp protein (Cartilage intermediate layer protein)	87	34867707	Arylsulfatase A (ASA) (Cerebrosidase-sulfatase)

Table 2-4. Continued.

No.	Gene ID	Identified proteins	No.	Gene ID	Identified proteins
22	27688933	collagen alpha1	88	10800128	beta ig-h3 (TGFBI transforming growth factor, beta-induced, 68 kDa)
23	62655388	collagen isoform 1, type VI, alpha 3	89	62653568	C1q and tumor necrosis factor related protein 5
24	4995838	collagen type XVIII, alpha (I) chain	90	13928758	cathepsin K
25	3164123 (62655017)	collagen, type V, alpha 2	91	60688149	Cathepsin Y
26	62648968	collagen, type XV	92	1262920	CD14; a myeloid cell-surface receptor and soluble plasma protein
27	22255878	colony stimulating factor-1 (macrophage)	93	8393087	cell adhesion molecule-related/down-regulated by oncogenes (Cdon)
28	28570180	complement component 6	94	20806123	cell growth regulator with EF hand domain 1
29	62642976	complement component 7	95	13929074	c-fos induced growth factor (Vascular endothelial growth factor D precursor (VEGF-D), FIGF)
30	25244377	complement component C2	96	62658149	chordin
31	11560085 (4753900)	connective tissue growth factor	97	62643068 (62662017)	Cln5 protein (Ceroid-lipofuscinosis, neuronal 5)
32	1213217	Cu/Zn superoxide dismutase (SOD 1)	98	62652432	collagen type XIV
33	33086684	Da1-24; Complement factors B (B-factor, properdin)	99	6007583	collagen XVIII
34	19924047	dickkopf homologue 3 (Dickkopf-3)	100	11120710	collagen, type V, alpha 3
35	27677818	early quiescence protein-1	101	29373916	collagen, type XXIII, alpha 1
36	34863280	Elastin microfibril interfacier 1 (EMILIN 1)	102	38541053	cyclophilin B (peptidylprolyl isomerase B)
37	12018274	endothelial cell-specific molecule 1	103	2288921	DRM protein (Down-regulated in Mos-transformed cells protein); Gremlin
38	58865654 (9973135)	epidermal growth factor (EGF)-containing fibulin-like extracellular matrix protein 1 (Fibulin-3)	104	51859271	Ectonucleotide pyrophosphatase/phosphodiesterase 2 (Enpp2 protein)
39	394739	epididymal secretory superoxide dismutase	105	4583509	embryonic vascular EGF repeat-containing protein EVEC
40	13929178	fibrillin 1	106	56090361	ependymin related protein 2
41	42476116	fibulin 5	107	18104933	fibromodulin
42	62652879	Fibulin-1 (Basement-membrane protein 90)	108	30841840	follistatin 288 variant
43	24210470	fibulin-2 isoform a	109	2564302	GDNFR-alpha/TrnR1-delta protein
44	62665389	Galactosamine (N-acetyl)-6-sulfate sulfatase	110	62655235	Glb11 protein (galactosidase, beta 1-like)

Table 2-4. Continued.

No.	Gene ID	Identified proteins	No.	Gene ID	Identified proteins
45	34861992	Glutaminy-peptide cyclotransferase (QC) (Glutaminy-tRNA cyclotransferase) (Glutaminy cyclase)	111	38181579	Gpc1 protein (Glypican 1)
46	6970046	GPI-anchored ceruloplasmin	112	47477840	Growth arrest specific 6 (Gas6 protein)
47	28849947	hemiferrin, transferrin-like protein	113	47718020	Interleukin 1 receptor antagonist (Il1rn protein)
48	62649892	heparan sulfate proteoglycan 2 (perlecan)	114	6981590	interleukin 1 receptor-like 1
49	62663812	interalpha-inhibitor H2 chain (Inter alpha trypsin inhibitor, heavy chain 2)	115	58400808	Lysyl oxidase-like 1 (predicted)
50	13591914	kidney aminopeptidase M (aminopeptidase N)	116	12275390	membrane attractin
51	62666140	Laminin alpha-4 chain	117	1228089	multifunctional acyl-CoA-binding protein (diazepam binding inhibitor)
52	56788965	Laminin, beta-2; Lamb2 protein	118	41054820	neurogenesis 1
53	62638338	laminin-2 alpha2 chain	119	4468965	NG2 proteoglycan
54	11136636	latent transforming growth factor beta binding protein 2 (Latent TGF beta binding protein 2)	120	47477878	Plasma glutamate carboxypeptidase (Pgcp protein)
55	62652278	lipoprotein receptor-related protein	121	16758116	proline arginine-rich end leucine-rich repeat protein
56	62664372	lysyl oxidase	122	34882048	protein S (alpha)
57	62655863	M6PR domain containing protein 1	123	62638555	Ribonuclease T2 (Ribonuclease 6)
58	27527940 (25244444)	MASP-3 protein (mannan-binding lectin serine peptidase 1, MASP 1/3)	124	62662853	secreted frizzled-related protein 1
59	127076	Matrix Gla-protein (MGP)	125	16758312	secreted frizzled-related protein 4
60	62651656	matrix metalloproteinase 19	126	62646703	Semaphorin 3C
61	27672001	microfibrillar-associated protein 4	127	50811823	Spinal cord injury-related protein 10 (SCIRP10-related protein); Neuron-derived neurotrophic factor spinal-cord derived growth factor-B (Platelet derived growth factor D)
62	6981200	milk fat globule-EGF factor 8 protein	128	11610601	stanniocalcin 2
63	11072106 (14549433)	nucleobindin 2	129	11560026	steroid-sensitive protein 1 (<i>Urb</i> protein)
64	62644339	Olfactomedin-like 3	130	62657881	talin
65	1871124 (205860)	osteopontin (secreted phosphoprotein 1)	131	62648889	Tumor protein, translationally controlled 1 (Lens epithelial protein)
66	62646367	Phospholipid transfer protein	132	30385204 (34877064, 62658399)	

Table 2-5. Rat adipocytokines regulated by insulin resistance^a

No.	Gene ID	Identified proteins	(HG+I)/LG	PUG/LG
1	51858619	Lipoprotein lipase	6.0(1), 1.6(2)	2.0(1), 1.6(2)
2	27721871	Tetranectin	5.3(1), 2.5(2)	3.0(1), 1.5 (2)
3	13928716	Serine protease inhibitor 2c	3.0(1), 2.4(2)	1.7(1), 1.5(2)
4	11464979	Tissue inhibitor of metalloproteinase 2	1.6(1), 1.7(2)	2.0(1), 1.6(2)
5	62640996	Spondin 1	[3/0](1), 1.5(2)	[5/0](1)
6	62661377	Cathepsin B	1.9(1), 1.5(2)	3.3(1)
7	21307593	Adiponectin (Acrp30)	1.5(1), 1.7(2)	2.0(2)
8	27465565	Niemann Pick type C2 (secretory protein 1)	1.7(1)	2.0(1), 2.0(2)
9	51854227	Gelsolin	3.0(1)	2.5(1)
10	394739	Epididymal secretory superoxide dismutase	2.0(1)	2.0(1)
11	28570180	Complement component 6	6.0(2)	3.0(2)
12	4558458	Glycoprotein-39, Chitinase 3 like 1	2.8(2)	3.0(2)
13	1041904	Protein S	2.6(2)	2.0(2)
14	6970046	Ceruloplasmin	2.3(2)	2.0(2)
15	27527940	Mannan-binding lectin serine peptidase MASP-3	2.0(2)	1.5(2)
No.	Gene ID	Identified proteins	LG/(HG+I)	LG/PUG
1	13786142	Slit homologue 3	[7/0](1), 2.2(2)	3.5(1), 1.6(2)
2	24210470	Fibulin-2 isoform a	[12/0](1), 1.8(2)	3.0(1)
3	19173736	Retinoid-inducible serine carboxypeptidase 1	3.5(1), 2.0(2)	2.0(2)
4	16758644	Thioredoxin	2.0(1)	[4/0](1), 1.5(2)
5	51859442	Protease, serine, 11	2.0(1)	4.0(1)

^a Shown in (HG+I)/LG and PUG/LG are the ratios of the average number of unique peptides from each condition. (1) refers to LC-MS/MS shotgun analysis and (2) refers to 2D-LC-MS/MS analysis; when no peptides were detected under a given condition, the total number of unique peptides assigned to the protein are shown in brackets [].

Table 2-6. Sites of N-linked glycosylation in rodent adipocytokines

No.	Gene ID	Proteins	N-linked peptides ^a
3T3-L1 and F442A Immortalized Adipocytokines			
1	6753484	(pro)collagen, type VI, alpha 1	(-)N@FTAADWGHSR
2	6753484	(pro)collagen, type VI, alpha 1	(R)GEDGPPGN@GTEGFPGFPGYPGNR
3	34328185	(pro)saposin	(-)TN@SSFIQGFVDHVKEDCDR
4	34328185	(pro)saposin	(-)TVVTEAGNLLKDN@ATQEEILHYLEK
5	34328185	(pro)saposin	(-)LVLYLEHNLEKN@STKKEILAALEK
6	34328185	(pro)saposin	(-)DN@ATQEEILHYLEK
7	34328185	(pro)saposin	(-)FSELIVNN@ATEELLVK
8	34328185	(pro)saposin	(-)N@STKKEILAALEK
9	7304867	adipsin (Complement factor D)	(-)LSQN@ASLGPHVR
10	7304867	adipsin (Complement factor D)	(-)LSQN@ASLGPHVRPLPLQYEDK
11	6753558	cathepsin L	(-)AEFAVAN@DTGFVDIPQQEK
12	51767794	chondroitin sulfate proteoglycan 2 (Versican)	(-)FEN@QTCFPLPDSR
13	51705198	collagen VI, alpha-3 polypeptide	(-)QLINALQIN@NTAVGHALVLPAR
14	51705198	collagen VI, alpha-3 polypeptide	(R)ALN@GSALYTGSSLDVFR
15	6679439	cyclophilin A (peptidylprolyl isomerase A)	(-)HTGPGILSMANAGPNTN@GSQFFICTAK
16	6681143	decorin	(-)ISDTN@ITAIPQGLPTSLTEVHLDGK
17	31982800	extracellular matrix protein 2; SPARC-like 1 (mast9, hevin)	(-)ILDQACGTDN@QTYASSCHLFATK
18	31560699	folliculin-like 1	(-)GSN@YSEILDK
19	8850219	haptoglobin	(-)N@LTSPVGVQPILNEHTFCAGLTK
20	8850219	haptoglobin	(-)NLFLN@HSETASAK
21	8850219	haptoglobin	(-)VVLHPN@HSVVDIGLIK
22	8850219	haptoglobin	(-)CVVHYEN@STVPEKK
23	23956086	hemopexin	(-)SLGPNTCSSN@GSSLYFIHGPNLYCYSSIDK
24	23956086	hemopexin	(-)SWSTVGN@CTAALR
25	6680397	interleukin 12b; IL-12 p40	(-)CEAPN@YSGRFTCSWLVRNMDLKFNIK
26	31791057	laminin B2	(-)TLAGEN@QTALEIEELNR
27	31791057	laminin B2	(-)LQRVN@SSLHSQISR
28	6755144	lectin, galactoside-binding, soluble, 3 binding protein (galectin 3)	(-)GLN@LTEDTYKPR

Table 2-6. Continued.

No.	Gene ID	Proteins	N-linked peptides ^a
29	6755144	lectin, galactoside-binding, soluble, 3 binding protein (galectin 3)	(-)APIPTALDTN@SSK
30	6755144	lectin, galactoside-binding, soluble, 3 binding protein (galectin 3)	(-)ALGYEN@ATQALGR
31	6678710	lipoprotein lipase	(-)TPEDTAEDTCHLIPGLADSVSNCHF@HSSK
32	6754854	nidogen 1 (entactin 1)	(-)CVAN@YTGNGR
33	6679182	orosomuroid 1	(-)ESQTIGDQCVYN@STHLGFQR
34	6678077	osteonectin; SPARC	(-)VCSNDN@KTFDSSCHFFATK
35	12963609	quiescin Q6	(-)N@GSGATLPGAGANVQTLR
36	31982755	vimentin	(-)QDVDN@ASLAR
37	31982755	vimentin	(-)QVQSLTCEVDALKGTN@ESLER
Rat Primary Adipocytokines			
1	5305687	(pro)collagen, alpha-2(I)	(-)ASQN@ITYHCK
2	56711254	(pro)collagen, type III, alpha 1	(-)GEN@GSPGAPGAPGHPGPPGVPVPSGK
3	56711254	(pro)collagen, type III, alpha 1	(-)GDRGEN@GSPGAPGAPGHPGPPGVPVPSGK
4	38512144	(pro)saposin	(-)TVVTEAGNLLKDN@ATEEEILHYLEK
5	38512144	(pro)saposin	(-)LSELIINN@ATEELLIK
6	34862337	adipsin (Complement factor D)	(-)LSHN@ASLGPHVRPLPLQR
7	34862337	adipsin (Complement factor D)	(-)LSHN@ASLGPHVR
8	8392983	biglycan	(-)LLQVVYLHSNN@ITK
9	8392983	biglycan	(-)MIEN@GSLSFLPTLR
10	38648869	cathepsin L	(-)AEYAVAN@DTGFVDIPQKEK
11	62642714	chondroitin sulfate proteoglycan 2 (Versican)	(-)FEN@QTCFPLPDSR
12	11127974	Clusterin; Clu protein	(-)QELN@DSLQVAER
13	38181879	Clusterin; Clu protein	(-)HN@STGCLK
14	62665833	collagen, type VI, alpha1	(-)GEDGPPGN@GTEGFPGFPGYPGNR
15	62665833	collagen, type VI, alpha1	(-)N@FTAADWGHRS
16	20302095	complement component 1, s subcomponent	(-)TCGVN@CSGDVFTALIGEIASPNYPNPYPENSR
17	38303991	complement component 1, s subcomponent	(-)TCGVN@CSGDVFTALIGEIASPNYPNPYPENSR
18	25244377	complement component C2	(-)LGSYPVGGN@LSFECEHGFTLR
19	54020664	decorin	(-)YVQVVYLHNNN@ISEVGQHDFCLPSYQTR
20	54020664	decorin	(-)LGLSFNSITVVEN@GSLANVPHLR
21	54020664	decorin	(-)ISDTN@ITAIPQGLPTSISELHLDGNK

Table 2-6. Continued.

No.	Gene ID	Proteins	N-linked peptides ^a
22	13929178	fibrillin 1	(-)AWGTPCELCPV@TSEYK
23	9506703	fibronectin 1	(-)DQCIVDDITYNVN@DTFHK
24	62652879	Fibulin-1 (Basement-membrane protein 90)	(-)NCQDIDECVTGIHN@CSIN@ETCFNIQGSFR
25	13242265	folliculin-like 1	(-)GSN@YSEILDK
26	13242265	folliculin-like 1	(-)GSN@YSEILDKYFK
27	25006237	GM2 activator protein	(-)EGTYSLPSSN@FTVPDLELPSWLSTGNYR
28	6981590	interleukin 1 receptor-like 1	(-)ITCPTIALYN@WTAPVQWFK
29	62666140	Laminin alpha-4 chain	(-)LSN@LSNLSHDLVQEAVDHAYNLQQEANELSR
30	62650567	laminin B1 (Laminin beta 3)	(-)QADEDIQGTQNLTSIESETAASEETLTN@ASQR
31	62650567	laminin B1 (Laminin beta 3)	(-)SN@STAGELDALQAEAGSLDK
32	62650567	laminin B1 (Laminin beta 3)	(-)VN@ASTTDPNSTVEQSALTR
33	62659497	laminin, gamma 1	(-)TAN@ETSAEAYNLLLR
34	62659497	laminin, gamma 1	(-)TLAGEN@QTALEIEELNR
35	62638338	laminin-2 alpha2 chain	(-)VCN@CSTVGLSSQCNINTGQCCHPK
36	20806135	lectin, galactoside-binding, soluble, 3 binding protein (galectin 3)	(-)ALGYEN@ATQALSR
37	13591983	lumican	(-)KLHINYNN@LTESVGPLPK
38	13591983	lumican	(-)LGSFDGLVN@LTFIYLQHNQLK
39	13591983	lumican	(-)LHINYNN@LTESVGPLPK
40	13591983	lumican	(-)AFEN@VTDLQWLILDHNLLENSK
41	13591983	lumican	(-)LSHNELADSGVPGNSFN@ISSLLELDLSYNK
42	49256641	matrix metalloproteinase 2 (collagenase, type IV)	(-)GYPKPLTSLGLPPDVQQVDAAFN@WSK
43	1174697	Metalloproteinase inhibitor 1 precursor (TIMP-1)	(-)GFDAVGN@ATGFR
44	1174697	Metalloproteinase inhibitor 1 precursor (TIMP-1)	(-)SQN@RSEEFILAGR
45	62644339	Olfactomedin-like 3	(-)IYVLDGTQN@DTAFVFPR
46	2196884	osteonectin; SPARC	(-)VCSNDN@KTFDSSCHFFATK
47	16758312	secreted frizzled-related protein 4	(-)DDCEPLMKMYN@HSWPESLACDELVPYDR
48	3309591	versican V3 isoform	(-)FEN@QTCFPLPDSR

^a An @ indicates the site of N-linked glycosylation.

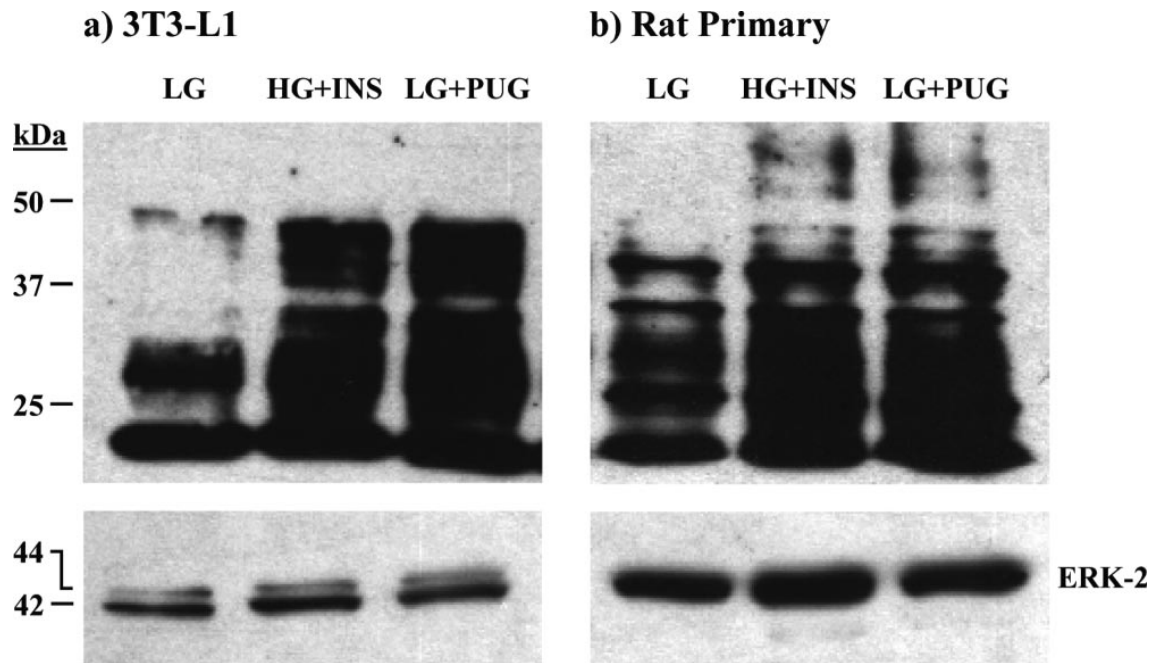


Figure 2-1. O-GlcNAc levels are elevated under insulin resistant conditions. 3T3-L1 adipocytes (A) or rat primary adipocytes (B) were maintained in an insulin responsive growth condition (low (physiological) glucose, LG) or grown under insulin responsive conditions (either high glucose and chronic insulin exposure (HG+INS) or treated with PUGNac (PUG)). Equal amounts of proteins from whole-cell extracts were separated by SDS-PAGE and Western blotting performed using the anti-O-GlcNAc antibody RL-2. ERK-2 Western blotting was performed as well to demonstrate equal loading.

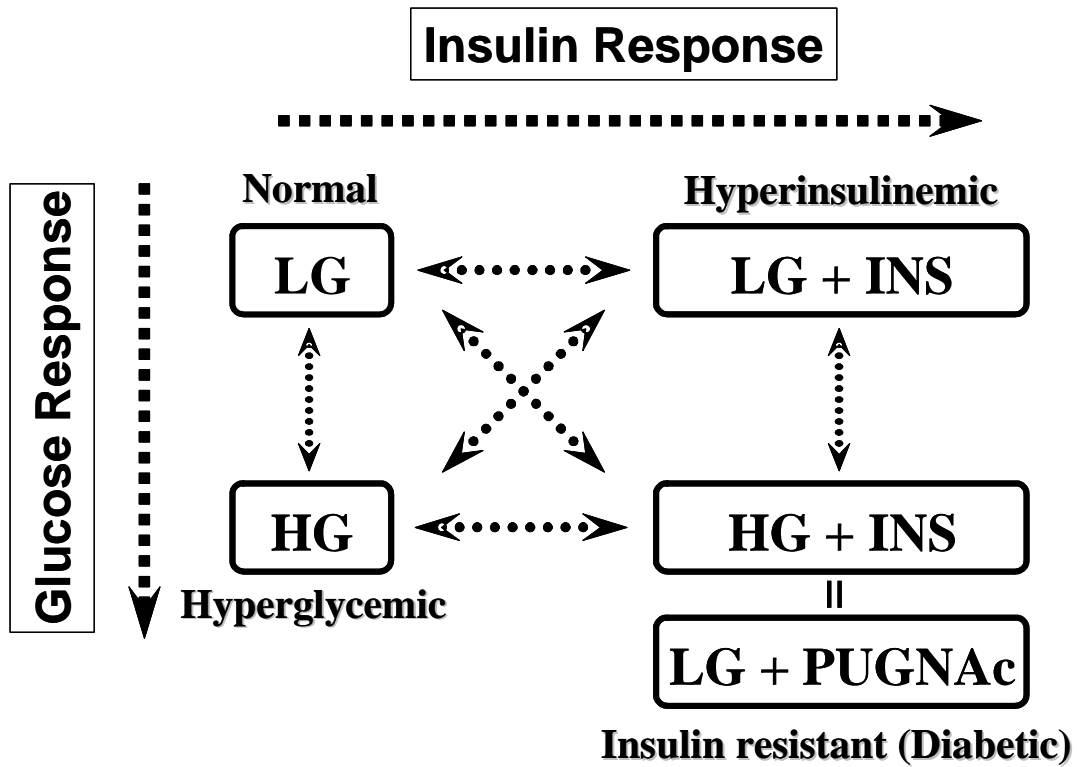


Figure 2-2. Schematic diagram of experimental approach. Adipocytokines are harvested from adipocytes that are insulin responsive (LG, low glucose) or that have been shifted to an insulin resistant state by the addition of PUGNac to elevate O-GlcNAc levels or by the combination of hyperglycemia (HG) and hyperinsulinemia (INS).

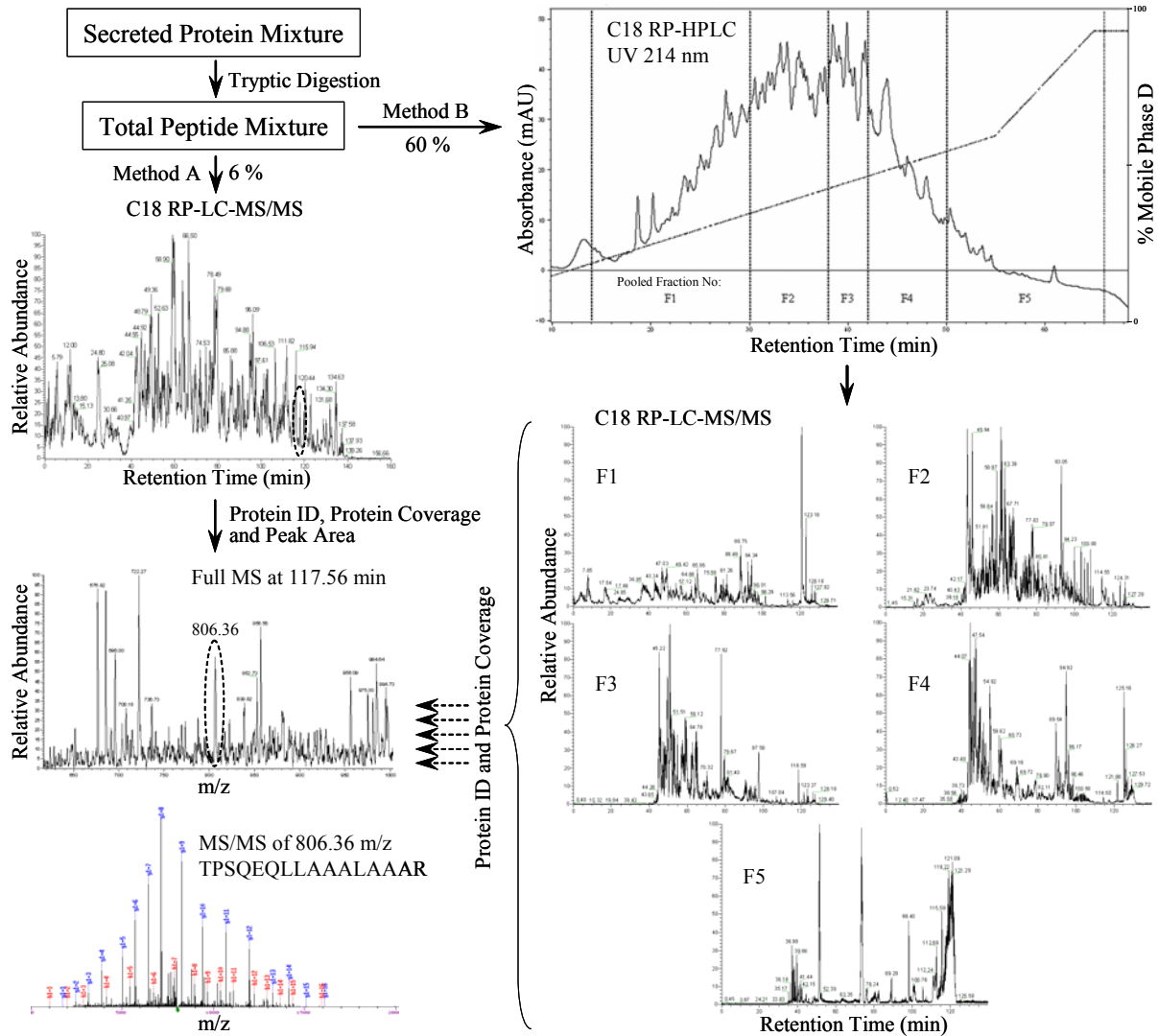


Figure 2-3. Assigning the secreted proteome of adipocytes. Following tryptic digest, the secreted proteome is analyzed by shotgun proteomics and off-line HPLC separation into 5 fractions each followed by LC-MS/MS.

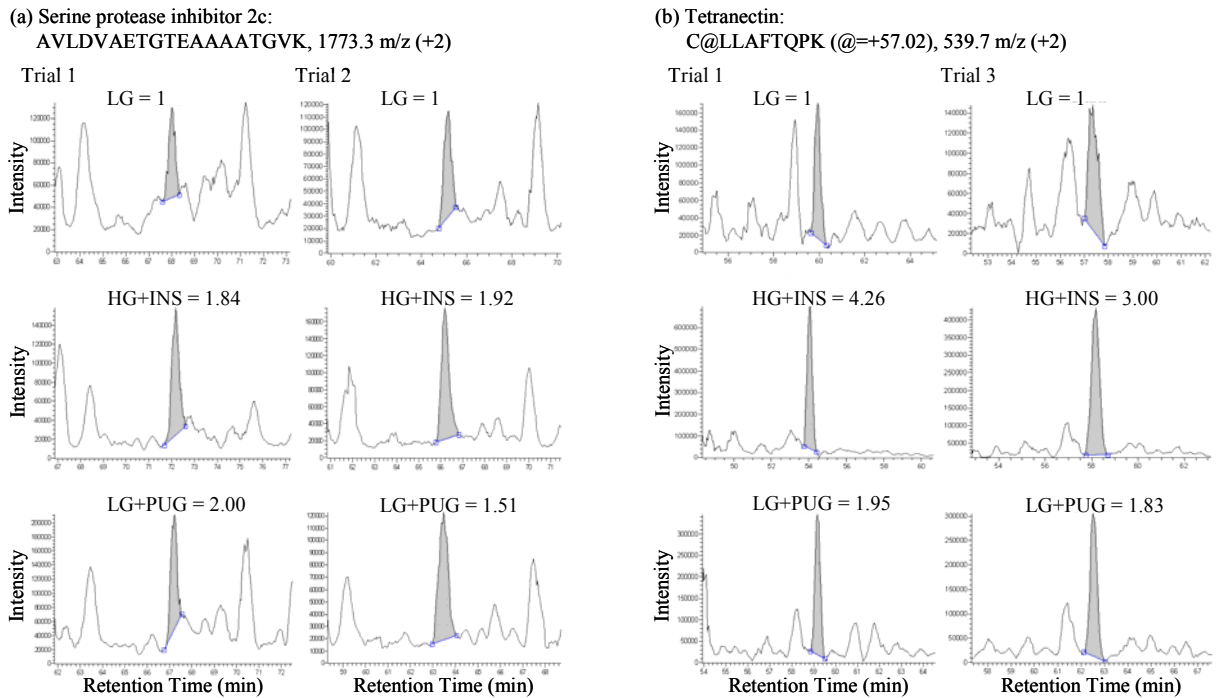


Figure 2-4. Differential secretion of adipocytokines determined by reconstructed ion chromatograms. A peptide from serine protease inhibitor 2C (A) or tetranectin (B) that was isolated and reconstructed from the secreted proteome of rat adipocytes is shown from two different biological replicates and three different culturing conditions. Reconstructed ion chromatograms for both peptides clearly shown an upregulation when the adipocytes are shifted from insulin responsive conditions (LG, normalized to 1.00) to insulin resistant conditions (HG+INS and LG+PUG).

SUPPORTING INFORMATION

Table 2-S1. The list of total secreted proteins identified from modulated 3T3-L1 and 3T3-F442A

Table 2-S2. Mouse adipocytokines regulated by insulin in high glucose

Table 2-S3. Mouse adipocytokines regulated by PUGNAc in low glucose

Table 2-S4. The list of total secreted proteins identified from treated rat primary adipocytes

Table 2-S5. Quantification of secreted proteins from rat primary adipocytes with insulin resistance conditions by LC-MS/MS

Table 2-S6. Comparison of common proteins identified with insulin resistance conditions [(a) and (b)] by RP and RP/RP-LC-MS/MS and by RP and RP/RP-LC-MS/MS with insulin resistance conditions [(c) and (d)]

Table 2-SI. The list of total secreted proteins identified from modulated 3T3-L1 and 3T3-F442A

(a) Protein level.

No.	Gene ID	PSORT Prediction	Signal Peptide	Identified Proteins	Detection	
					3T3-L1	3T3-F442A
1	34328108	exc	N	(pro)collagen, type I, alpha 1*	+	+
2	6680980	exc	N	(pro)collagen, type I, alpha 2 (osteogenesis imperfecta)*	+	+
3	33859526	exc	N	(pro)collagen, type III, alpha 1*	+	+
4	33859528	exc	N	(pro)collagen, type IV, alpha 1*	+	+
5	36031080	mit	N	(pro)collagen, type IV, alpha 2*	+	+
6	7656987	exc	N	(pro)collagen, type V, alpha 1*	+	+
7	6753484	mit	N	(pro)collagen, type VI, alpha 1*	+	+
8	34328185	exc	Y	(pro)saposin	+	+
9	31982423	exc	Y	adiponectin (Acrp30)*	+	+
10	7304867	exc	Y	adipsin (Complement factor D)*	+	+
11	33859506	exc	Y	albumin 1	+	+
12	19705566	exc	Y	angiotensinogen*	+	+
13	47271511	end	N	betaglycan; transforming growth factor (TGF), beta receptor 3	+	+
14	20137008	exc	Y	biglycan	+	+
15	21450325	exc	N	biliverdin reductase B	+	+
16	6681079	end	Y	cathepsin B*	+	+
17	6753556	mit	Y	cathepsin D*	+	+
18	51767794	nuc	N	chondroitin sulfate proteoglycan 2 (Versican)*	+	+
19	51705198	nuc	N	collagen VI, alpha-3 polypeptide*	+	+
20	12963529	cyt	Y	complement component 1, r subcomponent	+	+
21	21450097	exc	Y	complement component 1, s subcomponent*	+	+
22	23956044	exc	N	complement component 3*	+	+
23	6679439 (51770340)	cyt	N	cyclophilin A (peptidylprolyl isomerase A)*	+	+
24	6679441	exc	Y	cyclophilin C (peptidylprolyl isomerase C)*	+	+
25	6681143	exc	Y	decorin	+	+
26	10181164	nuc	Y	fibrinogen/angiopoietin-related protein*	+	+
27	46849812	nuc	N	fibronectin 1	+	+
28	6679757	nuc	N	fibulin 2 (Fbln 2)	+	+

Table 2-SI. Continued.

No.	Gene ID	PSORT Prediction	Signal Peptide	Identified Proteins	Detection	
					3T3-L1	3T3-F442A
29	31560699	exc	Y	follistatin-like 1	+	+
30	28916693	exc	Y	gelsolin*	+	+
31	6680107	exc	Y	granulin (Grn protein, Epithelin 1 & 2)	+	+
32	8850219	end	Y	haptoglobin*	+	+
33	51765519	cyt	N	hippocampal cholinergic neurostimulating peptide*	+	+
34	6981086	exc	Y	insulin-like growth factor binding protein 4	+	+
35	33859490	nuc	N	laminin B1 subunit 1	+	+
36	31791057	nuc	N	laminin B2*	+	+
37	6755144	exc	Y	lectin, galactoside-binding, soluble, 3 binding protein (galectin 3)	+	+
38	34328049	exc	Y	lipocalin 2	+	+
39	6678710	end	Y	lipoprotein lipase*	+	+
40	6754696	cyt	N	macrophage migration inhibitory factor*	+	+
41	6678902	mit	Y	matrix metalloproteinase 2 (collagenase, type IV)*	+	+
42	6754854	cyt	N	nidogen 1 (entactin 1)*	+	+
43	6679058	end	N	nidogen 2*	+	+
44	12963667	exc	Y	Niemann Pick type C2 (epididymal secretory protein 1)*	+	+
45	6754950	exc	Y	orosomuroid 2	+	+
46	7657429	exc	Y	osteoblast specific factor 2 (OSF-2, fasciclin I-like)*	+	+
47	6678077	exc	Y	osteonectin; SPARC*	+	+
48	6754976	cyt	N	peroxiredoxin 1*	+	+
49	31981504	end	Y	pigment epithelium-derived factor (PEDF)*	+	+
50	12963609	end	Y	quiescin Q6	+	+
51	12667798	exc	Y	resistin*	+	+
52	31982800	exc	Y	extracellular matrix protein 2; SPARC-like 1 (mast9, hevyn)*	+	+
53	31981237	cyt	N	thimet oligopeptidase 1	+	+
54	31982755	mit	N	vimentin*	+	+
55	13937349	mit	N	(pro)collagen, type XV	+	-
56	19527008	mit	Y	lysophospholipase 3	+	-
57	7305295	nuc	N	myosin heavy chain 11, smooth muscle	+	-

Table 2-SI. Continued.

No.	Gene ID	PSORT Prediction	Signal Peptide	Identified Proteins	Detection	
					3T3-L1	3T3-F442A
58	6679166	nuc	Y	osteoglycin	+	-
59	22203747	exc	N	(pro)collagen, type VI, alpha 2*	-	+
60	47059082	nuc	N	ADAMTS-1; a disintegrin-like and metalloprotease (reprolysin type) with thrombospondin type 1 motif, 1	-	+
61	22203763	exc	Y	carboxypeptidase E	-	+
62	6753558	exc	Y	cathepsin L	-	+
63	11968166	exc	Y	cathepsin X	-	+
64	6680816	mit	N	complement component 1, q subcomponent	-	+
65	31981822	exc	Y	cystatin C; cystatin 3*	-	+
66	6753642	exc	Y	delta-like 1 homolog	-	+
67	33859532	nuc	Y	dystroglycan 1	-	+
68	31982690	exc	Y	epidermal growth factor (EGF)-containing fibulin-like extracellular matrix protein 2 (Efemp2, fibulin 4)	-	+
69	7657067	exc	Y	ERO1-like (Endoplasmic Reticulum oxidoreductin-1)	-	+
70	6681257	exc	Y	extracellular matrix protein 1 (ECM1)	-	+
71	6806917	end	Y	GM2 ganglioside activator protein	-	+
72	23956086	exc	Y	hemopexin*	-	+
73	6678740	exc	Y	lumican	-	+
74	6678680	exc	Y	lunatic fringe gene homolog	-	+
75	6679158	exc	Y	nucleobindin 1*	-	+
76	21313658	exc	Y	retinoic acid receptor responder (tazarotene induced) 2	-	+
77	38075893	end	N	semaphorin sem2	-	+
78	6755600	end	Y	superoxide dismutase 3, extracellular	-	+
79	7657639	end	Y	transcobalamin 2	-	+

(b) Peptide level.

No.	Gene ID	PSORT Prediction	Signal Peptide	Identified Proteins	Detection	
					3T3-L1	3T3-F442A
1	21553309	mit	Y	apolipoprotein A-I binding protein	+	+
2	31981890	exc	Y	beta-2-microglobulin*	+	+
3	6679182	exc	Y	orosomuroid 1	+	+

Table 2-SI. Continued.

No.	Gene ID	PSORT Prediction	Signal Peptide	Identified Proteins	Detection	
					3T3-L1	3T3-F442A
4	6755112	exc	Y	phospholipid transfer protein	+	+
5	9903607	end	Y	putative secreted protein ZSIG9	+	+
6	33859636	end	Y	serine protease inhibitor 2*	+	+
7	33468851	exc	N	(pro)collagen, type IV, alpha 5	+	-
8	6754570	nuc	N	annexin A1 (Annexin I, lipocortin I)	+	-
9	6680816	mit	N	complement component 1, q subcomponent	+	protein level
10	31981822	exc	Y	cystatin C; cystatin 3	+	protein level
11	19526463	mit	Y	endoplasmic reticulum protein ERp29	+	-
12	31982690	exc	Y	epidermal growth factor (EGF)-containing fibulin-like extracellular matrix protein 2 (Efemp2, fibulin 4)	+	protein level
13	6806917	end	Y	GM2 ganglioside activator protein	+	protein level
14	6679869	exc	Y	insulin-like growth factor binding protein 7*	+	-
15	6680397	nuc	Y	interleukin 12b; IL-12 p40	+	-
16	18250288	end	Y	interleukin 25	+	-
17	6678740	exc	Y	lumican	+	protein level
18	6755600	end	Y	superoxide dismutase 3, extracellular	+	protein level
19	7657639	end	Y	transcobalamin 2	+	protein level
20	8393173	exc	N	(pro)collagen, type V, alpha 3	-	+
21	6755142	end	Y	cyclophilin B (peptidylprolyl isomerase B)	-	+
22	31560691	nuc	N	hepatoma-derived growth factor	-	+
23	6678792	mit	Y	mannosidase alpha class 2B member 2	-	+
24	6755779	nuc	N	thrombospondin 2	-	+
25	31543867	exc	Y	tissue inhibitor of metalloproteinase 2	-	+

* References: 18, 19, 20

Table 2-S2. Mouse adipocytokines regulated by insulin in high glucose

Cell Line	Gene ID	Identified Proteins	LG	HG+I	(HG+I)/LG
3T3-L1	36031080	(pro)collagen, type IV, alpha 2	N.A.	5	[5/0]
	7656987	(pro)collagen, type V, alpha 1	N.A.	6	[6/0]
	6753484	(pro)collagen, type VI, alpha 1	N.A.	18	[18/0]
	6981086	insulin-like growth factor binding protein 4	N.A.	6	[6/0]
	34328049	lipocalin 2	N.A.	26	[26/0]
	31981504	pigment epithelium-derived factor (PEDF)	N.A.	7	[7/0]
	6679757	fibulin 2 (Fbln 2)	2	31	15.5
	20137008	biglycan	2	20	10.0
	33859490	laminin B1 subunit 1	1	10	10.0
	6754854	nidogen 1 (entactin 1)	5	40	8.0
	12963609	quiescin Q6	2	14	7.0
	31982423	adiponectin (Acrp30)	4	23	5.8
	31982800	extracellular matrix protein 2; SPARC-like 1 (mast9, hevin)	2	10	5.0
	6678077	osteonectin; SPARC	7	24	3.4
	23956044	complement component 3	93	287	3.1
	8850219	haptoglobin	16	44	2.8
	51765519	hippocampal cholinergic neurostimulating peptide	5	13	2.6
	6755144	lectin, galactoside-binding, soluble, 3 binding protein (mama)	4	10	2.5
	6680980	(pro)collagen, type I, alpha 2 (osteogenesis imperfecta)	10	4	0.4
	6678902	matrix metalloproteinase 2 (collagenase, type IV)	9	1	0.1
3T3-F442A	34328108	(pro)collagen, type I, alpha 1	N.A.	35	[35/0]
	36031080	(pro)collagen, type IV, alpha 2	N.A.	12	[12/0]
	7656987	(pro)collagen, type V, alpha 1	N.A.	11	[11/0]
	22203747	(pro)collagen, type VI, alpha 2	N.A.	34	[34/0]
	33859506	albumin 1	N.A.	5	[5/0]
	6679439	cyclophilin A (peptidylprolyl isomerase A)	N.A.	9	[9/0]
	31981822	cystatin C; cystatin 3	N.A.	15	[15/0]
	7657067	ERO1-like (Endoplasmic Reticulum oxidoreductin-1)	N.A.	53	[53/0]
	23956086	hemopexin	N.A.	34	[34/0]
	34328049	lipocalin 2	N.A.	9	[9/0]
	7657639	transcobalamin 2	N.A.	5	[5/0]
51705198	collagen VI, alpha-3 polypeptide	8	156	19.5	

Table 2-S2. Continued.

	Gene ID	Identified Proteins	LG	HG+I	(HG+I)/LG
	6753484	(pro)collagen, type VI, alpha 1	7	62	8.9
	12667798	resistin	1	8	8.0
	33859526	(pro)collagen, type III, alpha 1	5	38	7.6
	51767794	chondroitin sulfate proteoglycan 2 (Versican)	4	26	6.5
	47271511	betaglycan; transforming growth factor (TGF), beta receptor 3	1	6	6.0
	12963609	quiescin Q6	8	48	6.0
	6679757	fibulin 2 (Fbln 2)	14	73	5.2
	6981086	insulin-like growth factor binding protein 4	4	20	5.0
3T3- F442A	46849812	fibronectin 1	20	84	4.2
	31982423	adiponectin (Acrp30)	6	24	4.0
	6755144	lectin, galactoside-binding, soluble, 3 binding protein (galectin 3)	8	32	4.0
	19705566	angiotensinogen	9	34	3.8
	23956044	complement component 3	95	357	3.8
	6754854	nidogen 1 (entactin 1)	21	66	3.1
	6678077	osteonectin; SPARC	16	47	2.9
	7304867	adipsin (Complement factor D)	12	34	2.8
	28916693	gelsolin	55	24	0.4
	6678902	matrix metalloproteinase 2 (collagenase, type IV)	7	1	0.1
	31981237	thimet oligopeptidase 1	3	N.A.	[0/3]
	10181164	fibrinogen/angiopoietin-related protein	9	N.A.	[0/9]

Table 2-S3. Mouse adipocytokines regulated by PUGNAc in low glucose

Cell Line	Gene ID	Identified Proteins	LG	LG+PUG	(LG+PUG)/LG
3T3-L1	33859490	laminin B1 subunit 1	1	12	12.0
	6681079	cathepsin B	2	12	6.0
	33859506	albumin 1	2	9	4.5
	31982423	adiponectin (Acrp30)	4	16	4.0
	51765519	hippocampal cholinergic neurostimulating peptide	5	15	3.0
	51705198	collagen VI, alpha-3 polypeptide	18	3	0.2
	33859528	(pro)collagen, type IV, alpha 1	6	N.A.	[0/6]
	8850219	haptoglobin	16	N.A.	[0/16]
	6679158	nucleobindin 1	6	N.A.	[0/6]
3T3-F442A	33859506	albumin 1	N.A.	6	[6/0]
	6679439	cyclophilin A (peptidylprolyl isomerase A)	N.A.	20	[20/0]
	19705566	angiotensinogen	9	28	3.1
	12963609	quiescin Q6	8	23	2.9
	31982423	adiponectin (Acrp30)	6	16	2.7
	51765519	hippocampal cholinergic neurostimulating peptide	5	13	2.6
	31981504	pigment epithelium-derived factor (PEDF)	17	8	0.5
	20137008	biglycan	30	9	0.3
	6679757	fibulin 2 (Fbln 2)	14	4	0.3
	6679158	nucleobindin 1	7	1	0.1
	6678902	matrix metalloproteinase 2 (collagenase, type IV)	7	1	0.1
	6680980	(pro)collagen, type I, alpha 2 (osteogenesis imperfecta)	9	1	0.1
	6679437	cathepsin A	12	N.A.	[0/12]
10181164	fibrinogen/angiopoietin-related protein	9	N.A.	[0/9]	
31560699	follicle-stimulating-like 1	11	N.A.	[0/11]	

Table 2-S4. The list of total secreted proteins identified from treated rat primary adipocytes

(a) Protein level

No.	Gene ID	Identified Proteins	Note
1	5305687	(pro)collagen, alpha-2(I)	*
2	6981424 (38512144)	(pro)saposin	*
3	13242316 (11095299)	ADAMTS-1; a disintegrin and metalloproteinase with thrombospondin motifs 1	*
4	55391508	Albumin	*
5	235879 (6978501)	annexin A1 (Annexin I, lipocortin I)	*
6	34849649	Beta-galactoside-binding lectin (Galectin 1)	*
7	8392983	biglycan	*
8	62665835	collagen isoform 2C2a, type VI, alpha 2	*
9	62665833	collagen, type VI, alpha 1	*
10	62648141	complement component 1, r subcomponent	*
11	54020664	decorin	*
12	34865933	dystroglycan 1	*
13	54400722	epidermal growth factor (EGF)-containing fibulin-like extracellular matrix protein 2 (Efemp2, fibulin 4)	*
14	9506703	fibronectin 1	*
15	55742713	extracellular matrix protein 1 (ECM1)	*
16	62647833	fibulin-2	*
17	13242265	folliculin-like 1	*
18	47939028 (56109)	granulin (Grn protein, Epithelin 1 & 2)	*
19	62656955	insulin-like growth factor-binding protein 4	*
20	62650567	laminin B1 (Laminin beta 3)	*
21	13929190 (20806135, 51859422)	lectin, galactoside-binding, soluble, 3 binding protein (galectin 3)	*
22	13591983	lumican	*
23	16758210	nucleobindin 1	*
24	27683465	osteoglycin	*
25	16758172	quiescin Q6	*
26	11464979	tissue inhibitor of metalloproteinase 2	*
27	11968124	transcobalamin 2	*
28	56711254	(pro)collagen, type III, alpha 1	**
29	59808775	(pro)collagen, type VI, alpha 2; Col6a2	**
30	21307593	adiponectin (Acrp30)	**

Table 2-S4. Continued.

No.	Gene ID	Identified Proteins	Note
31	34862337	adipsin (Complement factor D)	**
32	7549746 (818019)	beta-2-microglobulin	**
33	11693172	calreticulin	**
34	1524328 (62661377)	cathepsin B	**
35	38303993	cathepsin D	**
36	62642714	chondroitin sulfate proteoglycan 2 (Versican)	**
37	38181879 (11127974)	Clusterin; Clu protein	**
38	62662987	collagen alpha 1(IV) chain	**
39	62662985	collagen alpha 2(IV) chain	**
40	19745166	collagen, type V, alpha 1	**
41	20302095 (38303991)	complement component 1, s subcomponent	**
42	50657362 (29789265)	complement component 4a	**
43	56541029 (736290)	cystatin C; cystatin 3	**
44	51854227	gelsolin	**
45	25006237	GM2 activator protein	**
46	61556795	insulin-like growth factor binding protein 7	**
47	62659497	laminin, gamma 1	**
48	22001735	Legumain (Asparaginyl endopeptidase) (Protease, cysteine 1)	**
49	51858619	Lipoprotein lipase	**
50	38181546	Macrophage migration inhibitory factor	**
51	49256641	matrix metalloproteinase 2 (collagenase, type IV)	**
52	1174697	Metalloproteinase inhibitor 1 precursor (TIMP-1)	**
53	62663700	nidogen (1); entactin (1)	**
54	62661058	nidogen 2	**
55	27465565	Niemann Pick type C2 (Epididymal secretory protein 1)	**
56	62643453	osteoblast specific factor 2 (OSF-2, fasciclin I-like)	**
57	2196884	osteonectin; SPARC	**
58	21426805	resistin	**
59	62642230	retinol binding protein 4, plasma	**
60	13928716	serine protease inhibitor 2c	**
61	27721871	tetranectin	**

Table 2-S4. Continued.

No.	Gene ID	Identified Proteins	Note
62	16758644	thioredoxin	**
63	33340123	thrombospondin 1	**
64	57480	vimentin	**
65	4102819	(pro)collagen C-proteinase enhancer protein	***
66	28557685	(pro)collagen lysine, 2-oxoglutarate 5-dioxygenase 2	***
67	62644224	(pro)collagen type XI alpha 1	***
68	6978677	(pro)collagen, type II, alpha 1	***
69	62654019	(pro)collagen, type XII, alpha 1	***
70	16758678	(pro)collagen-lysine, 2-oxoglutarate 5-dioxygenase 1	***
71	28400779	(pro)collagen-lysine, 2-oxoglutarate 5-dioxygenase 3	***
72	53850608	acid sphingomyelinase-like phosphodiesterase 3A	***
73	62660765	AE binding protein 1	***
74	11990616	aggrecan 1	***
75	28932816	alpha-2 antiplasmin; serine (or cysteine) proteinase inhibitor, clade F, member 1	***
76	27436861 (930262)	amyloid beta (A4) protein; Beta-amyloid peptide	***
77	40018598	angiopoietin-like protein 4	***
78	2143593	annexin II (calpactin 1)	***
79	20301954 (37805241)	apolipoprotein E	***
80	58476724	Biotinidase (predicted)	***
81	62661703	bone morphogenetic protein 1 (procollagen C-proetinase)	***
82	20302073	cadherin 13	***
83	62645871	Carboxypeptidase X 1 (M14 family); Metalloproteinase CPX-1	***
84	4558458	Chitinase 3 like 1; glycoprotein-39	***
85	62653824	Cilp protein (Cartilage intermediate layer protein)	***
86	27688933	collagen alpha1	***
87	62655388	collagen isoform 1, type VI, alpha 3	***
88	4995838	collagen type XVIII, alpha (I) chain	***
89	3164123 (62655017)	collagen, type V, alpha 2	***
90	62648968	collagen, type XV	***
91	22255878	colony stimulating factor-1 (macrophage)	***
92	28570180	complement component 6	***

Table 2-S4. Continued.

No.	Gene ID	Identified Proteins	Note
93	62642976	complement component 7	***
94	25244377	complement component C2	***
95	11560085 (4753900)	connective tissue growth factor	***
96	1213217	Cu/Zn superoxide dismutase (SOD 1)	***
97	33086684	Da1-24; Complement factors B (B-factor, properdin)	***
98	19924047	dickkopf homolog 3 (Dickkopf-3)	***
99	27677818	early quiescence protein-1	***
100	34863280	Elastin microfibril interfacier 1 (EMILIN 1)	***
101	12018274	endothelial cell-specific molecule 1	***
102	58865654 (9973135)	epidermal growth factor (EGF)-containing fibulin-like extracellular matrix protein 1 (Fibulin-3)	***
103	394739	epididymal secretory superoxide dismutase	***
104	13929178	fibrillin 1	***
105	42476116	fibulin 5	***
106	62652879	Fibulin-1 (Basement-membrane protein 90)	***
107	24210470	fibulin-2 isoform a	***
108	62665389	Galactosamine (N-acetyl)-6-sulfate sulfatase	***
109	34861992	Glutaminyl-peptide cyclotransferase (QC) (Glutaminyl-tRNA cyclotransferase) (Glutaminyl cyclase)	***
110	6970046	GPI-anchored ceruloplasmin	***
111	28849947	hemiferrin, transferrin-like protein	***
112	62649892	heparan sulfate proteoglycan 2 (perlecan)	***
113	62663812	inter-alpha-inhibitor H2 chain (Inter alpha trypsin inhibitor, heavy chain 2)	***
114	13591914	kidney aminopeptidase M (aminopeptidase N)	***
115	62666140	Laminin alpha-4 chain	***
116	56788965	Laminin, beta-2; Lamb2 protein	***
117	62638338	laminin-2 alpha2 chain	***
118	11136636	latent transforming growth factor beta binding protein 2 (Latent TGF beta binding protein 2)	***
119	62652278	lipoprotein receptor-related protein	***
120	62664372	lysyl oxidase	***
121	62655863	M6PR domain containing protein 1	***
122	27527940 (25244444)	MASP-3 protein (mannan-binding lectin serine peptidase 1, MASP 1/3)	***
123	127076	Matrix Gla-protein (MGP)	***

Table 2-S4. Continued.

No.	Gene ID	Identified Proteins	Note
124	62651656	matrix metalloproteinase 19	***
125	27672001	microfibrillar-associated protein 4	***
126	6981200	milk fat globule-EGF factor 8 protein	***
127	11072106 (14549433)	nucleobindin 2	***
128	62644339	Olfactomedin-like 3	***
129	1871124 (205860)	osteopontin (secreted phosphoprotein 1)	***
130	62646367	Phospholipid transfer protein	***
131	13928880	plasma glutamate carboxypeptidase	***
132	62649105	pregnancy-associated plasma protein-A	***
133	51859442	Protease, serine, 11	***
134	1041904	protein S	***
135	62339361	retinoic acid receptor responder (tazarotene induced) 1	***
136	47477890	Ribonuclease, RNase A family 4	***
137	40018558	serine (or cysteine) proteinase inhibitor, clade G (C1 inhibitor), member 1, (angioedema, hereditary)	***
138	19173736	serine carboxypeptidase 1 (Retinoid-inducible serine carboxypeptidase)	***
139	30027645	short isoform growth hormone receptor	***
140	13786142	slit homolog 3	***
141	62640996 (25453372)	spondin 1	***
142	34880777	tenascin-N	***
143	8394446	betaglycan; transforming growth factor (TGF), beta receptor 3	***
144	57472 (58476812)	Vascular cell adhesion molecule 1	***
145	3309591	versican V3 isoform	***
146	38649303	Wfdc1 protein (WAP four-disulfide core domain 1); Prostate stromal protein ps20	***

(b) Peptide level

No.	Gene ID	Identified Peptides	Note
1	51948402	cyclophilin C (peptidylprolyl isomerase C)	*
2	6981568	superoxide dismutase 3, extracellular	*
3	19424254	angiopoietin-like 2	**
4	59808182	haptoglobin	**

Table 2-S4. Continued.

No.	Gene ID	Identified Peptides	Note
5	50400208	Interleukin-4 receptor alpha chain (IL-4R-alpha)	**
6	27676342	Macrophage migration inhibitory factor (MIF)	**
7	38677995	resistin	**
8	4519515	(pro)collagen C-proteinase 3	***
9	62900635	(Pro)collagen-lysine,2-oxoglutarate 5-dioxygenase 2 (Lysyl hydroxylase 2) (LH2)	***
10	37048700	ADAMTS-5; a disintegrin-like and metalloprotease (reprolysin type) with thrombospondin type 1 motif 5 (aggrecanase-2)	***
11	3776238	aminopeptidase N (CD13)	***
12	34867707	Arylsulfatase A (ASA) (Cerebroside-sulfatase)	***
13	10800128	beta ig-h3 (TGFBI transforming growth factor, beta-induced, 68kDa)	***
14	62653568	C1q and tumor necrosis factor related protein 5	***
15	13928758	cathepsin K	***
16	60688149	Cathepsin Y	***
17	1262920	CD14; a myeloid cell-surface receptor and soluble plasma protein	***
18	8393087	cell adhesion molecule-related/down-regulated by oncogenes (Cdon)	***
19	20806123	cell growth regulator with EF hand domain 1	***
20	13929074	c-fos induced growth factor (Vascular endothelial growth factor D precursor (VEGF-D), FIGF)	***
21	62658149	chordin	***
22	62643068 (62662017)	Cln5 protein (Ceroid-lipofuscinosis, neuronal 5)	***
23	62652432	collagen type XIV	***
24	6007583	collagen XVIII	***
25	11120710	collagen, type V, alpha 3	***
26	29373916	collagen, type XXIII , alpha 1	***
27	38541053	cyclophilin B (peptidylprolyl isomerase B)	***
28	2288921	DRM protein (Down-regulated in Mos-transformed cells protein); Gremlin	***
29	51859271	Ectonucleotide pyrophosphatase/phosphodiesterase 2 (Enpp2 protein)	***
30	4583509	embryonic vascular EGF repeat-containing protein EVEC	***
31	56090361	ependymin related protein 2	***
32	18104933	fibromodulin	***
33	30841840	follistatin 288 variant	***
34	2564302	GDNFR-alpha/TrnR1-delta protein	***

Table 2-S4. Continued.

No.	Gene ID	Identified Peptides	Note
35	62655235	Glb11 protein (galactosidase, beta 1-like)	***
36	38181579	Gpc1 protein (Glypican 1)	***
37	47477840	Growth arrest specific 6 (Gas6 protein)	***
38	47718020	Interleukin 1 receptor antagonist (Il1rn protein)	***
39	6981590	interleukin 1 receptor-like 1	***
40	58400808	Lysyl oxidase-like 1 (predicted)	***
41	12275390	membrane attractin	***
42	1228089	multifunctional acyl-CoA-binding protein (diazepam binding inhibitor)	***
43	41054820	neurogenesis 1	***
44	4468965	NG2 proteoglycan	***
45	47477878	Plasma glutamate carboxypeptidase (Pgcp protein)	***
46	16758116	proline arginine-rich end leucine-rich repeat protein	***
47	34882048	protein S (alpha)	***
48	62638555	Ribonuclease T2 (Ribonuclease 6)	***
49	62662853	secreted frizzled-related protein 1	***
50	16758312	secreted frizzled-related protein 4	***
51	62646703	Semaphorin 3C	***
52	50811823	Spinal cord injury-related protein 10 (SCIRP10-related protein); Neuron-derived neurotrophic factor	***
53	11610601	spinal-cord derived growth factor-B (Platelet derived growth factor D)	***
54	11560026	stanniocalcin 2	***
55	62657881	steroid-sensitive protein 1 (<i>Urb</i> protein)	***
56	62648889	talin	***
57	30385204 (34877064, 62658399)	Tumor protein, translationally-controlled 1 (Lens epithelial protein)	***

* 3T3-L1 and 3T3-F442A cell lines, ** rat primary adipose cell line, and *** novel proteins identified.

Table 2-S5. Quantification of secreted proteins from rat primary adipocytes with insulin resistance conditions by LC-MS/MS

(a) Classical insulin resistance condition

Gene ID	Identified Proteins	Unique peps		Ratio of protein coverage	Common peps	Ratio of peak area	↑↓
		HG+I	LG				
3164123	collagen, type V, alpha 2	4	N.A.	[4/0]	N.A.	N.A.	+
59808182	haptoglobin	3	N.A.	[3/0]	N.A.	N.A.	+
56541029	cystatin C; cystatin 3	2	N.A.	[2/0]	N.A.	N.A.	+
62640996	spondin 1	3	N.A.	[3/0]	N.A.	N.A.	+
51858619	Lipoprotein lipase	6	1	6.00	ITGLDPAGPNFEYAEAPSR	5.23	+
27721871	tetranectin	16	3	5.33	CLLAFTQPK	3.59	+
					AENCAALSGAANGK	1.36	
62642230	retinol binding protein 4, plasma	16	3	5.33	FSGLWYAIK	5.53	+
					YWGVASFLQR	4.57	
					LQNLDTGTCADSYSFVFSR	2.09	
13928716	serine protease inhibitor 2c	18	6	3.00	AVLDVAETGTEAAAATGVK	1.88	+
					KLINDYVSK	2.07	
					ALYQAEAFADTFQQR	3.50	
51854227	gelsolin	6	2	3.00	QTQVSVLPEGGETPLFK	0.91	+
62655388	collagen isoform 1, type VI, alpha 3	28	10	2.80	LLTPITTLTSQQIQQILASTR	1.50	+
					VGLVQYNSDPTDEFFLR	1.45	
394739	epididymal secretory superoxide dismutase	4	2	2.00	LACCVVGTNSSEAWESQTK	1.45	+
62661377	cathepsin B	13	7	1.86	NGPVEGAFTVFSDFLYK	2.18	+
					VGFSEDINLPESFDAR	2.82	+
62662987	collagen alpha 1(IV) chain	12	7	1.71	VVPLPGPPGAAGLPGSPGFPQPQ	1.21	+
					DR		
27465565	Niemann Pick type C2 (Epididymal secretory protein 1)	5	3	1.67	DNLFCWEIPVEIKG	1.36	+
					CGINCPQK	5.13	
25006237	GM2 activator protein	8	5	1.60	SLTLQPDPIVVPGDVIVSAEGK	1.71	+
11464979	tissue inhibitor of metalloproteinase 2	16	10	1.60	EVDSGNDIYGNPIKR	1.48	+
					GAAPPKQEFLDIEDP	1.21	
					AVSEKEVDSGNDIYGNPIKR	2.13	

Table 2-S5. Continued.

Gene ID	Identified Proteins	Unique peps		Ratio of protein coverage	Common peps	Ratio of peak area	↑↓
		HG+I	LG				
21307593	adiponectin (Acrp30)	6	4	1.50	AVLFTYDQYQEK VTVPNVPIR	1.58 14.36	+
11095299	ADAMTS-1; a disintegrin and metalloproteinase with thrombospondin motifs 1	3	2	1.50	N.A. LQPDSGFLAPGFTLQTVGR	N.A. 1.22	+
1213217	Cu/Zn superoxide dismutase (SOD 1)	N.A.	4	[0/4]	N.A.	N.A.	-
11560085	connective tissue growth factor	N.A.	5	[0/5]	N.A.	N.A.	-
13786142	slit homolog 3	N.A.	7	[0/7]	N.A.	N.A.	-
24210470	fibulin-2 isoform a	N.A.	12	[0/12]	N.A.	N.A.	-
38303993	cathepsin D	N.A.	5	[0/5]	N.A.	N.A.	-
6978677	(pro)collagen, type II, alpha 1	2	8	0.25	N.A.	N.A.	-
19173736	serine carboxypeptidase 1 (Retinoid-inducible serine carboxypeptidase)	4	14	0.29	GLAEVSDIAEQVLNAVNK EVWDYVTVR	0.34 0.65	-
34849649	Beta-galactoside-binding lectin (Galectin 1)	2	7	0.29	DDGTWGTEQR DSNNLCLHFNPR	0.22 0.49	-
62646367	Phospholipid transfer protein	2	5	0.40	FLEQELEDINIPDVYGAK	0.73	-
38181879	Clusterin; Clu protein	6	14	0.43	IDSLES DR LFSDPITVVLPEEVSK	0.18 2.26	-
38303991	complement component 1, s subcomponent	9	21	0.43	NQQFGPYCGNGFPGPLTIK MGPTVAPICLPETSSDYNPSEGD LG LISGWGR	1.45 0.45	-
62649892	heparan sulfate proteoglycan 2 (perlecan)	27	59	0.46	YELGSG LAVLR AQAGANTRPCPS SPGPNVAVNTK	0.49 1.23 0.49	-
16758644	thioredoxin	2	4	0.50	EAFQEALAAAGDK	0.64	-
51859442	Protease, serine, 11	2	4	0.50	GACGQGQEDPNSLR YNFIADVVEK FLNKEPY	0.61 0.57 0.81	-
47939028	granulin (Grn protein, Epithelin 1 & 2)	10	18	0.56	LNTGAWGCCPFTK	0.61	-

Table 2-S5. Continued.

Gene ID	Identified Proteins	Unique peps		Ratio of protein coverage	Common peps	Ratio of peak area	↑↓
		HG+I	LG				
19924047	dickkopf homolog 3 (Dickkopf-3)	3	5	0.60	DCQPGLCCAFQR	0.85	-
38512144	(pro)saposin	15	24	0.63	LGPGVSDICK	0.76	-
					ICSGGSVVCR	0.43	
					LVTDIQTAVR	0.52	
19745166	collagen, type V, alpha 1	13	20	0.65	SSKEPDVAYR	0.50	-
8394446	betaglycan; transforming growth factor (TGF), beta receptor 3	4	6	0.67	NFLSLNYLAEYLQPK	0.55	-

(b) Elevated O-GlcNAc level-induced insulin resistance condition

Gene ID	Identified Proteins	Unique peps		Ratio of protein coverage	Common peps	Ratio of peak area	↑↓
		LG+PUG	LG				
6981424	(pro)saposin	9	N.A.	[9/0]	N.A.	N.A.	+
11693172	calreticulin	2	N.A.	[2/0]	N.A.	N.A.	+
13242316	ADAMTS-1; a disintegrin and metalloproteinase with thrombospondin motifs 1	2	N.A.	[2/0]	N.A.	N.A.	+
27683465	osteoglycin	3	N.A.	[3/0]	N.A.	N.A.	+
28400779	(pro)collagen-lysine, 2-oxoglutarate 5-dioxygenase 3	2	N.A.	[2/0]	N.A.	N.A.	+
62640996	spondin 1	5	N.A.	[5/0]	N.A.	N.A.	+
62661377	cathepsin B	23	7	3.29	NGPVEGAFTVFSDFLYK	2.08	+
27721871	tetranectin	9	3	3.00	CLLAFTQPK	1.89	+
62653388	collagen isoform 1, type VI, alpha 3	29	10	2.90	NANPSELEQIVPSPAFILAAESLPK	1.31	+
61556795	insulin-like growth factor binding protein 7	11	4	2.75	VYLSCEVIGIPTPVLINWK	2.84	+
51854227	gelsolin	5	2	2.50	QTQVSVLPEGGETPLFK	1.29	+
62643453	osteoblast specific factor 2 (OSF-2, fasciclin I-like)	40	18	2.22	GFEPGVTNLIK	1.39	+
394739	epididymal secretory superoxide dismutase	4	2	2.00	VQPSAMLPPDQPQITGLVLFRR	7.47	+
11464979	tissue inhibitor of metalloproteinase 2	20	10	2.00	EVDSGNDIYGNPIKR	1.44	+
13928880	plasma glutamate carboxypeptidase	4	2	2.00	VGAVASLIR	1.45	+
				2.00	LGLLVDTVGPR	1.14	+

Table 2-S5. Continued.

Gene ID	Identified Proteins	Unique peps		Ratio of protein coverage	Common peps	Ratio of peak area	↑↓
		LG+PUG	LG				
27465565	Niemann Pick type C2 (Epididymal secretory protein 1)	6	3	2.00	DNLFCWEIPVEIKG	1.67	+
51858619	Lipoprotein lipase	2	1	2.00	ITGLDPAGPNFEYAEAPSR	1.28	+
62644339	Olfactomedin-like 3	2	1	2.00	LDPQTLTDEQQWDTPCPR	1.77	+
62665835	collagen isoform 2C2a, type VI, alpha 2	22	11	2.00	NLEWIAGGTWTPSALK	1.07	+
					GPQGALGEPGK	1.48	
11560085	connective tissue growth factor	9	5	1.80	DGAPCVFVGGSVYR	2.19	+
38303993	cathepsin D	9	5	1.80	VSSLPIITFK	1.59	+
59808775	(pro)collagen, type VI, alpha 2; Col6a2	17	10	1.70	RFVEEVSR	1.00	+
13928716	serine protease inhibitor 2c	10	6	1.67	AVLDVAETGTEAAAATGVK	1.74	+
62660765	AE binding protein 1	21	13	1.62	VVNEECPTITR	1.62	+
					TPSQEQLLAAALAAAR	1.49	
38181879	Clusterin; Clu protein	17	11	1.55	LFSDPITVVLPEEVSKDNPK	1.07	+
					CQEILSVDCSTNNPAQANLR	1.29	
13929178	fibrillin 1	41	27	1.52	AGYQSTLTR	0.73	+
					CECFPGLAVGLDGR	3.62	+
1213217	Cu/Zn superoxide dismutase (SOD 1)	6	4	1.50	HVGD LGNVAAGK	0.88	+
34862337	adipsin (Complement factor D)	15	10	1.50	DEVVQVLLGAHSLSSPEPYK	1.78	+
38181546	Macrophage migration inhibitory factor	3	2	1.50	ASVPEGFLSEL TQQLAQATGK	1.37	+
8392983	biglycan	65	44	1.50	AYYNGISLFNPNVPYWEVQPATFR	1.77	+
16758644	thioredoxin	N.A.	4	[0/4]	N.A.	N.A.	-
127076	Matrix Gla-protein (MGP)	1	4	0.25	NANTFISPQQR	0.31	-
51859442	Protease, serine, 11	1	4	0.25	N.A.	N.A.	-
13786142	slit homolog 3	2	7	0.29	QPAVGINSPLYLGGIPTSTGLSALR	0.39	-
24210470	fibulin-2 isoform a	4	12	0.33	TCRPDGGAPQLDTAR	0.61	-
6978677	(pro)collagen, type II, alpha 1	4	8	0.50	GAQGPPGATGFPGAAGR	0.66	-
8394446	betaglycan; transforming growth factor (TGF), beta receptor 3	3	6	0.50	NFLSLNYLAEYLQPK	0.30	-

Table 2-S6. Comparison of common proteins identified with insulin resistance conditions [(a) and (b)] by RP and RP/RP-LC-MS/MS and by RP and RP/RP-LC-MS/MS with insulin resistance conditions [(c) and (d)]

(a) Common proteins between insulin resistance conditions with RP

Gene ID	Identified Proteins	Unique peps		Ratio of protein coverage	Unique peps		Ratio of protein coverage	↑↓
		HG+I	LG		LG+PUG	LG		
62640996	spondin 1	3	N.A.	[3/0]	5	N.A.	[5/0]	+
51858619	Lipoprotein lipase	6	1	6.00	2	1	2.00	+
27721871	tetranectin	16	3	5.33	9	3	3.00	+
13928716	serine protease inhibitor 2c	18	6	3.00	10	6	1.67	+
51854227	gelsolin	6	2	3.00	5	2	2.50	+
62655388	collagen isoform 1, type VI, alpha 3	28	10	2.80	29	10	2.90	+
394739	epididymal secretory superoxide dismutase	4	2	2.00	4	2	2.00	+
62661377	cathepsin B	13	7	1.86	23	7	3.29	+
27465565	Niemann Pick type C2 (Epididymal secretory protein 1)	5	3	1.67	6	3	2.00	+
11464979	tissue inhibitor of metalloproteinase 2	16	10	1.60	20	10	2.00	+
13786142	slit homolog 3	N.A.	7	[0/7]	2	7	0.29	-
24210470	fibulin-2 isoform a	N.A.	12	[0/12]	4	12	0.33	-
6978677	(pro)collagen, type II, alpha 1	2	8	0.25	4	8	0.50	-
8394446	betaglycan; transforming growth factor (TGF), beta receptor 3	4	6	0.67	3	6	0.50	-
16758644	thioredoxin	2	4	0.50	N.A.	4	[0/4]	-
51859442	Protease, serine, 11	2	4	0.50	1	4	0.25	-

(b) Common proteins between insulin resistance conditions with RP/RP

Gene ID	Identified Proteins	Unique peps		Ratio of protein coverage	Unique peps		Ratio of protein coverage	↑↓
		HG+I	LG		LG+PUG	LG		
28570180	complement component 6	12	2	6.00	6	2	3.00	+
4558458	Chitinase 3 like 1; glycoprotein-39	11	4	2.75	12	4	3.00	+
1041904	protein S	13	5	2.60	10	5	2.00	+
27721871	tetranectin	27	11	2.45	16	11	1.50	+
13928716	serine protease inhibitor 2c	24	10	2.40	15	10	1.50	+

Table 2-S6. Continued.

Gene ID	Identified Proteins	Unique peps		Ratio of protein coverage	Unique peps		Ratio of protein coverage	↑↓
		HG+I	LG		LG+PUG	LG		
6970046	GPI-anchored ceruloplasmin	7	3	2.33	6	3	2.00	+
27527940	MASP-3 protein (mannan-binding lectin serine peptidase 1, MASP 1/3)	12	6	2.00	9	6	1.50	+
38181879	Clusterin; Clu protein	38	21	1.81	31	21	1.50	+
8394446	betaglycan; transforming growth factor (TGF), beta receptor 3	9	5	1.80	8	5	1.60	+
11464979	tissue inhibitor of metalloproteinase 2	15	9	1.67	14	9	1.56	+
21307593	adiponectin (Acrp30)	5	3	1.67	6	3	2.00	+
13929178	fibrillin 1	66	41	1.61	61	41	1.50	+
34849649	Beta-galactoside-binding lectin (Galectin 1)	8	5	1.60	8	5	1.60	+
51858619	Lipoprotein lipase	8	5	1.60	8	5	1.60	+
62662985	collagen alpha 2(IV) chain	11	7	1.57	11	7	1.57	+
7549746	beta-2-microglobulin	6	4	1.50	6	4	1.50	+
13591914	kidney aminopeptidase M (aminopeptidase N)	3	2	1.50	3	2	1.50	+
47477890	Ribonuclease, RNase A family 4	3	2	1.50	3	2	1.50	+
13786142	slit homolog 3	5	11	0.45	7	11	0.64	-
19173736	serine carboxypeptidase 1 (Retinoid-inducible serine carboxypeptidase)	5	10	0.50	5	10	0.50	-

(c) Common proteins between RP and RP/RP with (High Glucose + Insulin)/Low Glucose

Gene ID	Identified Proteins	RP			RP/RP			↑↓
		Unique peps		Ratio of protein coverage	Unique peps		Ratio of protein coverage	
		HG+I	LG		HG+I	LG		
56541029	cystatin C; cystatin 3	2	N.A.	[2/0]	9	5	1.80	+
59808182	haptoglobin	3	N.A.	[3/0]	2	N.A.	[2/0]	+
62640996	spondin 1	3	N.A.	[3/0]	19	13	1.50	+
51858619	Lipoprotein lipase	6	1	6.00	8	5	1.60	+
27721871	tetranectin	16	3	5.33	27	11	2.45	+
62642230	retinol binding protein 4, plasma	16	3	5.33	16	5	3.20	+
13928716	serine protease inhibitor 2c	18	6	3.00	24	10	2.40	+
62661377	cathepsin B	13	7	1.86	15	10	1.50	+

Table 2-S6. Continued.

Gene ID	Identified Proteins	RP			RP/RP			↑↓
		Unique peps		Ratio of protein coverage	Unique peps		Ratio of protein coverage	
		HG+I	LG		HG+I	LG		
62662987	collagen alpha 1(IV) chain	12	7	1.71	9	5	1.80	+
11464979	tissue inhibitor of metalloproteinase 2	16	10	1.60	15	9	1.67	+
25006237	GM2 activator protein	8	5	1.60	7	4	1.75	+
21307593	adiponectin (Acrp30)	6	4	1.50	5	3	1.67	+
62661058	nidogen 2	3	2	1.50	12	8	1.50	+
1213217	Cu/Zn superoxide dismutase (SOD 1)	N.A.	4	[0/4]	3	5	0.60	-
13786142	slit homolog 3	N.A.	7	[0/7]	5	11	0.45	-
24210470	fibulin-2 isoform a	N.A.	12	[0/12]	4	7	0.57	-
19173736	serine carboxypeptidase 1 (Retinoid-inducible serine carboxypeptidase)	4	14	0.29	5	10	0.50	-

(d) Common proteins between RP and RP/RP with (Low Glucose + PUGNAc)/Low Glucose

Gene ID	Identified Proteins	RP			RP/RP			↑↓
		Unique peps		Ratio of protein coverage	Unique peps		Ratio of protein coverage	
		LG+PUG	LG		LG+PUG	LG		
27683465	osteoglycin	3	N.A.	[3/0]	2	N.A.	[2/0]	+
27721871	tetranectin	9	3	3.00	16	11	1.50	+
62655388	collagen isoform 1, type VI, alpha 3	29	10	2.90	54	37	1.50	+
61556795	insulin-like growth factor binding protein 7	11	4	2.75	15	9	1.67	+
27465565	Niemann Pick type C2 (Epididymal secretory protein 1)	6	3	2.00	4	2	2.00	+
51858619	Lipoprotein lipase	2	1	2.00	8	5	1.60	+
11464979	tissue inhibitor of metalloproteinase 2	20	10	2.00	14	9	1.56	+
13928716	serine protease inhibitor 2c	10	6	1.67	15	10	1.50	+
38181879	Clusterin; Clu protein	17	11	1.55	31	21	1.50	+
13929178	fibrillin 1	41	27	1.52	61	41	1.50	+
38181546	Macrophage migration inhibitory factor	3	2	1.50	5	3	1.67	+
16758644	thioredoxin	N.A.	4	[0/4]	2	3	0.67	-
13786142	slit homolog 3	2	7	0.29	7	11	0.64	-

CHAPTER 3

QUANTITATIVE SECRETOME AND GLYCOME OF PRIMARY HUMAN ADIPOCYTES UNDER INSULIN RESISTANT CONDITIONS

Jae-Min Lim, Chin Fen Teo, Dorothy B. Hausman and Lance Wells, Quantitative secretome and glycome of primary human adipocytes under insulin resistant conditions, To be submitted to *Molecular & Cellular Proteomics*.

ABSTRACT

Insulin resistance, characterized by impairment in insulin-mediated signaling, is a prerequisite condition for the disease progression of type 2 diabetes. Under this condition, the insulin responsive cells such as adipocytes and skeletal muscle cells fail to execute blood glucose clearance upon insulin stimulation and eventually lead to pancreatic beta-cell dysfunction. Prolonged hyperglycemia and hyperinsulinemia are both required for the development of classical insulin resistance. In recent years, accumulative evidence has established that, direct elevated O-GlcNAc levels via either genetic or pharmacological methods lead to insulin resistance in both cultured adipocytes and animal models (non-canonical insulin resistance). While adipocytes have long been considered as an important tissue for energy storage, recent studies have revealed that adipose tissue is also a major endocrine gland releasing a broad spectrum of proteins, termed adipocytokines or adipokines. In this study, we aimed at addressing the quantitative secretome of human primary adipocytes under insulin responsive and two insulin resistant conditions by using a shotgun proteomic approach. Of the 190 secreted proteins identified, we report 20 up-regulated and 6 down-regulated proteins detected in both insulin resistant conditions. Moreover, we applied glycomic techniques to examine (A) the N-glycan structures and sites from the pool of secreted proteins and (B) the relative abundance of complex N- and O-glycans structures released from adipocytes exposed to different conditions. We identified 91 N-glycosylation sites on the secreted proteins derived from 51 proteins, as well as 155 and 29 released N- and O-glycans respectively. There were moderate alterations in the observed N- and O-linked glycan structures under the different conditions by $^{13}\text{C}/^{12}\text{C}$ ratios from sum of peak area and prevalence ratios.

Keywords: O-GlcNAc, insulin resistance, type 2 diabetes, metabolic syndrome, adipocytokine, tandem mass spectrometry, shotgun proteomics, glycosylation, glycomics, N-linked, O-linked

3.1. INTRODUCTION

Type 2 diabetes, which accounts for the vast majority cases of diabetes mellitus, generally arises from the presence of insulin resistance (a combination of chronic hyperglycemia and hyperinsulinemia conditions) and pancreatic beta-cells dysfunction (1). At the molecular levels, insulin resistance is due to a defect in insulin signaling in target tissues. The development of insulin resistance in peripheral tissue such as skeletal muscle and adipocytes is an early defect in the pathogenesis of type 2 diabetes. Adipocytes are known to secrete a variety of cytokines, termed adipocytokines and some of these (e.g. leptin, adiponectin and resistin) can modulate insulin sensitivity and other metabolic disorders associated with diabetes (2, 3). Thus, changes of these adipocytokines in adipocytes could represent a key role in predisposition to diabetes and related diseases.

The increased prevalence of type 2 diabetes is largely correlated to excessive caloric intake which is reflected in an induction of insulin resistance (4). In this condition, adipocytes become desensitized to the biological effects of insulin. In the body, 2 to 5% of incoming glucose enters the hexosamine biosynthetic pathway (HBP), whose final product is the upstream precursor for the formation of O-linked β -N-acetylglucosamine (O-GlcNAc) modification of the serine and threonine residues of intracellular proteins (5). Marshall and colleagues (6, 7) demonstrated that prolonged incubation of adipocytes with insulin, glucose, and glutamine resulted in desensitization of glucose transport. This phenomenon has been further supported by

McClain *et al.* (8) using animal models to be one of the key mechanisms responsible for “glucose toxicity” (9, 10). Patti *et al.* also reported that the glucosamine-induced insulin resistance is closely associated with increased in O-GlcNAc modified proteins in rat skeletal muscle (11). In addition, administration of PUGNAc [O-(2-acetamido-2-deoxy-D-glucopyranosylidene)amino-N-phenylcarbamate], a GlcNAc mimetic and potent inhibitor of O-GlcNAcase, globally elevated intracellular O-GlcNAc levels (12) caused insulin resistance in 3T3-L1 adipocytes (13), rat skeletal muscle (14) and rat primary adipocytes (15). From signaling perspectives, many proteins can be O-GlcNAc modified under insulin resistant condition. For instance, Vosseller *et al.* demonstrated that elevated O-GlcNAc levels associated with insulin resistance was detected in 3T3-L1 adipocytes as a reduction in insulin signaling (13). Also, multiple groups have reported that proteins involved in the insulin signaling pathway are O-GlcNAcylated (15, 16).

While HBP and chronic hyperinsulinemia or O-GlcNAc mediated insulin resistance have long been studied in the intracellular signaling context, we are particularly interested in comparing secreted adipocytokine levels under these conditions. To address this issue, we examined the secretome in primary human adipocytes with both classically induced-insulin resistant (chronic hyperglycemia and hyperinsulinemia) and the pharmacologically induced-insulin resistant (by PUGNAc to elevate global O-GlcNAc levels) conditions. The approaches of proteomic researches for secreted proteins from 3T3-L1 preadipocytes and adipocytes have been performed by Kratchmarova *et al.*, Wang *et al.* and Lim *et al.* (17-20). In recent years, Chen *et al.* have developed a 2D-LC-MS/MS technique to identify the secreted proteins from rat primary adipose cells and quantify them upon induction by insulin treatment by adapting proteolytic ¹⁸O labeling strategy (20). This has resulted in 84 proteins identified as adipocytokines and in several

secreted proteins quantified with insulin modulation. Many researchers have begun to define the secreted proteome of primary human adipocytes by gel-based and liquid chromatography-based mass spectrometry (21-25). We studied previously the full secreted proteins and altered expression of the mouse and rat adipocytokines under insulin resistant conditions by hyperglycemia and hyperinsulinemia or elevated O-GlcNAc levels using two complementary differentiated mouse adipocyte cell lines (both 3T3-L1 and 3T3-F442A) and rat primary adipocytes (19). In the present study, we aimed to address the spectrum of secreted adipocytokines in primary human adipocytes in association with two insulin resistant conditions as in the previously reported rodent models. By comparing the identified proteome under different conditions, we defined the adipocytokines whose release is regulated by nutritional and/or hormonal perturbations. Proteomic approaches with reverse phase (RP) liquid chromatography-nanospray-tandem mass spectrometry (LC-NS-MS/MS) were employed to experimentally identify and quantify the secreted proteins. Proteins that were compared by normalized spectral counts were classified as abundant. We have identified total 190 secreted proteins from primary human adipocytes and quantified 20 unregulated and 4 downregulated secreted proteome by spectral counts comparing the insulin responsive condition and both insulin resistance conditions.

Glycosylation is one of the most common post-translational modifications (PTM) of proteins and is essential for regulation of many physiological events such as cell-cell recognition, signal transduction, and inflammation during development, differentiation, and disease progression (26-34). The complex structures of glycans found on the cells are dictated by highly specific glycosyltransferases and glycosidases present in the endoplasmic reticulum (ER) and Golgi apparatus. Alteration in the expression of these enzymes can lead to changes of the

glycomic profiles of glycoproteins in certain diseases (35, 36). The analysis of glycosylation sites is becoming increasingly important in the discovery of diagnostic biomarkers. The identification of sites of N-linked glycosylation has become an integral part of proteomic examinations to define the interface for protein-protein interactions (19, 37, 38). In this study, we identified 91 N-glycosylation sites on the secreted proteins derived from 51 proteins using PNGase F digestion in ^{18}O water and parents mass list method. For glycan analysis, mass spectrometry was employed as the recent development of sensitive analytical techniques to characterize the structure of glycans (36, 39-47). Isotopic labeling was used for the quantitative comparison of glycans in complex glycoprotein mixtures obtained from biological samples entailed permethylation using heavy/light iodomethane ($^{13}\text{CH}_3\text{I}$ and $^{12}\text{CH}_3\text{I}$) and isobaric pairs of iodomethane ($^{13}\text{CH}_3\text{I}$ or $^{12}\text{CH}_2\text{DI}$) (48, 49). Given the important physiological roles of protein glycosylation, the characterization of specific glycan structures and how these glycans change in adipocytes under insulin resistant conditions would be significant. We characterized a total of 155 of N-linked glycans and total 29 of O-linked glycans using MS/MS spectra by total ion mapping (TIM) scan respectively. Predominant N-linked and O-linked glycans were quantified by ^{13}C isotopic labeling of the glycans with different conditions. Total 48 of N-linked glycans and total 12 of O-linked glycans were compared between the insulin responsive condition and both insulin resistance conditions by calculated $^{13}\text{C}/^{12}\text{C}$ ratios from sum of peak area and prevalence ratios.

Given that diabetes is a chronic and incurable disease, interest in detection of the prediabetic condition that precedes the onset of diabetes is vastly invested in because it can be subjected to early disease detection and intervention. For this reason, the discovery of new biomarkers for the prediabetic stage is rapidly on the rises. The research of the novel and

advanced proteomic technologies in recent years has generated many candidate biomarkers in relatively low concentration in complex mixtures. In our current study, we provide high throughput profiles of secretome and glycome and relevant novel biomarkers some of which have become useful in diagnostics and prognostic for prediabetes in association with insulin resistance.

3.2. EXPERIMENTAL PROCEDURES

Tissue Culture and Conditioned Cell Treatments. Cryopreserved human subcutaneous preadipocytes (number of donors: 6-7, gender of donors: female, average age: 39, and average BMI: 27.32) were purchased from Zen-Bio, Inc. (Research Triangle Park, NC). The adipose tissue culture protocols for the maintenance and differentiation from preadipocytes to adipocytes were based on Zen-Bio instruction manual (ZBM0001.01). Briefly approximately 6.7×10^5 cells were cultured in a T-75 cm² culture flask using preadipocyte medium (PM-1, consisting of DMEM/Ham's F-12 medium, HEPES, fetal bovine serum: FBS, penicillin, streptomycin, amphotericin B; Zen-Bio, Inc.), under a humidified atmosphere containing 5% CO₂ in air at 37 °C until they were 85-90% confluent, and then trypsinized for 5 minutes at 37 °C. After neutralization and centrifugation steps, the cell pellet was resuspended in PM-1 and seeded at an average density of 2.67×10^4 cells/cm² in 10 cm cell culture dishes for differentiation. After 2 days of confluence (referred to as day 0), the medium was replaced with adipocyte differentiation medium (DM-2, similar to PM-1 but also containing biotin, pantothenate, human insulin, dexamethasone, isobutylmethylxanthine, PPAR γ agonist; Zen-Bio, Inc.). On day 7, the DM-2 was removed and the cells were maintained in adipocyte maintenance medium (AM-1, consisting of PM-1, biotin, pantothenate, human insulin, dexamethasone; Zen-Bio, Inc.), and the

medium was changed every 3 days. On day 15, at which time the majority of the cells contained large lipid droplets, the AM-1 medium was replaced with low glucose DMEM (Cellgro[®], Mediatech, Inc.) containing 10% FBS (GIBCO[®], Invitrogen) and antibiotics (100 units/mL penicillin and 100 µg/mL streptomycin: P/S, Cellgro[®], Mediatech, Inc.) and the medium was changed every 2 days, until treatments were applied. On day 20, human adipocytes were induced with the induction media composed of (A) low glucose (LG, DMEM containing 10% FBS and P/S), (B) insulin (100 nM, human, Roche) in high glucose (HG, DMEM containing 10% FBS and P/S), or (C) PUGNAc (100 µM, TRC, Inc.) in LG (DMEM containing 10% FBS and P/S) according to the experimental conditions described in the results. After the first 24 h of incubation, the cells were washed five times with low or high glucose serum-free DMEM without antibiotics and incubated for 15 min during the last rinse. After the final wash, the conditioned serum-free media supplemented with insulin (INS, 1 nM) in HG and PUGNAc (PUG, 100 µM) in LG was added to obtain conditions. The induced cells and media were harvested after 16 h of incubation.

Secreted Protein Sample Preparation. The conditioned media were harvested with extreme care and then centrifuged once at 1800 rpm, 4 °C for 7 min. The supernatants were filtered using 1 µm syringe filters (PALL). The samples were then collected in centrifuge tubes and centrifuged again at 30000 × g, 4 °C for 30 min. The samples were then transferred to equilibrated spin columns (Centriprep YM-3, Amicon, Millipore) and buffer-exchanged at 2800 × g, 4 °C into 40 mM ammonium bicarbonate (NH₄HCO₃) in the presence of 1 mM dithiothreitol (DTT, Fisher Scientific) and concentrated. The concentrated samples were denatured with 1 M urea (Sigma), reduced with 10 mM DTT for 1 h at 56 °C, carboxyamidomethylated with 55 mM iodoacetamide

(ICH₂CONH₂, Sigma) in the dark for 45 min, and then digested with 4 μg of trypsin (Promega) in 40 mM NH₄HCO₃ overnight at 37 °C. After digestion, the peptides were acidified with 200 μL of 1% trifluoroacetic acid (TFA). Desalting was subsequently performed with C18 spin columns (Vydac Silica C18, The Nest Group, Inc.) and the resulting peptides were dried down in a Speed Vac and stored at -20 °C until analysis. For the subset of samples to be analyzed for N-linked glycosylation, peptides were resuspended in 19 μL of ¹⁸O water (H₂¹⁸O, 95%, Cambridge Isotope Laboratories, Inc.) and 1 μL of N-Glycosidase F (PNGase F, Prozyme) and allowed to incubate for 18 h at 37 °C. Peptides were dried back down and resuspended in 50 μL of 40 mM NH₄HCO₃, with 1 μg of trypsin, to remove any possible C-terminal incorporation of ¹⁸O from residual trypsin activity for 4 h and then dried down and stored at -20 °C until analysis.

Whole Cell Extracts and Western Blots. After culture medium was removed for secreted proteins analysis, the cell monolayer was washed once with 10 ml of ice-cold PBS and scraped in the presence of 0.5 ml PBS. After removing PBS by centrifugation at 18,000 x g for 15 min at 4 °C, the pellet was snap frozen on dry ice and stored at -80 °C. To prepare a cell lysate for immunoblotting, the pellet was incubated on ice for 15 min in the presence of lysis buffer (1 x TBS, 1% NP-40, 0.1% SDS, protease inhibitor cocktail, phosphatase inhibitor cocktail, 1 mM EDTA, 1 mM DTT and 10 μM PUGNAc), and centrifuged at 15,000 x g for 30 min at 4 °C. Protein concentration was determined using Bradford assay reagent (Bio-Rad) and boiled in Laemli sample buffer. 20 μg of whole cell lysates were resolved by 4-15% Tris-HCl precast minigels (Bio-Rad) and transferred to Immobilon-P transfer membrane (Millipore). After blocking with 3% BSA in TBS containing 0.1 % Tween 20, the blots were probed with CTD 110.6 (for O-GlcNAc modified proteins) and ERK-2 (as a positive control for loading)

antibodies. The final detection of HRP activity conjugating to the secondary antibodies was performed using SuperSignal West Pico chemiluminescent substrate and exposed to CL-XPosure film (Pierce/Thermo Scientific).

Whole Proteins Extracts for Glycan Analysis. After the conditioned media was collected, the adipose cells for each condition were immediately washed with ice-cold PBS twice and harvested for glycan analysis. The cells were centrifuged at 12,000 x g, 4 °C for 15 min to remove the supernatant and debris, snap frozen and stored at -20 °C until analysis. As the samples thawed on ice, the samples were subjected to Dounce homogenization in 100% of ice-cold methanol. The homogenized samples were delipidated by extraction twice for 3 h at room temperature on the rocker with a mixture of chloroform/methanol/water (4:8:3, v/v/v) as described previously (36, 38). The emulsion was centrifuged at 2800 × g for 15 min at 4 °C to remove the supernatant. The pellets were resuspended in an acetone/water (10:1, v/v) mixture and incubated on ice for 15 min to wash the pellets twice. The protein pellets were collected by centrifugation and dried on a heating module at 45 °C with a mild nitrogen stream (Reacti-Therm™ and Reacti-Vap™, Pierce). The dried protein powder was weighted and stored at -20 °C until analyzed.

Preparation of N-linked Glycans. 3 mg of the protein powder was resuspended in 200 µL of 40 mM NH₄HCO₃ by sonication and boiled at 100 °C for 5 min. After cooling to room temperature, 25 µL of trypsin (2 mg/mL in 40 mM NH₄HCO₃, Sigma) and chymotrypsin (2 mg/mL in 40 mM NH₄HCO₃, Sigma) was added respectively. The samples were denatured with 250 µL of 2 M urea in 40 mM NH₄HCO₃ (resulting in 1 M urea) and incubated overnight (18 h) at 37 °C. After

digestion, the peptide samples were centrifuged and 10 μ L of the supernatant was collected for protein assay. The peptide amounts were measured by using micro BCA (Bicinchoninic acid) protein assay kit (Pierce). The samples were boiled at 100 $^{\circ}$ C for 5 min and acidified by addition of 500 μ L of 10% acetic acid (AcOH) (resulting in 5% AcOH) to deactivate proteases. The samples were loaded onto the equilibrated C18 extraction column (BakerBondTM, J.T.Baker), washed with 1 mL of 5% AcOH for three times, and eluted stepwise by 1 mL of 20% isopropanol in 5% AcOH, 40% isopropanol in 5% AcOH, and 100% isopropanol respectively. The resulting glycopeptides were dried down in a Speed Vac, resuspended in 48 μ L of 1 \times reaction buffer of PNGase F and 2 μ L of PNGase F, and then allowed to incubate for 18 h at 37 $^{\circ}$ C. Following PNGase F digestion, released oligosaccharides were separated by the C18 extraction column. The mixture was reconstituted in 5% AcOH and loaded onto the equilibrated C18 extraction column. The N-linked oligosaccharides were eluted by 1 mL of 5% AcOH three times and collected as purified N-linked glycans and dried down in a Speed Vac for permethylation processes.

Preparation of O-linked Glycans. O-linked oligosaccharides were released by reductive β -elimination and were purified by cation exchange resin as follows. 3 mg of delipidated protein powder was weighed and transferred into a clean glass tube. 500 μ L of 50 mM sodium hydroxide (NaOH) and 500 μ L of alkaline borohydride solution (a mixture of 2 M sodium borohydride: NaBH₄, Sigma-Aldrich, in 50 mM NaOH resulted in 1 M of NaBH₄) were added in the sample tube. The mixture was incubated for 16 h at 45 $^{\circ}$ C on the heating block and the reaction was stopped by addition of 10% AcOH with vortexing, resulting in 5% AcOH. The acidified mixture was loaded on an equilibrated cation exchange resin cartridge (AG 50W-X8, Bio-Rad) with 5%

AcOH. O-linked glycans were eluted with 6 mL of 5% AcOH and dried down in a Speed Vac. The sample was resuspended in 1 mL of a methanol/glacial acetic acid (9:1, v/v) solution and dried on the heating module at 45 °C with a mild nitrogen stream to remove borates twice for permethylation.

Permethylation of Glycans. To facilitate analysis of oligosaccharides by mass spectrometry (MS), the released oligosaccharide mixtures were permethylated as described previously (36, 38, 50). Briefly, glycans were suspended in 200 μ L of anhydrous dimethyl sulfoxide (DMSO, Sigma-Aldrich) and 250 μ L of the fresh dehydrated NaOH/DMSO reagent (mixture of 50 mg NaOH in 2 mL of anhydrous DMSO). After sonication and vortexing under nitrogen gases, 100 μ L of ^{12}C or ^{13}C -iodomethane ($^{12}\text{CH}_3\text{I}$ and $^{13}\text{CH}_3\text{I}$, 99% of ^{13}C , Sigma-Aldrich) was added and the mixtures were vortexed vigorously for 5 min. 2 mL of distilled water was added and the excess iodomethane was removed by bubbling with a nitrogen stream and 2 mL of dichloromethane (CH_2Cl_2 , Sigma-Aldrich) was added. After vigorous mixing and phase separation by centrifugation, the upper aqueous layer was removed and discarded. The nonpolar organic phase was then extracted 4 times with distilled water. Dichloromethane was evaporated on the heating module at 45 °C with the mild nitrogen stream. The permethylated glycans were dissolved in adjusted volumes (15-30 μ L) of 100% methanol based on the results of protein assay and then ^{12}C and ^{13}C -labeled permethylated glycans were mixed in the same proportion of each experimental condition before mass spectrometric analysis.

Mass Spectrometric Analysis. Proteome analysis of secreted proteins by liquid chromatography tandem mass spectrometry (LC-MS/MS): The peptides were resuspended with 19.5 μ L of mobile

phase A (0.1% formic acid, FA, in water) and 0.5 μ L of mobile phase B (80% acetonitrile, ACN, and 0.1% formic acid in water) and filtered with 0.2 μ m filters (Nanosep, PALL). The samples were loaded off-line onto a nanospray tapered capillary column/emitter (360 \times 75 \times 15 μ m, PicoFrit[®], New Objective) self-packed with C18 reverse phase (RP) resin (8.5 cm, Waters) in a nitrogen pressure bomb for 10 min at 1000 psi (\sim 5 μ L load) and then separated via a 160 min linear gradient of increasing mobile phase B at a flow rate of \sim 200 nL/min directly into the mass spectrometer. One-dimensional LC-MS/MS analysis was performed on a linear ion trap and an Orbitrap mass spectrometer (LTQ and LTQ Orbitrap XL, Thermo Fisher Scientific Inc., San Jose, CA) equipped with a nanoelectrospray ion source at 2.0 kV capillary voltage and 200 $^{\circ}$ C capillary temperature. For secretome analysis, a full ITMS (Ion trap mass spectrometry) spectrum in positive ion and profile mode was collected at 300-2000 m/z followed by 8 MS/MS events on the 8 most intense peaks with enabled dynamic exclusion using a repeat count of 2, a maximum exclusion list size of 100 and an exclusion duration of 30 s. each MS/MS scan event was followed by CID (34% normalized collision energy), 0.25 activation Q, and 30.0 ms activation time. For N-linked glycosylation site mapping, a full FTMS (Fourier transform mass spectrometry) spectrum, typically recorded at 60000 resolution in positive ion and profile mode, was acquired at 300-2000 m/z followed by 5 data dependent MS/MS spectra of ITMS on the most intense ion peaks following CID (36 % normalized collision energy), 0.25 activation Q, and 30.0 ms activation time. Dynamic exclusion was set at a repeat count of 2, a maximum exclusion list of 100 and an exclusion duration of 60 s.

Glycome analysis by direct infusion nanospray MS: For MS analysis for complex glycome of adipose cells, permethylated glycans were dissolved in total 50 μ L of sample with 15 μ L of the isotopically mixed sample in 100% methanol plus 35 μ L of 1 mM NaOH in 50%

methanol and infused directly into a linear ion trap and an Orbitrap mass spectrometer using a nanospray ion source with a fused-silica emitter ($360 \times 75 \times 30 \mu\text{m}$, SilicaTip™, New Objective) at 2.0 kV capillary voltage, 200 °C capillary temperature, and a syringe flow rate of 0.4 $\mu\text{L}/\text{min}$. The full ITMS spectra and FTMS spectra, typically recorded at 60000 resolution in positive ion and profile mode, were collected at 400-2000 m/z for 30 s with 5 microscans and 150 maximum injection times (ms). The centroid MS/MS spectra following collision-induced dissociation (CID) were obtained from 400 to 2000 m/z at 34% and 28% normalized collision energy for N- and O-linked glycans respectively, 0.25 activation Q, and 30.0 ms activation time by total ion mapping (TIM). Parent mass step size and isolation width were set at 2.0 m/z and 2.8 m/z respectively for automated MS/MS spectra with TIM scans.

Data Analysis. The resulting data was searched against a target nonredundant human (*Homo sapiens*, 5-2-07) database including the common contaminants database obtained from the human International Protein Index (IPI) protein sequence database (European Bioinformatics Institute, www.ebi.ac.uk/IPI/) using the TurboSequest algorithm (BioWorks 3.3.1 SP1, Thermo Fisher Scientific Inc.) as well as a decoy human database to statistically validate peptide identification. DTA files were generated for spectra with a threshold of 15 ions and a TIC of $2e^3$ over a range of $[\text{MH}]^+ = 600\text{-}4000$ for only IT data. The SEQUEST parameters were set to allow 2.0 Da (20 ppm for FT) of precursor ion mass tolerance and 0.5 Da of fragment ion tolerance with monoisotopic mass. Only strict tryptic peptides were allowed with up to two missed internal cleavage sites. Dynamic mass increases of 15.99 and 57.02 Da (15.9949 and 57.0215 Da for FT) were allowed for oxidized methionine and alkylated cysteine, respectively. In the cases where sites of N-linked glycosylation were investigated with PNGase F and ^{18}O water, a dynamic mass

increase of 3.0 Da (2.9883 Da for FT) was allowed for Asn residues. The identified peptides and proteins were statistically validated between the target and decoy database search results and protein ratios were determined by normalized spectral count using ProteoIQ 1.1 (BIOINQUIRE, GA). Proteins identified by two peptides were only considered to be statistically significant at less than 1% protein false discovery rate (FDR) using the ProValT algorithm as implemented in ProteoIQ (51, 52) From the results, the subcellular location of secreted proteins was manually determined for each protein from the Human Protein Reference Database (<http://www.hprd.org/>), Bioinformatic Harvester III (<http://harvester.fzk.de/harvester/>) and the UniProtKB/Swiss-Prot (<http://www.ebi.ac.uk/swissprot/>) databases and the functional categories of secretome were annotated by the Ingenuity Pathways Analysis (IPA, Ingenuity Systems, Inc.).

The N- and O-linked glycans released from the protein powder of adipose tissues were analyzed by full MS following permethylation and subsequent MS/MS fragmentations for specific glycan structures. The areas of each isotopic peak were calculated by the Gaussian distribution and summed to compare relative abundances of each glycan between different samples. The ratio of peak areas from isotopic permethylation defined the relative abundance of each glycan.

3.3. RESULTS

Elevated Global O-GlcNAc Levels of Nucleocytoplasmic Proteins by Insulin Resistance Conditions in Human Adipocytes. In rodent adipocytes, chronic insulin exposure combined with hyperglycemia (classical) or PUGNAc treatment (pharmacological inhibition of OGA) induce insulin resistance by global elevation of O-GlcNAcylated nucleocytoplasmic proteins (13, 15). Both insulin resistance conditions also elevated global O-GlcNAc levels in primary human

subcutaneous adipose tissues as determined by western blotting of whole-cell lysates with an O-GlcNAc-specific antibody CTD 110.6 (Figure 3-1). In previous study with rodent adipose tissue, we demonstrated that insulin resistance mediated by the flux through hexosamine biosynthetic pathway (HSP) and PUGNAc-induced by elevated O-GlcNAc levels modulated multiple adipocytokine secretion (53, 54) This result shows that both the increased flux through the HSP and O-GlcNAc inhibitor PUGNAc cause insulin resistance.

The Secretome Profiling of Primary Human Adipose Tissues by LC-MS/MS. The primary human adipocytes were derived from subcutaneous preadipocytes in culture using the human adipose tissue culture protocol. The human adipocytes were then maintained with serum-free media in two insulin resistance conditions (Insulin in HG: HGINS and PUGNAc in LG: LGPUG) and an insulin responsive condition (LG) shown in Figure 3-2A. The proteins secreted into the medium for 16 h were harvested and analyzed by LC-MS/MS shown in Figure 3-2B. The mass spectra of 24 mass spectrometric analyses were searched against a target human database as well as a decoy human database using SEQUEST. The identified proteins were validated at 1% FDR with 2 peptide coverage for statistic by ProteoIQ and secreted proteins were manually determined by reference search. By these criteria, a total of 190 secreted proteins were identified with 28 mass spectrometric analyses. Table 3-1 shows the complete list of 173 secreted proteins with 2 peptide coverage and 17 of the secreted proteins identified based on a single peptide are presented in the Supplemental Table 3-S1. Each protein of those tables also includes a subcellular location using the Ingenuity Pathways Analysis (IPA). Finally, the secretome was clustered in 9 main groups of functional categories by the IPA, as indicated in Figure 3-3. The functional categories of the

secretome include kinase, cytokine, transcription regulator, growth factor, transmembrane receptor, transporter, peptidase, enzyme and other proteins.

Quantification of the Secretome from Primary Human Adipocytes. Mass spectrometry (MS) techniques provide the quantitative analysis of proteins in complex protein samples using peptide isotopic labeling (55-64). However, label-free MS-based quantitative analyses are an alternative to isotopic labeling for high-throughput quantitative protein analysis focused on ion intensity using quantitative software tools and observed peptide spectral count (66-74). Peptide spectral counts attempt to quantify protein abundance by counting the number of MS/MS spectra identifying each protein. In this study, quantification of the secretome was performed on three conditioned media samples that differ in their complex proteome profiles and the relative number of normalized spectral counts. Functionality of ProteoIQ enables to export of annotated MS/MS spectra for identified peptides and normalized spectral counts were determined for proteins identified at 1% FDR and two peptides for statistic. Three biological samples (LG, LGPUG and HGINS) were subjected to reverse phase LC-MS/MS which repeated twice as technical replicate. Each of the three biological conditions was performed in triplicate leading to 18 total LC-MS/MS experiments. MS data files from each LC-MS/MS run were searched against a forward and reversed human database using SEQUEST. ProteoIQ was used to cluster peptides to proteins with three biological conditions and output lists of proteins had a protein false discovery rate (ProFDR) less than 1% at two peptides for statistic. Normalized spectral counts from technical replicate were averaged between runs and comparative ratios between the two insulin resistant conditions and the insulin responsive condition were obtained. The comparative ratios were then averaged between the biological triplicate experiments. We set the threshold for reporting differences at $\geq 150\%$ (1.5-

fold) under ≥ 5 averaged total spectral count and ≥ 3 averaged each condition's normalized spectral count. Table 3-2 shows the 20 human adipocytokines that upregulated secretion levels by at least 1.5-fold under both insulin resistant conditions and 4 proteins that downregulated under the same conditions. The 28 and 8 proteins regulated by at least 1.5-fold under one of the insulin resistant conditions are reported in supporting information (Table 3-S2).

N-Glycan Site Mapping of the Secretome of Human Adipocytes. To determine N-linked glycosylation of human adipocytokines, the tryptic peptides were digested with PNGase F in the presence of ^{18}O water to convert the glycan-modified Asn to ^{18}O -Asp residue. The resulting peptides were analyzed by LC-MS/MS using the previous normal shotgun method for ITMS and parent mass list method for FTMS. To obtain the parent mass list, the protein sequences of 190 total secreted proteins from Table 3-1 and 3-S1 were extracted from the database. The tryptic peptides including the consensus sequences, N-X-S/T, of asparagine residues and allowing for two internal missed cleavage sites were obtained for theoretical mass calculations. These peptides were allowed for dynamic modification with oxidized methionine, alkylated cysteine and asparagine (15.9949, 57.0215 and 2.9883 Da) respectively and then calculated with up to quintuply charge states. The masses were selected between 300-2000 m/z at each charge state and 7352 total masses were obtained for parent mass list. Each sample was analyzed by four of LC-MS/MS runs with different parent mass list up to 2000 because of maximum number of parent masses for FTMS and mass complexity. The results from shotgun method and parent mass list method were combined and filtered at ≥ 0.60 Final Score (Sf). Table 3-3 shows 91 total N-linked glycosylation sites on 52 proteins. These sites covered 10.3% sites in 882 total possible consensus sequences of N-linked glycosylation sites from the secreted protein list.

Characterization of Glycome in Human Adipocytes. Glycans were released from whole extracted proteins of human adipocyte by PNGase F for N-linked glycans and β -elimination for O-linked glycans as shown in Figure 3-2C. The permethylated glycans were directly infused to full FTMS in the LTQ Orbitrap XL and MS/MS by TIM scan in the ion trap. Figure 3-4A shows that N-linked glycans were characterized by full FTMS spectrum and MS/MS fragmentation by TIM analysis. We used the GlycoWorkbench (<http://www.dkfz-heidelberg.de/spec/EUROCarbDB/GlycoWorkbench/>) to manually interpret the glycan structure from the MS/MS spectra by TIM scan. 155 total N-linked glycans were characterized from MS² spectra at different charge states shown in supporting information (Table 3-S3). In right panel of Figure 3-4A, 28 of predominant N-linked glycans were assigned on a full FTMS spectrum and a MS/MS spectrum (No. 19) shows the fragmentation of biantennary N-linked glycan. Figure 3-4B shows a full FTMS spectrum from O-linked glycan mixture. 10 of predominant O-linked glycans were assigned on the full FTMS spectrum and one of core 2 O-linked glycans shows its fragmentation (No. 10). 29 total O-linked glycans were characterized from MS/MS spectra at singly and doubly charge state as shown in a supplemental table (Table 3-S4).

Relative Quantification of Human Adipocyte Glycome upon Insulin Resistance using ¹³C

Labeling and Prevalence. The comparative glycan quantifications from biological samples were performed by *in-vivo* isotopic labeling using heavy/light iodomethane (¹³CH₃I and ¹²CH₃I) and isobaric pairs of iodomethane (¹³CH₃I or ¹²CH₂DI) at permethylation step (48, 49) In this study, relative quantification data were obtained by ¹³C/¹²C ratio from the sum of peak area and prevalence ratio between the different biological conditions (insulin resistance vs. insulin response). Glycans permethylated with ¹³CH₃I or ¹²CH₃I were mixed in a 1:1 protein ratio and

analyzed in quadruplicate using an LTQ Orbitrap XL. Figure 3-5A shows the isotopic pairs of N-linked glycans on a full FTMS spectrum and calculated $^{13}\text{C}/^{12}\text{C}$ ratio from sum of peak area between HGINs and LG. 18 total predominant N-linked glycans were listed with the ratios of one of the quadruplicates. In Table 3-4, 48 total N-linked glycans were relatively quantified from human adipocytes between insulin resistant conditions and insulin responsive condition by average $^{13}\text{C}/^{12}\text{C}$ ratio and average prevalence ratio. This approach quantified simultaneously a broad range of glycan structures in a complex mixture. Figure 3-5B shows the isotopic pairs of O-linked glycans on a full FTMS spectrum and calculated $^{13}\text{C}/^{12}\text{C}$ ratio from sum of peak area between LGPUG and LG. 6 total predominant O-linked glycans were listed with the ratios of one of the quadruplicates and in Table 3-5, 12 total O-linked glycans were relatively quantified by average $^{13}\text{C}/^{12}\text{C}$ ratio and average prevalence ratio.

3.4. DISCUSSION

The secreted proteins of rodent and human adipocytes have been defined by previous studies focused on differential expression during mesenchymal stem cells and adipocyte differentiation (17-19, 21-25). Chen *et al.* have performed the identification of adipocytokines based on the presence of insulin in rat adipose tissue (20). In our previous study, we have characterized differential secretome levels of rodent adipocytes under the insulin resistant conditions by chronic hyperglycemia and hyperinsulinemia (classical insulin resistance) or elevated intracellular O-GlcNAc levels (with PUGNAc treatment) (19). Here, we characterized the secretome and differential expression of primary human adipocytes under both insulin resistant conditions using a proteomic approach. In order to identify the proteins of the secretory events under these conditions, we allowed a 16 h secretion which likely limits the levels of

secretome but prevents cell lysis. A total of 190 secreted proteins were identified and classified into subcellular locations and 9 functional categories using IPA. The largest pool of identified proteins corresponds to extracellular matrix proteins, confirming the secretome by previous studies and reference search. Manually validation of the list revealed that proteins assigned to be in the intracellular compartment by IPA were previously reported by other groups as secreted proteins. 57% of secretome with unknown biological function (under “other” category, Figure 3-3) is contributed by extracellular matrix proteins. 15% of enzymes and 13% of peptidases were mostly represented from the list of secretome.

Adipose tissue is recognized as an endocrine organ for the regulation of the whole-body energy metabolism through the secretion of adipocytokines. Changes of adipocytokines from insulin responsive to insulin resistant conditions are a potential key to sugar metabolism in diabetes. The quantitative profiling of secreted proteins between the conditions was performed by normalized spectral count which is a label-free quantification method of confident proteins assignment for a minor peptide associated with low abundance protein. Proteins found to have 1.5-fold difference in the number of spectral counts when compared between two distinct conditions were considered in up- or down-regulation. In both insulin resistant conditions on Table 3-2, 20 proteins were upregulated and 13 proteins were significantly different with > 2-fold such as reticulocalbin-3, olfactomedin-like protein 3, macrophage colony-stimulating factor 1, laminin alpha 2 subunit isoform b, procollagen C-endopeptidase enhancer 1, procollagen C-endopeptidase enhancer 1, dermatopontin, procollagen-lysine,2-oxoglutarate 5-dioxygenase 1, chitinase-3-like protein 1, collagen alpha-2(V) chain, C-type lectin domain family 11 member A, fibromodulin, sulfhydryl oxidase 1, and aminopeptidase N. Importantly, chitinase-3-like protein 1 and laminin subunit beta-1 were detected in previous rat adipocytes and 3T3s study as

upregulated proteins respectively. We also defined the downregulated proteins with slightly decreases including beta-2-microglobulin, insulin-like growth factor-binding protein 7, integrin beta-like protein 1. We also reported regulated proteins under one of insulin resistant conditions. The most increases were obtained from classical insulin resistance. A total of 22 proteins were identified from chronic exposure to insulin and high glucose and 6 proteins were from PUGNAc treatment as upregulated proteins. A total of 8 proteins were downregulated under either one of the insulin resistant conditions. From the experimental conditions on human adipocytes, these results have application as possible prognostic/diagnostic biomarkers for metabolic syndrome, type 2 diabetes, and other complications.

Given the importance of secretory proteins from adipocytes as a crucial source for early diagnostic biomarker of type 2 diabetes, defining the secreted proteins required an explicit feature of post-translational modification (PTM) status of these proteins. Our laboratory is particularly interested in complex glycosylation (N- and O-linked) as all the secreted proteins are exposed to glycosylation machinery *en route* that reside in ER and Golgi apparatus. Glycans expressed by cells depends on multiple factors such as the developmental stage and tissue specificity and are affected by the genetic and physiological state of the cells. The structural diversity of glycoproteins is determined by the expression and regulation of glycosyltransferase activities. Adipose tissues in insulin resistant conditions could change glycan expression patterns in response to their environment. Most secreted proteins are relatively heavily glycosylated and N-linked glycosylation is prevalent in the proteins for extracellular matrix location. For the analysis of N-linked glycosylation sites on the secreted proteins, we used PNGase F and ^{18}O water to convert the glycan-modified Asn to an ^{18}O -Asp residue. We identified 91 sites on 51 proteins of N-linked glycosylation by Orbitrap mass spectrometer using the parent mass list

obtained from theoretical consensus sequence in the secretome list. We have focused on determining the full diversity and changes of major and minor glycans from the adipocytes under the insulin resistant conditions. The results presented here demonstrate that the human adipocytes are expressing extended hybrid and complex N-linked glycans, in addition to the expected family of predominant high mannose glycans. Adipose tissues possess the biosynthetic ability to generate diverse O-linked glycans such as core structures and O-glucose glycan. We determined the changes of glycans under the insulin resistant conditions using $^{13}\text{C}/^{12}\text{C}$ ratio by permethylation and prevalence ratio. The results showed that changes of glycans under these conditions were not affected in mature adipocytes because of the short incubation period.

In summary, we have characterized the secretome of human adipocytes under the insulin resistant conditions using a proteomic approach. The secretome from adipocytes was regulated under the two insulin resistant conditions. We presented the diverse N- and O-linked glycans by TIM analysis and quantified some of those glycans from full FTMS by isotopic labeling of ^{13}C .

REFERENCES

1. Brownlee, M. The pathobiology of diabetic complications: a unifying mechanism. *Diabetes* **2005**, *54* (6), 1615-1625.
2. Havel, P. J. Update on adipocyte hormones: regulation of energy balance and carbohydrate/lipid metabolism. *Diabetes* **2004**, *53* (Suppl 1), S143-151.
3. Hazel, M.; Cooksey, R. C.; Jones, D.; Parker, G.; Neidigh, J. L.; Witherbee, B.; Gulve, E. A.; McClain, D. A. Activation of the hexosamine signaling pathway in adipose tissue results in decreased serum adiponectin and skeletal muscle insulin resistance. *Endocrinology* **2004**, *145* (5), 2118-2128.
4. Brownlee, M. Biochemistry and molecular cell biology of diabetic complications. *Nature* **2001**, *414* (6865), 813-820.
5. Wells, L.; Vosseller, K.; Hart, G. W. A role for N-acetylglucosamine as a nutrient sensor and mediator of insulin resistance. *Cell. Mol. Life Sci.* **2003**, *60* (2), 222-228.
6. Garvey, W. T.; Olefsky, J. M.; Matthaei, S.; and Marshall, S. Glucose and insulin coregulate the glucose transport system in primary cultured adipocytes: a new mechanism of insulin resistance. *J. Biol. Chem.* **1987**, *262*, 189-197.
7. Marshall, S.; Bacote, V.; Traxinger, R. R. Discovery of a metabolic pathway mediating glucose-induced desensitization of the glucose transport system: role of hexosamine biosynthesis in the induction of insulin resistance. *J. Biol. Chem.* **1991**, *266*, 4706-4712.
8. McClain, D. A.; Crook, E. D. Hexosamines and insulin resistance. *Diabetes* **1996**, *45*, 1003-1009.

9. Cooksey, R. C.; McClain, D. A. Transgenic mice overexpressing the rate-limiting enzyme for hexosamine synthesis in skeletal muscle or adipose tissue exhibit total body insulin resistance. *Ann N Y Acad Sci.* **2002**, *967*, 102-111.
10. Cooksey, R. C.; Pusuluri, S.; Hazel, M.; McClain, D. A. Hexosamines regulate sensitivity of glucose-stimulated insulin secretion in beta-cells. *Am J Physiol Endocrinol Metab.* **2006**, *290* (2), E334-340.
11. Patti, M. E.; Virkamaki, A.; Landaker, E. J.; Kahn, C. R.; Yki-Jarvinen, H. Activation of the hexosamine pathway by glucosamine *in vivo* induces insulin resistance of early postreceptor insulin signaling events in skeletal muscle. *Diabetes* **1999**, *48*, 1562-1571.
12. Haltiwanger, R. S.; Grove, K.; Philipsberg, G. A. Modulation of O-linked N-acetylglucosamine levels on nuclear and cytoplasmic proteins *in vivo* using the peptide O-GlcNAc-beta-N-acetylglucosaminidase inhibitor O-(2-acetamido-2-deoxy D-glucopyranosylidene) amino-N-phenylcarbamate. *J. Biol. Chem.* **1998**, *273*, 3611-3617.
13. Vosseller, K.; Wells, L.; Lane, M. D.; Hart, G. W. Elevated nucleocytoplasmic glycosylation by O-GlcNAc results in insulin resistance associated with defects in Akt activation in 3T3-L1 adipocytes. *Proc. Natl. Acad. Sci.* **2002**, *99*, 5313-5318.
14. Arias, E. B.; Kim, J.; Cartee, G. D. Prolonged incubation in PUGNAc results in increased protein O-Linked glycosylation and insulin resistance in rat skeletal muscle. *Diabetes* **2004**, *53*, 921-930.
15. Park, S. Y.; Ryu, J.; Lee W. O-GlcNAc modification on IRS-1 and Akt2 by PUGNAc inhibits their phosphorylation and induces insulin resistance in rat primary adipocytes. *Exp. Mol. Med.* **2005**, *37*, 220-229.

16. Federici, M.; Menghini, R.; Mauriello, A.; Hribal, M. L.; Ferrelli, F.; Lauro, D.; Sbraccia, P.; Spagnoli, L. G.; Sesti, G.; Lauro, R. Insulin-dependent activation of endothelial nitric oxide synthase is impaired by O-linked glycosylation modification of signaling proteins in human coronary endothelial cells. *Circulation* **2002**, *106* (4), 466-472.
17. Kratchmarova, I.; Kalume, D. E.; Blagoev, B.; Scherer, P. E.; Podtelejnikov, A. V.; Molina, H.; Bickel, P. E.; Andersen, J. S.; Fernandez, M. M.; Bunkenborg, J.; Roepstorff, P.; Kristiansen, K.; Lodish, H. F.; Mann, M.; Pandey, A. A proteomic approach for identification of secreted proteins during the differentiation of 3T3-L1 preadipocytes to adipocytes. *Mol. Cell. Proteomics* **2002**, *1*, 213-222.
18. Wang, P.; Mariman, E.; Keijer, J.; Bouwman, F.; Noben, J.-P.; Robben, J.; Renes, J. Profiling of the secreted proteins during 3T3-L1 adipocyte differentiation leads to the identification of novel adipokines. *Cell. Mol. Life Sci.* **2004**, *61*, 2405-2417.
19. Lim, J. M.; Sherling, D.; Teo, C. F.; Hausman, D. B.; Lin, D.; Wells, L. Defining the regulated secreted proteome of rodent adipocytes upon the induction of insulin resistance *Journal of Proteome Research* **2008**, *7*, 1251-1263.
20. Chen, X.; Cushman, S. W.; Pannell, L. K.; Hess, S. Quantitative proteomic analysis of the secretory proteins from rat adipose cells using a 2D liquid chromatography-MS/MS approach. *J. Proteome Res.* **2005**, *4*, 570-577.
21. Chiellini, C.; Cochet, O.; Negroni, L.; Samson, M.; Poggi, M.; Ailhaud, G.; Alessi, M. C.; Dani, C.; Amri, E. Z. Characterization of human mesenchymal stem cell secretome at early steps of adipocyte and osteoblast differentiation. *BMC Mol Biol.* **2008**, *9*, 26.
22. Adachi, J.; Kumar, C.; Zhang, Y.; Mann, M. In-depth analysis of the adipocyte proteome by mass spectrometry and bioinformatics. *Mol Cell Proteomics* **2007**, *6* (7):1257-1273.

23. Alvarez-Llamas, G.; Szalowska, E.; de Vries, M. P.; Weening, D.; Landman, K.; Hoek, A.; Wolffenbuttel, B. H.; Roelofsen, H.; Vonk, R. J. Characterization of the human visceral adipose tissue secretome. *Mol Cell Proteomics* **2007**, *6* (4), 589-600.
24. Zvonic, S.; Lefevre, M.; Kilroy, G.; Floyd, Z. E.; DeLany, J. P.; Kheterpal, I.; Gravois, A.; Dow, R.; White, A.; Wu, X.; Gimble, J. M. Secretome of primary cultures of human adipose-derived stem cells: modulation of serpins by adipogenesis. *Mol Cell Proteomics* **2007**, *6* (1), 18-28.
25. Lee, H. K.; Lee, B. H.; Park S. A.; Kim C. A. The proteomic analysis of an adipocyte differentiated from human mesenchymal stem cells using twodimensional gel electrophoresis. *Proteomics* **2006**, *6*, 1223-1229.
26. Varki, A. Biological roles of oligosaccharides: all of the theories are correct. *Glycobiology* **1993**, *3* (2), 97-130.
27. Krueger, K. E.; Srivastava, S. Posttranslational Protein Modifications: Current Implications for Cancer Detection, Prevention, and Therapeutics. *Mol. Cell. Proteomics* **2006**, *5* (10), 1799-1810.
28. Isaji, T.; Gu, J.; Nishiuchi, R.; Zhao, Y.; Takahashi, M.; Miyoshi, E.; Honke, K.; Sekiguchi, K.; Taniguchi, N. Introduction of bisecting GlcNAc into integrin alpha5 beta1 reduces ligand binding and down-regulates cell adhesion and cell migration. *J. Biol. Chem.* **2004**, *279*, 19747-19754.
29. Stanley, P. Biological consequences of overexpressing or eliminating N-acetylglucosaminyltransferase-TIII in the mouse. *Biochim. Biophys. Acta* **2002**, *1573*, 363-368.

30. Schachter, H. Congenital disorders involving defective N-glycosylation of proteins. *Cell Mol. Life Sci.* **2001**, *58*, 1085-1104.
31. Dennis, J. W.; Granovsky, M.; Warren, C.E. Glycoprotein glycosylation and cancer progression. *Biochim. Biophys. Acta* **1999**, *1473*, 21-34.
32. Delves, P. J. The role of glycosylation in autoimmune disease. *Autoimmunity* **1998**, *27*, 239-253.
33. Gleeson, P. A. Glycoconjugates in autoimmunity. *Biochim. Biophys. Acta* **1994**, *1197*, 237-255.
34. Chui, D.; Sellakumar, G.; Green, R.; Sutton-Smith, M.; McQuistan, T.; Marek, K.; Morris, H.; Dell, A.; Marth, J. Genetic remodeling of protein glycosylation in vivo induces autoimmune disease. *Proc. Natl. Acad. Sci. USA* **2001**, *98*, 1142-1147.
35. Kudo, T.; Nakagawa, H.; Takahashi, M.; Hamaguchi, J.; Kamiyama, N.; Yokoo, H.; Nakanishi, K.; Nakagawa, T.; Kamiyama, T.; Deguchi, K.; Nishimura, S.; Todo, S. N-glycan alterations are associated with drug resistance in human hepatocellular carcinoma. *Mol Cancer* **2007**, *6*, 32.
36. Aoki, K.; Perlman, M.; Lim, J. M.; Cantu, R.; Wells, L.; Tiemeyer, M. Dynamic developmental elaboration of N-linked glycan complexity in the *Drosophila melanogaster* embryo. *J Biol Chem.* **2007**, *282* (12), 9127-9142.
37. Lim, J. M.; Aoki, K.; Angel, P.; Garrison, D.; King, D.; Tiemeyer, M.; Bergmann, C.; Wells, L. Mapping glycans onto specific N-linked glycosylation sites of *Pyrus communis* PGIP redefines the interface for EPG-PGIP interactions. *J Proteome Res.* **2009**, *8* (2), 673-680.

38. Koles, K.; Lim, J. M.; Aoki, K.; Porterfield, M.; Tiemeyer, M.; Wells, L.; Panin, V. Identification of N-glycosylated proteins from the central nervous system of *Drosophila melanogaster*. *Glycobiology* **2007**, *17* (12), 1388-1403.
39. Dell, A.; Reason, A. J.; Khoo, K. H.; Panico, M.; McDowell, R. A.; Morris, H. R. Mass spectrometry of carbohydrate-containing biopolymers. *Methods Enzymol.* **1994**, *230*, 108-132.
40. Wuhrer, M.; Deelder, A. M.; Hokke, C. H. Protein glycosylation analysis by liquid chromatography-mass spectrometry. *J Chromatogr B Analyt Technol Biomed Life Sci.* **2005**, *825* (2), 124-133.
41. Morelle, W.; Faid, V.; Michalski, J. C. Structural analysis of permethylated oligosaccharides using electrospray ionization quadrupole time-of-flight tandem mass spectrometry and deuteroreduction. *Rapid Commun. Mass Spectrom.* **2004**, *18* (20), 2451-2464.
42. Reinhold, V. N.; Sheeley, D. M. Detailed characterization of carbohydrate linkage and sequence in an ion trap mass spectrometer: glycosphingolipids. *Anal. Biochem.* **1998**, *259* (1), 28-33.
43. Sheeley, D. M.; Reinhold, V. N. Structural characterization of carbohydrate sequence, linkage, and branching in a quadrupole Ion trap mass spectrometer: neutral oligosaccharides and N-linked glycans. *Anal. Chem.* **1998**, *70* (14), 3053-3059.
44. Viseux, N.; de Hoffmann, E.; Domon, B. Structural analysis of permethylated oligosaccharides by electrospray tandem mass spectrometry. *Anal. Chem.* **1997**, *69* (16), 3193-3198.

45. Prien, J. M.; Huysentruyt, L. C.; Ashline, D. J.; Lapadula, A. J.; Seyfried, T. N.; Reinhold, V. N. Differentiating N-linked glycan structural isomers in metastatic and nonmetastatic tumor cells using sequential mass spectrometry. *Glycobiology* **2008**, *18* (5), 353-366.
46. Aoki, K.; Porterfield, M.; Lee, S. S.; Dong, B.; Nguyen, K.; McGlamry, K. H.; Tiemeyer, M. The diversity of O-linked glycans expressed during *Drosophila melanogaster* development reflects stage- and tissue-specific requirements for cell signaling. *J Biol Chem.* **2008**, *283* (44), 30385-30400.
47. Abbott, K. L.; Aoki, K.; Lim, J. M.; Porterfield, M.; Johnson, R.; O'Regan, R. M.; Wells, L.; Tiemeyer, M.; Pierce, M. Targeted glycoproteomic identification of biomarkers for human breast carcinoma. *J Proteome Res.* **2008**, *7* (4), 1470-1480.
48. Alvarez-Manilla, G.; Warren, N. L.; Abney, T.; Atwood, J., III; Azadi, P.; York, W. S.; Pierce, M.; Orlando, R. Tools for glycomics: relative quantitation of glycans by isotopic permethylation using $^{13}\text{CH}_3\text{I}$. *Glycobiology* **2007**, *17* (7), 677-687.
49. Atwood III, J. A.; Cheng, L.; Alvarez-Manilla, G.; Warren, N. L.; York, W. S.; Orlando, R. Quantitation by Isobaric Labeling: Applications to Glycomics *J. Proteome Res.* **2008**, *7* (01), 367-374.
50. Ciucanu, I.; Kerek, F. A simple and rapid method for the permethylation of carbohydrates. *Carbohydrate Research* **1984**, *131*, 209-217.
51. Weatherly, D. B.; Atwood, J. A. 3rd.; Minning, T. A.; Cavola, C.; Tarleton, R. L.; Orlando, R. A. Heuristic method for assigning a false-discovery rate for protein identifications from Mascot database search results. *Mol Cell Proteomics* **2005**, *4* (6), 762-772.

52. Shah, P.; Atwood, J. A.; Orlando, R.; El Mubarek, H.; Podila, G. K.; Davis, M. R. Comparative Proteomic Analysis of *Botrytis cinerea* Secretome. *J. Proteome Res.* **2009**, *8* (3), 1123-1130.
53. Wang, J.; Liu, R.; Hawkins, M.; Barzilai, N.; Rossetti, L. A nutrientsensing pathway regulates leptin gene expression in muscle and fat. *Nature* **1998**, *393* (6686), 684-688.
54. Student, A. K.; Hsu, R. Y.; Lane, M. D.; McClain, D. A.; Alexander, T.; Cooksey, R. C.; Considine, R. V. Hexosamines stimulate leptin production in transgenic mice. *Endocrinology* **2000**, *141* (6), 1999-2002.
55. Gygi, S. P.; Rist, B.; Gerber, S. A.; Turecek, F.; Gelb, M. H.; Aebersold, R. Quantitative analysis of complex protein mixtures using isotope-coded affinity tags. *Nat Biotechnol* **1999**, *17*, 994-999.
56. Haqqani, A. S.; Nesic, M.; Preston, E.; Baumann, E.; Kelly, J.; Stanimirovic, D. Characterisation of vascular protein expression patterns in cerebral ischemia/reperfusion using laser capture microdissection and ICAT-nanoLC-MS/MS. *FASEB J* **2005**, *19*, 1809-1821.
57. Haqqani, A. S.; Kelly, J.; Baumann, E.; Haseloff, R. F.; Blasig, I. E.; Stanimirovic, D. B. Protein markers of ischemic insult in brain endothelial cells identified using 2D gel electrophoresis and ICAT-based quantitative proteomics. *J Proteome Res* **2007**, *6*, 226-239.
58. Haqqani, A. S.; Hutchison, J. S.; Ward, R.; Stanimirovic, D. B. Protein biomarkers in serum of pediatric patients with severe traumatic brain injury identified by ICAT-LC-MS/MS. *J Neurotrauma* **2007**, *24*, 54-74.
59. Shevchenko, A.; Chernushevich, I.; Standing, K. G.; Thompson, B.; Wilm, M.; Mann, M. Rapid “*de novo*” peptide sequencing by a combination of nanoelectrospray, isotopic

- labeling and a quadrupole/time-of-flight mass spectrometer. *Rapid Commun. Mass Spectrom.* **1997**, *11*, 1015-1024.
60. Schnolzer, M.; Jedrzejewski, P.; Lehmann, W. D. Proteasecatalyzed incorporation of ^{18}O into peptide fragments and its application for protein sequencing by electrospray and matrix-assisted laser desorption/ionization mass spectrometry. *Electrophoresis* **1996**, *17*, 945-953.
 61. Uttenweiler-Joseph, S.; Neubauer, G.; Christoforidis, S.; Zerial, M.; Wilm, M. Automated *de novo* sequencing of proteins using the differential scanning technique. *Proteomics* **2001**, *1*, 668-682.
 62. Ong, S. E.; Mann, M. Mass spectrometry-based proteomics turns quantitative. *Nat Chem Biol.* **2005**, *1* (5), 252-262.
 63. Ong, S. E.; Blagoev, B.; Kratchmarova, I.; Kristensen, D. B.; Steen, H.; Pandey, A.; Mann, M. Stable isotope labeling by amino acids in cell culture, SILAC, as a simple and accurate approach to expression proteomics. *Mol Cell Proteomics* **2002**, *1* (5), 376-386.
 64. Ong, S. E.; Kratchmarova, I.; Mann, M. Properties of ^{13}C -substituted arginine in stable isotope labeling by amino acids in cell culture (SILAC). *J Proteome Res.* **2003**, *2* (2), 173-181.
 65. Lu, P.; Vogel, C.; Wang, R.; Yao, X.; Marcotte, E. M. Absolute protein expression profiling estimates the relative contributions of transcriptional and translational regulation. *Nat. Biotechnol.* **2007**, *25*, 117-124.
 66. Mallick, P.; Schirle, M.; Chen, S. S.; Flory, M. R.; Lee, H.; Martin, D.; Ranish, J.; Raught, B.; Schmitt, R.; Werner, T.; Kuster, B.; Aebersold, R. Computational prediction of proteotypic peptides for quantitative proteomics. *Nat. Biotechnol.* **2007**, *25*, 125-131.

67. Wiener, M. C.; Sachs, J. R.; Deyanova, E. G.; Yates, N. A. Differential mass spectrometry: a label-free LC-MS method for finding significant differences in complex peptide and protein mixtures. *Anal. Chem.* **2004**, *76*, 6085-6096.
68. Liu, H.; Sadygov, R. G.; Yates, J. R. III. A model for random sampling and estimation of relative protein abundance in shotgun proteomics. *Anal. Chem.* **2004**, *76*, 4193-4201.
69. Bondarenko, P. V.; Chelius, D.; Shaler, T. A. Identification and relative quantitation of protein mixtures by enzymatic digestion followed by capillary reversed-phase liquid chromatography tandem mass spectrometry. *Anal. Chem.* **2002**, *74*, 4741-4749.
70. Chelius, D.; Bondarenko, P. V. Quantitative profiling of proteins in complex mixtures using liquid chromatography and mass spectrometry. *J. Proteome Res.* **2002**, *1*, 317-323.
71. Old, W. M.; Meyer-Arendt, K.; Aveline-Wolf, L.; Pierce, K. G.; Mendoza, A.; Sevinsky, J. R.; Resing, K. A.; Ahn, N. G. Comparison of label-free methods for quantifying human proteins by shotgun proteomics. *Mol. Cell. Proteomics* **2005**, *4*, 1487-1502.
72. Higgs, R. E.; Knierman, M. D.; Gelfanova, V.; Butler, J. P.; Hale, J. E. Comprehensive label-free method for the relative quantification of proteins from biological samples. *J. Proteome Res.* **2005**, *4*, 1442-1450.
73. Andreev, V. P.; Li, L.; Cao, L.; Gu, Y.; Rejtar, T.; Wu, S. L.; Karger, B. L. A New Algorithm Using Cross-Assignment for Label-Free Quantitation with LC-LTQ-FT MS. *J. Proteome Res.* **2007**, *6*, 2186-2194.
74. Nesvizhskii, A. I.; Keller, A.; Kolker, E.; Aebersold, R. A statistical model for identifying proteins by tandem mass spectrometry. *Anal. Chem.* **2003**, *75*, 4646-4658.

Table 3-1. Total secreted proteins from human adipose tissues by LC-MS/MS

No.	Protein ID	Identified Proteins	Subcellular Location ^a
1	Q92484	Acid sphingomyelinase-like phosphodiesterase 3a	Extracellular
2	P07108	Acyl-CoA-binding protein	Cytoplasm
3	Q8IUX7	Adipocyte enhancer-binding protein 1	Membrane
4	P01023	Alpha-2-macroglobulin	Nucleus
5	P06733	Alpha-enolase	Extracellular
6	P15144	Aminopeptidase N	Cytoplasm
7	P01019	Angiotensinogen	Membrane
8	P07355	Annexin A2	Extracellular
9	P08758	Annexin A5	Membrane
10	Q8NCW5	Apolipoprotein A-I binding protein	Extracellular
11	P05090	Apolipoprotein D	Extracellular
12	P02649	Apolipoprotein E	Extracellular
13	P15289	Arylsulfatase A	Cytoplasm
14	P61769	Beta-2-microglobulin	Membrane
15	P21810	Biglycan	Extracellular
16	P43251	Biotinidase	Extracellular
17	P55290	Cadherin-13	Membrane
18	P27797	Calreticulin	Cytoplasm
19	O43852	Calumenin	Cytoplasm
20	P16870	Carboxypeptidase E	Membrane
21	P49747	Cartilage oligomeric matrix protein	Extracellular
22	P07858	Cathepsin B	Cytoplasm
23	P07339	Cathepsin D	Cytoplasm
24	P43235	Cathepsin K	Cytoplasm
25	P07711	Cathepsin L	Cytoplasm
26	Q9UBR2	Cathepsin Z	Cytoplasm
27	P36222	Chitinase-3-like protein 1	Extracellular
28	Q15782	Chitinase-3-like protein 2	Extracellular
29	Q59FG9	Chondroitin sulfate proteoglycan 2 (versican) variant	Extracellular

Table 3-1. Continued.

No.	Protein ID	Identified Proteins	Subcellular Location ^a
30	P10909	Clusterin	Extracellular
31	P02452	Collagen alpha-1(I) chain	Extracellular
32	P02458	Collagen alpha-1(II) chain	Extracellular
33	P02461	Collagen alpha-1(III) chain	Extracellular
34	P02462	Collagen alpha-1(IV) chain	Extracellular
35	P20908	Collagen alpha-1(V) chain	Extracellular
36	P12109	Collagen alpha-1(VI) chain	Extracellular
37	Q02388	Collagen alpha-1(VII) chain	Extracellular
38	P12107	Collagen alpha-1(XI) chain	Extracellular
39	Q99715	Collagen alpha-1(XII) chain	Extracellular
40	P39059	Collagen alpha-1(XV) chain [Contains: Endostatin]	Extracellular
41	P39060	Collagen alpha-1(XVIII) chain [Contains: Endostatin]	Extracellular
42	P08123	Collagen alpha-2(I) chain	Extracellular
43	P08572	Collagen alpha-2(IV) chain [Contains: Canstatin]	Extracellular
44	P05997	Collagen alpha-2(V) chain	Extracellular
45	P12110	Collagen alpha-2(VI) chain	Extracellular
46	P25940	Collagen alpha-3(V) chain	Extracellular
47	P12111	Collagen alpha-3(VI) chain	Extracellular
48	P08253	Collagenase (72 kDa type IV)	Extracellular
49	P00736	Complement C1r subcomponent	Extracellular
50	P09871	Complement C1s subcomponent	Extracellular
51	P01024	Complement C3	Extracellular
52	P29279	Connective tissue growth factor	Extracellular
53	Q9Y240	C-type lectin domain family 11 member A	Extracellular
54	O75462	Cytokine receptor-like factor 1	Extracellular
55	P07585	Decorin	Extracellular
56	Q07507	Dermatopontin	Extracellular
57	Q4VWZ6	Diazepam binding inhibitor, splice form 1c	Cytoplasm
58	Q9UBP4	Dickkopf-related protein 3	Extracellular
59	Q14118	Dystroglycan	Membrane
60	Q13822	Ectonucleotide pyrophosphatase/phosphodiesterase 2	Membrane

Table 3-1. Continued.

No.	Protein ID	Identified Proteins	Subcellular Location ^a
61	Q12805	EGF-containing fibulin-like extracellular matrix protein 1	Extracellular
62	O95967	EGF-containing fibulin-like extracellular matrix protein 2	Extracellular
63	Q9Y6C2	EMILIN-1	Extracellular
64	Q9BXX0	EMILIN-2	Extracellular
65	P61916	Epididymal secretory protein E1	Extracellular
66	Q9Y2E5	Epididymis-specific alpha-mannosidase	Cytoplasm
67	Q16610	Extracellular matrix protein 1	Extracellular
68	P08294	Extracellular superoxide dismutase [Cu-Zn]	Extracellular
69	P35555	Fibrillin-1	Extracellular
70	Q53TP5	Fibroblast activation protein, alpha subunit	Cytoplasm
71	Q06828	Fibromodulin	Extracellular
72	P02751	Fibronectin	Membrane
73	P23142	Fibulin-1	Extracellular
74	P98095	Fibulin-2	Extracellular
75	Q9UBX5	Fibulin-5	Extracellular
76	Q12841	Follistatin-related protein 1	Extracellular
77	P16930	Fumarylacetoacetase	Cytoplasm
78	P09382	Galectin-1	Extracellular
79	Q08380	Galectin-3-binding protein	Membrane
80	Q92820	Gamma-glutamyl hydrolase	Cytoplasm
81	P06396	Gelsolin	Extracellular
82	Q9UJJ9	GlcNAc-1-phosphotransferase subunit gamma	Cytoplasm
83	P07093	Glia-derived nexin	Extracellular
84	P04406	Glyceraldehyde-3-phosphate dehydrogenase	Cytoplasm
85	P35052	Glypican-1	Membrane
86	P28799	Granulins	Extracellular
87	Q14393	Growth-arrest-specific protein 6	Extracellular
88	P00738	Haptoglobin	Extracellular
89	P00739	Haptoglobin-related protein	Extracellular
90	O75629	Human Protein CREG1	Nucleus
91	P17936	Insulin-like growth factor-binding protein 3	Extracellular

Table 3-1. Continued.

No.	Protein ID	Identified Proteins	Subcellular Location ^a
92	P22692	Insulin-like growth factor-binding protein 4	Extracellular
93	P24592	Insulin-like growth factor-binding protein 6	Extracellular
94	Q16270	Insulin-like growth factor-binding protein 7	Extracellular
95	O95965	Integrin beta-like protein 1	Unknown
96	P19823	Inter-alpha-trypsin inhibitor heavy chain H2	Extracellular
97	O14498	ISLR	Extracellular
98	Q08431	Lactadherin	Extracellular
99	Q8NHP8	LAMA-like protein 2	Extracellular
100	Q59H37	Laminin alpha 2 subunit isoform b	Extracellular
101	Q16363	Laminin subunit alpha-4	Extracellular
102	P07942	Laminin subunit beta-1	Extracellular
103	P55268	Laminin subunit beta-2	Extracellular
104	P11047	Laminin subunit gamma-1	Extracellular
105	Q14767	Latent-transforming growth factor beta-binding protein 2	Extracellular
106	Q99538	Legumain	Cytoplasm
107	Q07954	Low-density lipoprotein receptor-related protein 1	Membrane
108	P51884	Lumican	Extracellular
109	P10619	Lysosomal protective protein	Cytoplasm
110	P13473	Lysosome-associated membrane glycoprotein 2	Membrane
111	Q9Y4K0	Lysyl oxidase homolog 2	Extracellular
112	P09603	Macrophage colony-stimulating factor 1	Extracellular
113	Q9UM22	Mammalian ependymin-related protein 1	Nucleus
114	P48740	Mannan-binding lectin serine protease 1	Extracellular
115	P50281	Matrix metalloproteinase-14	Extracellular
116	P01033	Metalloproteinase inhibitor 1	Extracellular
117	P16035	Metalloproteinase inhibitor 2	Extracellular
118	Q71SW6	Muscle type neuropilin 1	Membrane
119	P14543	Nidogen-1	Extracellular
120	Q14112	Nidogen-2	Extracellular
121	Q02818	Nucleobindin-1	Cytoplasm
122	Q9NRN5	Olfactomedin-like protein 3	Extracellular

Table 3-1. Continued.

No.	Protein ID	Identified Proteins	Subcellular Location ^a
123	Q86UD1	Out at first protein homolog	Unknown
124	P26022	Pentraxin-related protein PTX3	Extracellular
125	P62937	Peptidyl-prolyl cis-trans isomerase A	Cytoplasm
126	P23284	Peptidylprolyl isomerase B	Cytoplasm
127	Q15063	Periostin	Extracellular
128	P98160	Perlecan	Membrane
129	Q92626	Peroxidasin homolog	Unknown
130	P30086	Phosphatidylethanolamine-binding protein 1	Cytoplasm
131	P55058	Phospholipid transfer protein	Extracellular
132	P36955	Pigment epithelium-derived factor	Extracellular
133	Q9BTY2	Plasma alpha-L-fucosidase	Extracellular
134	Q9Y646	Plasma glutamate carboxypeptidase	Extracellular
135	P05155	Plasma protease C1 inhibitor	Extracellular
136	P05121	Plasminogen activator inhibitor 1	Extracellular
137	Q9GZP0	Platelet-derived growth factor D	Extracellular
138	P07602	Proactivator polypeptide [Contains: Saposin-A]	Extracellular
139	Q15113	Procollagen C-endopeptidase enhancer 1	Extracellular
140	Q02809	Procollagen-lysine,2-oxoglutarate 5-dioxygenase 1	Cytoplasm
141	P07737	Profilin-1	Cytoplasm
142	P41222	Prostaglandin-H2 D-isomerase	Cytoplasm
143	Q6UXB8	Protease inhibitor 16	Membrane
144	P07237	Protein disulfide-isomerase	Cytoplasm
145	Q15084	Protein disulfide-isomerase A6	Cytoplasm
146	P14618	Pyruvate kinase isozymes M1/M2	Cytoplasm
147	Q96D15	Reticulocalbin-3	Cytoplasm
148	Q99969	Retinoic acid receptor responder protein 2	Membrane
149	O75326	Semaphorin-7A	Membrane
150	Q12884	Seprase	Cytoplasm
151	Q92743	Serine protease HTRA1	Extracellular
152	P02787	Serotransferrin	Extracellular
153	P09486	SPARC	Extracellular

Table 3-1. Continued.

No.	Protein ID	Identified Proteins	Subcellular Location ^a
154	Q9BUD6	Spondin-2	Extracellular
155	Q9BRK5	Stromal cell-derived factor 4	Cytoplasm
156	O00391	Sulfhydryl oxidase 1	Cytoplasm
157	P00441	Superoxide dismutase [Cu-Zn]	Cytoplasm
158	Q9Y490	Talin-1	Membrane
159	P24821	Tenascin	Extracellular
160	P22105	Tenascin-X	Extracellular
161	Q08629	Testican-1	Extracellular
162	P10599	Thioredoxin	Cytoplasm
163	Q16881	Thioredoxin reductase 1	Cytoplasm
164	P07996	Thrombospondin-1	Extracellular
165	P35442	Thrombospondin-2	Extracellular
166	Q6FGX5	TIMP1 protein	Extracellular
167	Q15582	Transforming growth factor-beta-induced protein ig-h3	Extracellular
168	O14773	Tripeptidyl-peptidase 1	Cytoplasm
169	Q6EMK4	Vasorin	Membrane
170	P13611	Versican core protein	Extracellular
171	P08670	Vimentin	Cytoplasm
172	P04004	Vitronectin	Extracellular
173	O76076	WNT1-inducible-signaling pathway protein 2	Extracellular

^a The subcellular location was determined for each protein based on the Ingenuity Pathway Analysis software (Ingenuity Systems).

Table 3-2. Human adipocytokines regulated a minimum of 150% under both insulin resistant conditions^a

No.	Protein ID	Identified Proteins	LGPUG/LG	HGINS/LG	Ave. SC	SD	Ave. Peptides	SD
1	Q96D15	Reticulocalbin-3	9.00	8.52	11.50	2.89	3.00	1.15
2	Q9NRN5	Olfactomedin-like protein 3	5.40	7.57	13.60	6.31	3.00	0.00
3	P09603	Macrophage colony-stimulating factor 1	2.98	5.02	5.00	1.87	1.60	0.55
4	Q59H37	Laminin alpha 2 subunit isoform b	1.73	4.60	11.50	6.45	4.50	1.91
5	Q15113	Procollagen C-endopeptidase enhancer 1	1.53	4.11	14.00	3.56	3.75	0.50
6	Q07507	Dermatopontin	2.01	2.93	10.40	2.88	2.00	0.00
7	Q02809	Procollagen-lysine,2-oxoglutarate 5-dioxygenase 1	2.70	2.80	11.17	4.83	3.83	0.98
8	P36222	Chitinase-3-like protein 1	1.49	2.68	26.00	8.05	6.33	0.52
9	P05997	Collagen alpha-2(V) chain	1.55	2.44	9.33	2.89	2.67	0.58
10	Q9Y240	C-type lectin domain family 11 member A	2.07	2.44	11.00	2.00	3.00	0.00
11	Q06828	Fibromodulin	1.76	2.38	15.75	2.06	2.00	1.15
12	O00391	Sulfhydryl oxidase 1	2.20	2.27	8.17	3.06	2.67	0.52
13	P15144	Aminopeptidase N	2.19	2.03	22.00	13.34	4.33	1.86
14	Q99538	Legumain	1.60	1.92	11.67	4.18	1.83	0.98
15	Q6UXB8	Protease inhibitor 16	1.97	1.75	15.75	1.50	2.50	0.58
16	P09486	SPARC	1.48	1.74	263.00	169.53	10.33	1.37
17	P07942	Laminin subunit beta-1	1.48	1.69	63.67	13.34	16.83	1.72
18	O75326	Semaphorin-7A	1.95	1.66	21.17	8.89	3.67	1.03
19	P10909	Clusterin	1.77	1.63	17.00	6.39	3.17	0.75
20	P24821	Tenascin	1.61	1.54	37.33	4.76	9.83	1.72
No.	Protein ID	Identified Proteins	LG/LGPUG	LG/HGINS	Ave. SC	SD	Ave. Peptides	SD
1	P61769	Beta-2-microglobulin	2.40	1.90	68.17	35.76	3.17	0.98
2	P00739	Haptoglobin-related protein	1.87	1.66	5.67	0.58	2.00	0.00
3	Q16270	Insulin-like growth factor-binding protein 7	1.75	1.59	19.00	9.76	4.33	1.03
4	O95965	Integrin beta-like protein 1	1.68	1.57	9.00	1.41	3.00	0.00

^a LGPUG: low glucose plus PUGNAC; HGINS: high glucose plus insulin as two insulin resistant conditions; Ave. SC: average total spectral count and SD: standard deviation.

Table 3-3. Identification of N-linked glycosylation sites using PNGase F with the incorporation of ¹⁸O water in human adipocytokines

No.	Protein ID	Identified Proteins	N-linked Peptides ^a
1	P15144	Aminopeptidase N	KLN@YTLSQGHR
2	P21810	Biglycan	LLQVVYLHSNN@ITK
3	P16870	Carboxypeptidase E	GN@ETIVNLIHSTR
4	P07339	Cathepsin D	GSLSYLN@VTR
5	P43235	Cathepsin K	SN@DTLYIPEWEGR
6	P07711	Cathepsin L	YSVAN@DTGFVDIPK
7	P07711	Cathepsin L	YSVAN@DTGFVDIPKQEK
8	P10909	Clusterin	LAN@LTQGEDQYYLR
9	P02461	Collagen alpha-1(III) chain	ASQN@ITYHCK
10	P02461	Collagen alpha-1(III) chain	DGSPGGKGDRCEN@GSPGAPGAPGHPGPPGVPAGK
11	P20908	Collagen alpha-1(V) chain	VYCN@FTAGGSTCVFPDKK
12	P12109	Collagen alpha-1(VI) chain	ENYAELLEDAFLKN@VTAQICIDKK
13	P12109	Collagen alpha-1(VI) chain	GEDGPAGN@GTEGFPGFPGYPGNR
14	P12109	Collagen alpha-1(VI) chain	N@FTAADWGQSR
15	P12109	Collagen alpha-1(VI) chain	RN@FTAADWGQSR
16	Q02388	Collagen alpha-1(VII) chain	TAPEPVGRVSRQLLN@ASSDVLR
17	Q99715	Collagen alpha-1(XII) chain	EAGN@ITTDGYEILGK
18	P08123	Collagen alpha-2(I) chain	LLANYASQN@ITYHCK
19	P05997	Collagen alpha-2(V) chain	EASQN@ITYICK
20	P12111	Collagen alpha-3(VI) chain	GNPGEPLN@GTTGPKGIR
21	P12111	Collagen alpha-3(VI) chain	GPPGVN@GTQGFQGCPCQR
22	P12111	Collagen alpha-3(VI) chain	GYPGDEGGPGERGPPGVN@GTQGFQGCPCQR
23	P09871	Complement C1s subcomponent	NCGVN@CSGDVFTALIGEIASPNYPKYPENS
24	O75462	Cytokine receptor-like factor 1	VLN@ASTLALALANLN@GSR
25	O75462	Cytokine receptor-like factor 1	VVDDVSN@QTSCR
26	P07585	Decorin	IADTN@ITSIPQGLPSSLTELHLDGNK
27	P07585	Decorin	LGLSFNSISAVDN@GSLANTPHLR

Table 3-3. Continued.

No.	Protein ID	Identified Proteins	N-linked Peptides ^a
28	Q9UBP4	Dickkopf-related protein 3	GSN@GTICDNQR
29	Q13822	Ectonucleotide pyrophosphatase/phosphodiesterase 2	AEGWEEGPPTVLSDSPWTN@ISGSCK
30	Q13822	Ectonucleotide pyrophosphatase/phosphodiesterase 2	AIAN@LTCK
31	Q9Y6C2	EMILIN-1	LGALN@SSLQLLEDR
32	P35555	Fibrillin-1	TAIFAFN@ISHVSNK
33	P02751	Fibronectin	DQCIVDDITYNVN@DTFHKR
34	P02751	Fibronectin	DQCIVDDITYNVN@DTFHK
35	P02751	Fibronectin	LDAPTNLQFVN@ETDSTVLVR
36	Q12841	Follistatin-related protein 1	GSN@YSEILDK
37	Q12841	Follistatin-related protein 1	GSN@YSEILDKYFK
38	P09382	Galectin-1	FNAHGDANTIVCNSK
39	Q08380	Galectin-3-binding protein	ALGFEN@ATQALGR
40	Q08380	Galectin-3-binding protein	DAGVVCTN@ETR
41	Q08380	Galectin-3-binding protein	TVIRPFYLTN@SSGVD
42	P00738	Haptoglobin	VVLHPN@YSQVDIGLIK
43	O75629	Human Protein CREG1	LN@ITNIWVLDYFGGPK
44	P17936	Insulin-like growth factor-binding protein 3	GLCVN@ASAVSR
45	O14498	ISLR	SLDLSHNLISDFAWSDLHN@LSALQLLK
46	Q8NHP8	LAMA-like protein 2	SDLNPAN@GSYPFKALR
47	Q16363	Laminin subunit alpha-4	DAVRN@LTEVVPQLLDQLR
48	Q16363	Laminin subunit alpha-4	FYFGGSPISAQYAN@FTGCISNAYFTR
49	Q16363	Laminin subunit alpha-4	LITEEAN@R
50	Q16363	Laminin subunit alpha-4	LTLSELDDIKN@ASGIYAEIDGAK
51	Q16363	Laminin subunit alpha-4	RPASN@VSASIQR
52	P07942	Laminin subunit beta-1	LSDTTSQSN@STAK
53	P11047	Laminin subunit gamma-1	VN@NTLSSQISR
54	P11047	Laminin subunit gamma-1	KYEQAKN@ISQDLEK
55	P11047	Laminin subunit gamma-1	LLNN@LTSIK
56	P11047	Laminin subunit gamma-1	TAN@DTSTEAYNLLLR
57	P11047	Laminin subunit gamma-1	TLAGEN@QTAFEIEELNR
58	P11047	Laminin subunit gamma-1	VNDN@KTAAEEALR

Table 3-3. Continued.

No.	Protein ID	Identified Proteins	N-linked Peptides ^a
59	Q14767	Latent-transforming growth factor beta-binding protein 2	DGTQQAVPLEHPSSPWGLN@LTEK
60	P51884	Lumican	AFEN@VTDLQWLILDHNLENSK
61	P51884	Lumican	LGSFEGLVN@LTFIHLQHNR
62	P51884	Lumican	LHINHNN@LTESVGPLPK
63	P13473	Lysosome-associated membrane glycoprotein 2	IAVQFGPGFSWIAN@FTK
64	P01033	Metalloproteinase inhibitor 1	AKFVGTPEVN@QTTLYQR
65	P01033	Metalloproteinase inhibitor 1	FVGTPEVN@QTTLYQR
66	P01033	Metalloproteinase inhibitor 1	SHN@RSEEFLIAGK
67	Q9NRN5	Olfactomedin-like protein 3	IYVLDGTQN@DTAFVFPFR
68	P26022	Pentraxin-related protein PTX3	ATDVLN@K
69	Q15063	Periostin	EVN@DTLLVNELK
70	Q15063	Periostin	IFLKEVN@DTLLVNELK
71	P98160	Perlecan	SLTQGSIVGDLPVN@GTSQ GK
72	P55058	Phospholipid transfer protein	VSN@VSCQASVSR
73	P36955	Pigment epithelium-derived factor	VTQN@LTLIEESLTSEFIHDIDR
74	P36955	Pigment epithelium-derived factor	VTQN@LTLIEESLTSEFIHDIDRELK
75	P05155	Plasma protease C1 inhibitor	VGQLQLSHN@LSLVILVPQNLK
76	P05155	Plasma protease C1 inhibitor	VLSN@NSDANLELINTWVAK
77	P07602	Proactivator polypeptide [Contains: Saposin-A]	TN@STFVQALVEHVK
78	P07602	Proactivator polypeptide [Contains: Saposin-A]	LIDNN@KTEK
79	P07602	Proactivator polypeptide [Contains: Saposin-A]	LIDNN@KTEKEILDADF K
80	P07602	Proactivator polypeptide [Contains: Saposin-A]	NLEKN@STK
81	P07602	Proactivator polypeptide [Contains: Saposin-A]	NLEKN@STKQEILAALEK
82	P07602	Proactivator polypeptide [Contains: Saposin-A]	TN@STFVQALVEHVKEECDR
83	P09486	SPARC	VCSNDN@K
84	P09486	SPARC	VCSNDN@KTFDSSCHFFATK
85	P24821	Tenascin	N@TTSYVLR
86	P24821	Tenascin	LN@YSLPTGQWVGVQLPR
87	P07996	Thrombospondin-1	VVN@STTGPGHEHLR
88	P35442	Thrombospondin-2	VVN@STTGTGEHLR

Table 3-3. Continued.

No.	Protein ID	Identified Proteins	N-linked Peptides ^a
89	Q6FGX5	TIMP1 protein	FVGTPEVN@QTTLYQR
90	Q6FGX5	TIMP1 protein	SHN@RSEEFLIAGK
91	Q6EMK4	Vasorin	LHEITN@ETFR

^a An @ indicates the site of N-linked glycosylation.

Table 3-4. Relative quantification of N-linked glycans from human adipocytes between insulin resistant conditions and insulin response condition by $^{13}\text{C}/^{12}\text{C}$ ratio and prevalence ratio

No.	N-linked oligosaccharide composition	Z	[M+zNa] ^{z+} (mono)		ΔM (m/z)	LGPUG/LG		HGINS/LG		Ave. prevalence (%)			Prevalence ratios	
			¹² C	¹³ C		¹³ C/ ¹² C ratios	SD	¹³ C/ ¹² C ratios	SD	LGPUG	HGINS	LG	LGPUG /LG	HGINS /LG
1	(Man)2(GlcNAc)2	1	967.484	981.531	14.047	0.49	0.31	0.58	0.34	0.20	0.23	0.46	0.45	0.50
2	(Man)2(GlcNAc)2(Fuc)1	1	1141.573	1157.626	16.054	0.30	0.14	0.39	0.15	0.52	0.66	1.81	0.29	0.37
3	(Man)3(GlcNAc)2	1	1171.583	1188.640	17.057	0.35	0.12	0.49	0.13	0.68	0.93	1.87	0.36	0.50
4	(Man)3(GlcNAc)2(Fuc)1	1	1345.673	1364.736	19.064	0.32	0.01	0.55	0.01	1.42	2.30	3.79	0.38	0.61
5	(Man)4(GlcNAc)2	1	1375.683	1395.750	20.067	0.52	0.06	0.59	0.10	0.71	0.78	1.15	0.61	0.68
6	(Man)5(GlcNAc)2	1	1579.783	1602.860	23.077	0.74	0.25	0.80	0.31	7.74	7.60	8.44	0.92	0.90
		2	801.386	812.925	11.539	0.64	0.33	0.79	0.33	0.85	0.85	1.05	0.82	0.81
7	(GlcNAc)1(Man)3(GlcNAc)2(Fuc)1	1	1590.799	1612.873	22.074	0.97	0.28	0.73	0.35	0.87	0.59	0.73	1.19	0.81
8	(Gal)1(GlcNAc)1(Man)3(GlcNAc)2	1	1620.810	1643.887	23.077	0.86	0.51	0.91	0.68	0.59	0.56	0.61	0.97	0.92
		2	821.900	833.438	11.539	1.92	1.65	1.82	1.32	0.12	0.11	0.06	1.93	1.85
9	(Man)6(GlcNAc)2	1	1783.883	1809.970	26.087	0.78	0.26	0.90	0.36	8.28	8.91	8.67	0.95	1.03
		2	903.436	916.480	13.044	0.75	0.29	0.88	0.40	3.26	3.29	3.47	0.94	0.95
10	(Gal)1(GlcNAc)1(Man)3(GlcNAc)2(Fuc)1	1	1794.899	1819.983	25.084	0.51	0.27	0.80	0.51	0.56	0.81	0.95	0.59	0.85
		2	908.944	921.486	12.542	0.92	0.51	1.75	1.79	0.20	0.21	0.17	1.16	1.24
11	(GlcNAc)1(Man)5(GlcNAc)2	1	1824.909	1850.997	26.087	1.13	0.83	1.37	1.10	2.14	2.30	1.80	1.19	1.28
		2	923.950	936.993	13.044	1.22	0.93	1.61	1.37	1.28	1.36	0.97	1.32	1.41
12	(GlcNAc)2(Man)3(GlcNAc)2(Fuc)1	1	1835.925	1861.009	25.084	2.14	0.25	0.66	0.22	0.77	0.22	0.30	2.58	0.75
		2	929.458	942.000	12.542	0.76	0.15	0.17	0.09	0.22	0.09	0.36	0.60	0.25
13	(Gal)1(GlcNAc)2(Man)3(GlcNAc)2	2	944.463	957.506	13.044	1.68	1.26	1.24	0.78	0.28	0.27	0.18	1.55	1.47
14	(NeuAc)1(Gal)1(GlcNAc)1(Man)3(GlcNAc)2	2	1002.487	1016.534	14.047	0.23	0.04	0.40	0.22	0.07	0.10	0.23	0.29	0.41
15	(Man)7(GlcNAc)2	2	1005.486	1020.035	14.549	0.83	0.36	0.97	0.50	4.01	4.10	3.94	1.02	1.04
16	(GlcNAc)1(Man)5(GlcNAc)2(Fuc)1	2	1010.994	1025.041	14.047	0.98	0.63	1.08	0.81	0.56	0.51	0.49	1.15	1.04
17	(Gal)1(GlcNAc)1(Man)5(GlcNAc)2	2	1025.999	1040.548	14.549	1.20	0.80	1.31	1.05	2.05	1.94	1.54	1.33	1.26
18	(Gal)1(GlcNAc)2(Man)3(GlcNAc)2(Fuc)1	2	1031.507	1045.554	14.047	1.22	0.77	0.98	0.79	1.28	0.84	0.90	1.42	0.93

Table 3-4. Continued.

No.	N-linked oligosaccharide composition	Z	[M+zNa] ^{z+} (mono)		ΔM (m/z)	LGPUG/LG		HGINS/LG		Ave. prevalence (%)			Prevalence ratios	
			¹² C	¹³ C		¹³ C/ ¹² C ratios	SD	¹³ C/ ¹² C ratios	SD	LGPUG	HGINS	LG	LGPUG /LG	HGINS /LG
19	(Gal)2(GlcNAc)2(Man)3(GlcNAc)2	2	1046.513	1061.061	14.549	1.01	0.67	1.21	0.88	3.72	3.93	3.29	1.13	1.20
20	(GlcNAc)3(Man)3(GlcNAc)2(Fuc)1	2	1052.021	1066.068	14.047	3.63	4.08	2.19	2.20	0.03	0.02	0.01	2.99	2.13
21	(NeuAc)1(Gal)1(GlcNAc)1(Man)3(GlcNAc)2 (Fuc)1	2	1089.531	1104.582	15.050	0.62	0.67	1.46	1.04	0.20	0.50	0.34	0.59	1.46
22	(NeuAc)1(Gal)1(GlcNAc)1(Man)1(Man)3 (GlcNAc)2	2	1104.536	1120.088	15.552	0.92	0.64	1.16	0.89	1.59	1.63	1.51	1.06	1.08
23	(Man)8(GlcNAc)2	2	1107.536	1123.590	16.054	0.80	0.36	0.97	0.53	7.76	8.26	7.96	0.97	1.04
24	(Gal)1(GlcNAc)1(Man)5(GlcNAc)2(Fuc)1	2	1113.044	1128.596	15.552	1.18	0.90	1.17	1.06	0.27	0.20	0.20	1.31	0.99
25	(NeuAc)1(Gal)1(GlcNAc)2(Man)3(GlcNAc)2	2	1125.050	1140.602	15.552	1.45	0.72	2.45	2.40	0.27	0.23	0.14	1.95	1.70
26	(Gal)2(GlcNAc)2(Man)3(GlcNAc)2(Fuc)1	2	1133.557	1149.109	15.552	1.03	0.66	1.13	0.75	10.46	10.46	8.97	1.17	1.17
27	(NeuAc)1(Gal)2(GlcNAc)1(Man)3(GlcNAc)2 (Fuc)1	2	1191.581	1208.136	16.555	1.73	1.80	2.26	2.45	0.22	0.21	0.15	1.45	1.44
28	(NeuAc)1(Gal)3(GlcNAc)1(Man)3(GlcNAc)2	2	1206.586	1223.643	17.057	0.95	0.59	0.94	0.71	1.05	0.92	0.98	1.07	0.94
29	(Man)9(GlcNAc)2	2	1209.586	1227.145	17.559	0.90	0.47	1.19	0.74	7.32	8.67	6.91	1.06	1.25
30	(Gal)2(GlcNAc)2(Fuc)1(Man)3(GlcNAc)2 (Fuc)1	2	1220.602	1237.157	16.555	1.27	1.11	1.51	1.50	0.60	0.53	0.46	1.32	1.16
31	(NeuAc)1(Gal)2(GlcNAc)2(Man)3(GlcNAc)2	2	1227.100	1244.157	17.057	0.93	0.56	1.02	0.68	2.72	2.62	2.53	1.08	1.03
32	(Gal)2(GlcNAc)3(Man)3(GlcNAc)2(Fuc)1	2	1256.121	1273.178	17.057	1.43	1.51	2.15	2.50	0.13	0.11	0.09	1.42	1.22
33	(Gal)3(GlcNAc)3(Man)3(GlcNAc)2	2	1271.126	1288.685	17.559	3.01	3.65	2.33	2.67	0.28	0.33	0.19	1.47	1.75
34	(NeuAc)1(Gal)2(GlcNAc)2(Man)3(GlcNAc)2 (Fuc)1	2	1314.144	1332.205	18.060	1.07	0.71	1.14	0.82	6.36	6.01	5.30	1.20	1.13
35	(Gal)3(GlcNAc)3(Man)3(GlcNAc)2(Fuc)1	2	1358.171	1376.733	18.562	1.53	0.93	1.78	1.38	1.72	1.64	0.97	1.77	1.69
36	(NeuAc)1(Gal)2(GlcNAc)2(Fuc)1(Man)3 (GlcNAc)2(Fuc)1	2	1401.189	1420.253	19.064	1.08	1.02	1.70	1.87	0.37	0.37	0.35	1.08	1.06
37	(NeuAc)2(Gal)2(GlcNAc)2(Man)3(GlcNAc)2	3	1407.687	1427.252	19.565	0.67	0.28	0.54	0.33	1.62	1.16	2.01	0.81	0.58
38	(NeuAc)1(Gal)3(GlcNAc)3(Man)3(GlcNAc)2	2	1451.713	1471.780	20.067	1.41	1.29	1.33	1.25	0.74	0.65	0.57	1.30	1.15
39	(NeuAc)2(Gal)2(GlcNAc)2(Man)3(GlcNAc)2 (Fuc)1	2	1494.731	1515.300	20.569	0.99	0.69	1.07	0.83	3.58	3.36	3.27	1.10	1.03
40	(NeuAc)2(Gal)3(GlcNAc)2(Man)3(GlcNAc)2	3	1509.736	1530.807	21.070	0.88	0.83	1.10	1.08	0.40	0.39	0.46	0.86	0.84
41	(NeuAc)1(Gal)3(GlcNAc)3(Man)3(GlcNAc)2 (Fuc)1	2	1538.757	1559.828	21.070	0.91	0.61	0.96	0.66	2.17	2.04	2.11	1.03	0.96

Table 3-4. Continued.

No.	N-linked oligosaccharide composition	Z	[M+zNa] ^{z+} (mono)		ΔM (m/z)	LGPUG/LG		HGINS/LG		Ave. prevalence (%)			Prevalence ratios	
			¹² C	¹³ C		¹³ C/ ¹² C ratios	SD	¹³ C/ ¹² C ratios	SD	LGPUG	HGINS	LG	LGPUG /LG	HGINS /LG
42	(NeuAc)2(Gal)3(GlcNAc)3(Man)3(GlcNAc)2	2	1632.300	1654.875	22.575	0.81	0.55	0.63	0.59	0.73	0.44	0.80	0.91	0.55
		3	1095.863	1110.913	15.050	1.08	0.85	0.83	0.98	0.14	0.06	0.11	1.21	0.55
43	(NeuAc)2(Gal)3(GlcNAc)3(Man)3(GlcNAc)2 (Fuc)1	2	1719.344	1742.923	23.579	1.22	1.01	0.99	0.82	1.75	1.40	1.47	1.19	0.95
		3	1153.893	1169.612	15.719	1.29	1.42	1.35	1.34	0.38	0.33	0.34	1.14	0.98
44	(NeuAc)1(Gal)4(GlcNAc)4(Man)3(GlcNAc)2 (Fuc)1	2	1763.370	1787.451	24.081	1.92	1.70	2.11	2.06	0.63	0.56	0.35	1.78	1.57
		3	1183.244	1199.297	16.054	0.75	0.59	1.15	1.30	0.06	0.05	0.07	0.96	0.74
45	(NeuAc)3(Gal)3(GlcNAc)3(Man)3(GlcNAc)2	2	1812.887	1837.970	25.084	0.42	0.28	0.18	0.12	0.48	0.19	1.01	0.47	0.19
		3	1216.254	1232.977	16.723	0.70	0.36	0.68	0.38	0.24	0.17	0.26	0.90	0.66
46	(NeuAc)3(Gal)3(GlcNAc)3(Man)3(GlcNAc)2 (Fuc)1	2	1899.931	1926.018	26.087	1.08	1.11	1.13	1.25	0.43	0.39	0.51	0.85	0.78
		3	1274.284	1291.675	17.391	1.72	1.91	1.86	2.09	0.13	0.13	0.11	1.23	1.24
47	(NeuAc)2(Gal)4(GlcNAc)4(Man)3(GlcNAc)2 (Fuc)1	2	1943.957	1970.546	26.589	1.15	1.10	1.45	1.66	0.36	0.34	0.37	0.98	0.93
		3	1303.635	1321.361	17.726	1.65	1.93	1.19	1.33	0.15	0.13	0.14	1.05	0.89
48	(NeuAc)3(Gal)4(GlcNAc)4(Man)3(GlcNAc)2 (Fuc)1	3	1424.026	1443.424	19.398	0.93	0.84	1.48	1.60	0.13	0.12	0.13	1.04	0.90

Table 3-5. Relative quantification of O-linked glycans from human adipocytes between insulin resistant conditions and insulin responsive condition by $^{13}\text{C}/^{12}\text{C}$ ratio and prevalence ratio

No.	O-linked oligosaccharide composition	Z	[M+zNa] ^{z+} (mono)		ΔM (m/z)	LGPUG/LG		HGINS/LG		Ave. prevalence (%)			Prevalence ratios	
			¹² C	¹³ C		¹³ C/ ¹² C ratios	SD	¹³ C/ ¹² C ratios	SD	LGPUG	HGINS	LG	LGPUG/LG	HGINS/LG
1	(Hex)1(HexNAc)1	1	534.289	543.319	9.030	1.46	0.66	1.51	0.62	4.95	3.94	3.52	1.41	1.12
2	(Xyl)2(Glc)1	1	609.310	619.343	10.034	1.81	1.05	1.53	0.66	0.89	0.63	0.51	1.75	1.24
3	(NeuAc)1(Hex)1	1	650.337	661.374	11.037	1.34	0.42	1.43	0.40	1.35	1.15	1.22	1.11	0.95
4	(Hex)1(HexNAc)1(Hex)1	1	738.389	750.429	12.040	1.56	1.55	1.87	1.24	0.18	0.14	0.11	1.60	1.22
5	(Hex)1(HexNAc)2	1	779.415	791.455	12.040	2.28	0.51	1.26	0.37	1.09	0.50	0.57	1.91	0.89
6	(NeuAc)1(Hex)1(HexNAc)1	1	895.463	909.510	14.047	1.20	0.38	1.32	0.35	27.95	27.68	27.90	1.00	0.99
7	(Hex)2(HexNAc)2	1	983.515	998.565	15.050	1.25	0.48	1.32	0.38	6.89	6.58	6.14	1.12	1.07
8	(NeuAc)1(Hex)1(HexNAc)2	1	1140.589	1157.810	17.221	1.70	0.44	1.32	0.42	3.53	2.28	3.02	1.17	0.75
9	(NeuAc)2(Hex)1(HexNAc)1	1	1256.636	1275.700	19.064	1.10	0.19	1.32	0.16	21.65	24.34	25.28	0.86	0.96
10	(NeuAc)1(Hex)2(HexNAc)2	1	1344.689	1364.756	20.067	1.38	0.37	1.63	0.29	13.32	13.49	12.28	1.08	1.10
11	(NeuAc)2(Hex)2(HexNAc)2	1	1705.862	1730.946	25.084	1.10	0.29	1.40	0.27	12.14	14.00	13.85	0.88	1.01
		2	864.426	876.968	12.542	1.18	0.31	1.51	0.31	4.53	4.15	4.33	1.05	0.96
12	(NeuAc)1(Hex)4(HexNAc)4	2	1133.065	1149.119	16.054	1.31	0.56	1.31	0.28	1.55	1.11	1.27	1.21	0.87

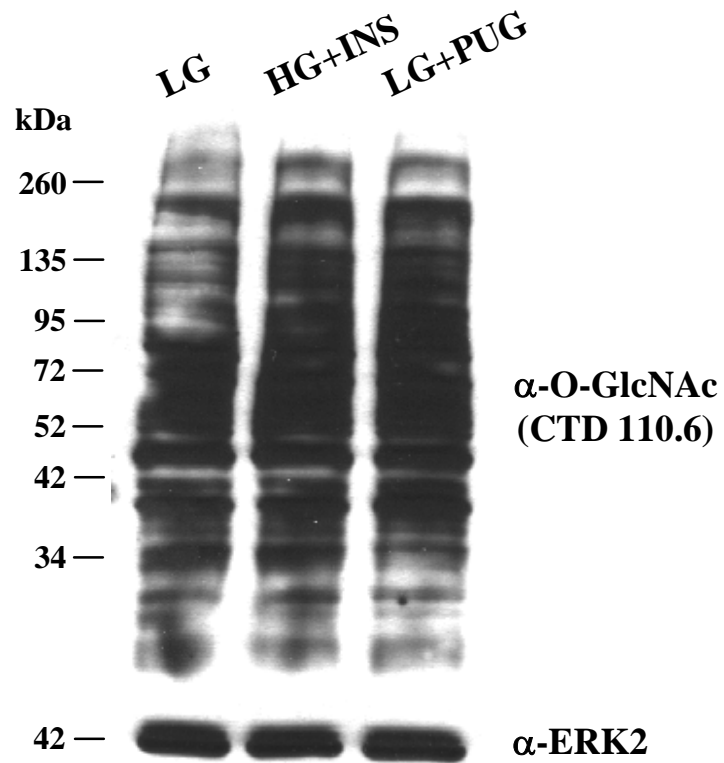


Figure 3-1. Detection of O-GlcNAc levels from nucleocytoplasmic proteins of human adipocytes. Global O-GlcNAc levels are moderately elevated under two insulin resistant conditions by either high glucose plus chronic insulin exposure (HG+INS) or PUGNac (PUG).

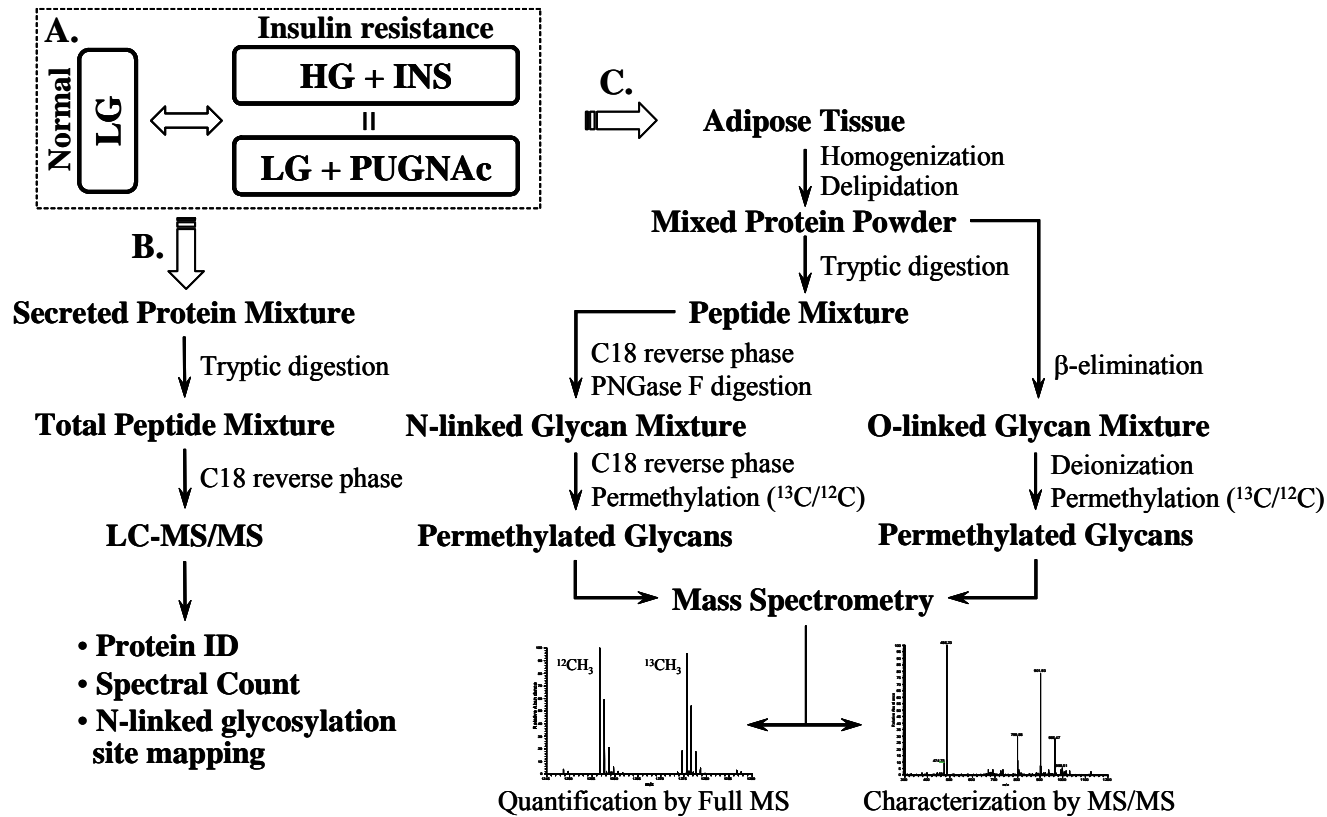


Figure 3-2. Schematic flow diagram of the experimental procedure. (A) Human adipose tissues are conditioned by insulin responsive (LG, low glucose) or two insulin resistance conditions (hyperglycemia plus hyperinsulinemia, HG+INS and PUGNAc). (B) Identification and quantification of the secretory proteome analysis and N-linked glycosylation site mapping by ¹⁸O water labeling with PNGase F using LC-MS/MS. (C) Characterization and relative abundance of N- and O-linked glycans from whole protein extract in human adipose tissues.

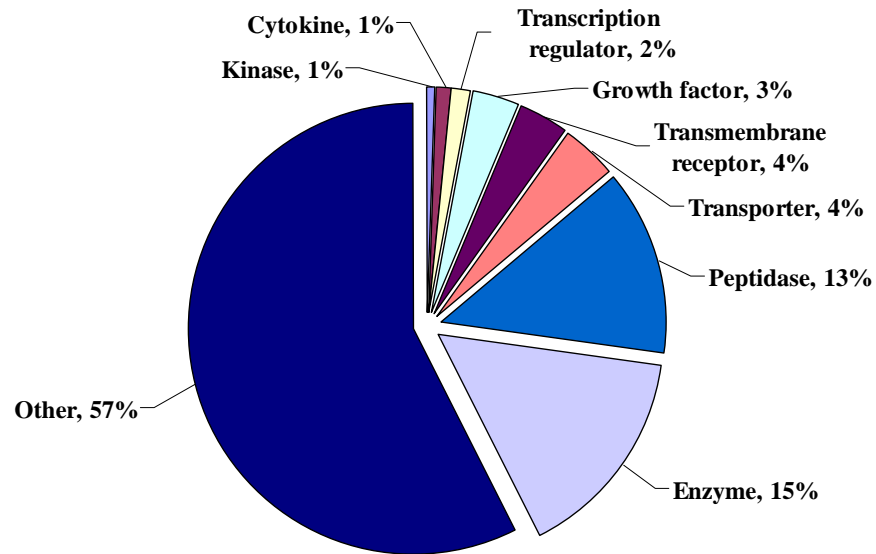


Figure 3-3. The functional categories of secretome from human adipocytes. The biological function analysis was determined for each protein based on the Ingenuity Pathway Analysis software (Ingenuity Systems).

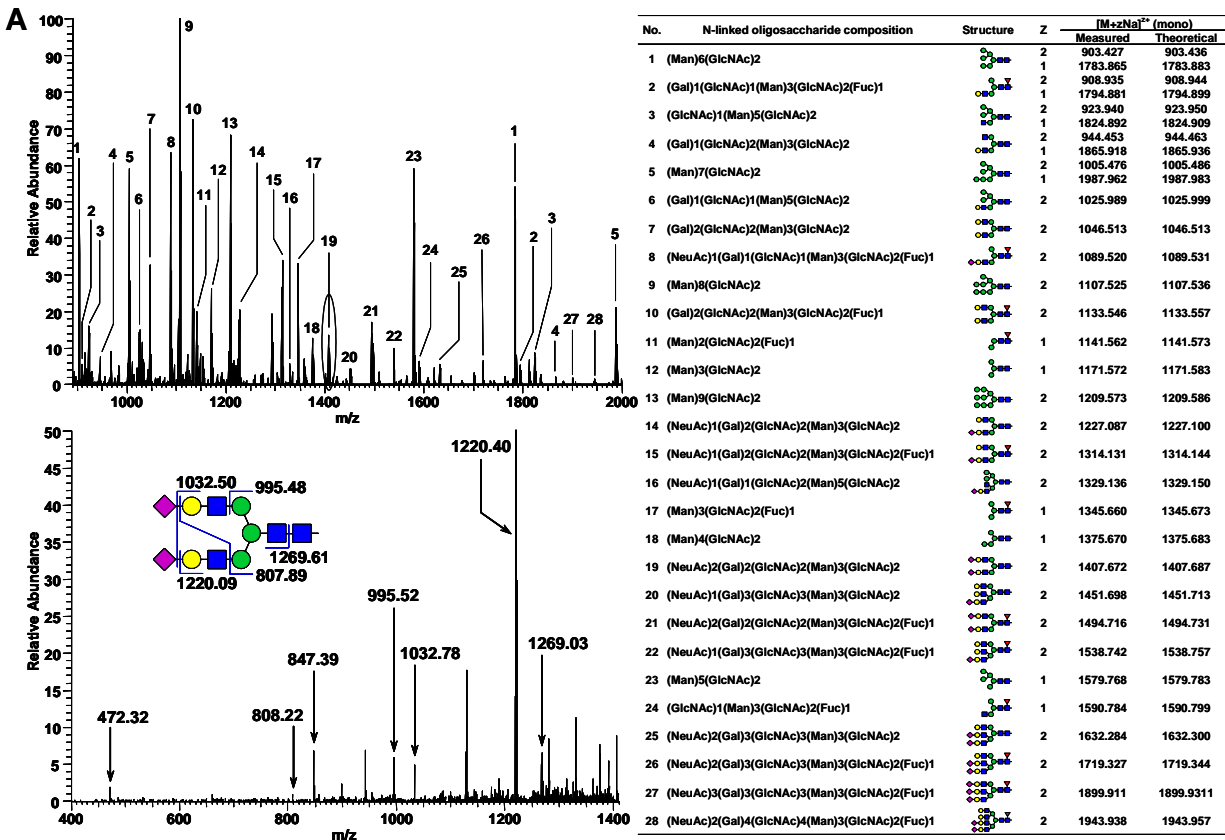


Figure 3-4. Characterization of glycome from human adipocytes by NS-MS and TIM scan. (A) Upper left panel: a full FTMS spectrum of the N-linked glycan mixture, lower left panel: the characterization of a biantennary complex N-linked glycan structure by MS/MS fragmentation, right panel: a list of predominant N-linked glycans. (B) Upper left panel: a full FTMS spectrum of the O-linked glycan mixture, upper right panel: the characterization of a core 2 O-linked glycan structure by MS/MS fragmentation, lower panel: a list of predominant O-linked glycans.

☆: Xyl, ▼: Fuc, ●: Glc, ●: Man, ●: Gal, ■: GlcNAc, ■: GalNAc, and ◆: NeuAc

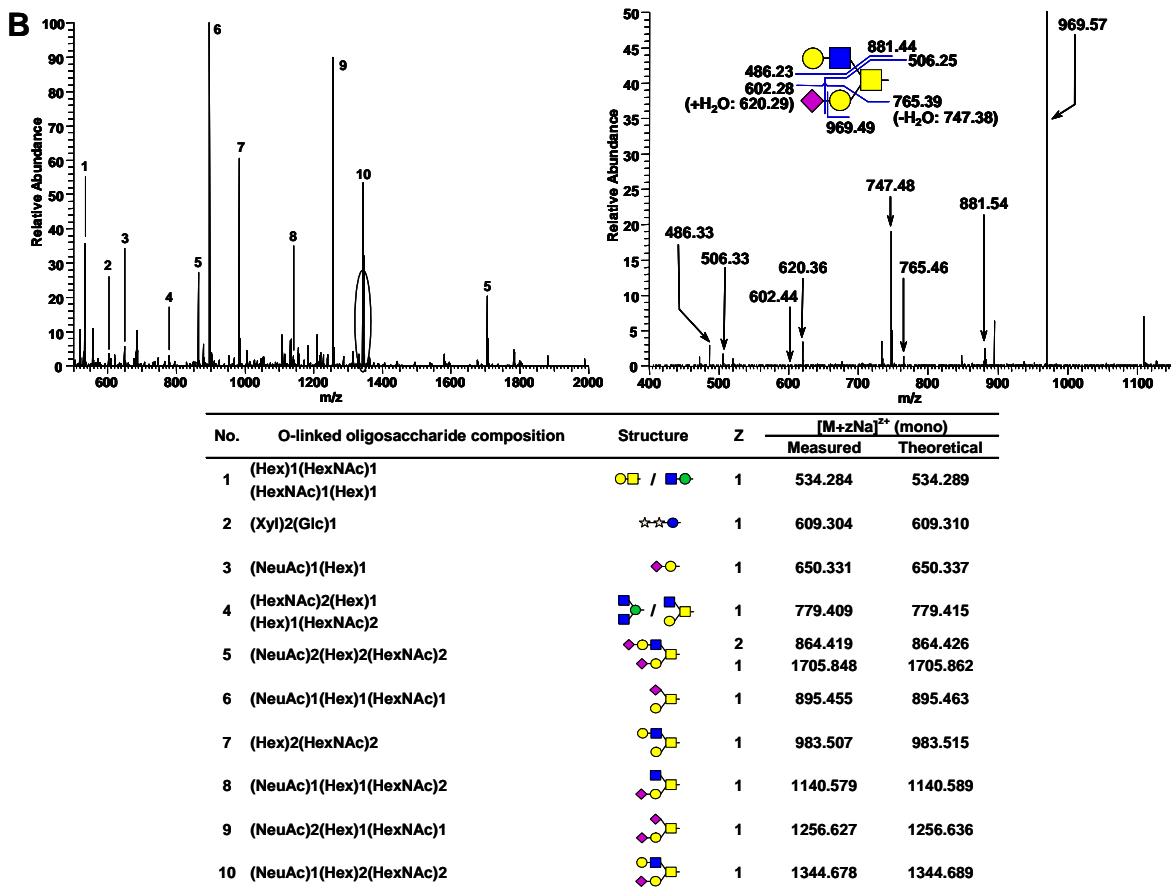


Figure 3-4. Continued.

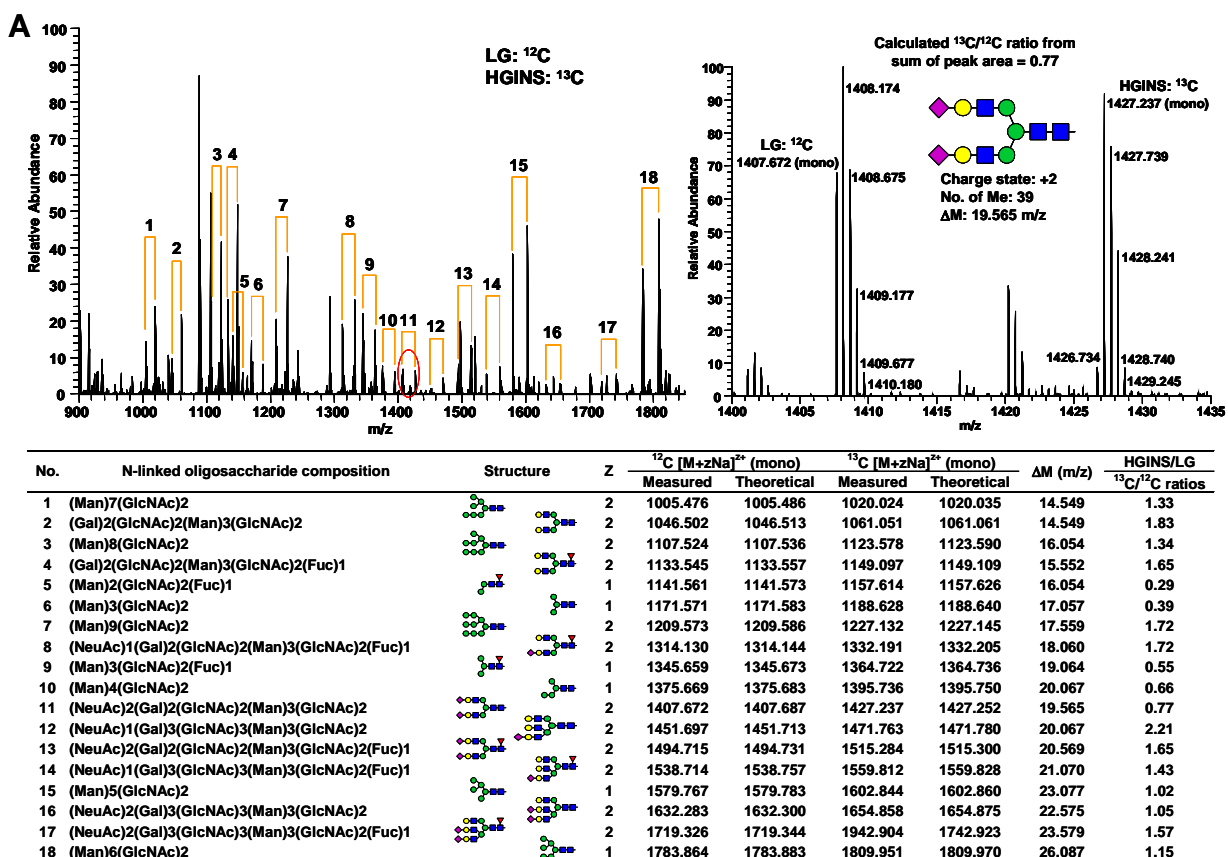


Figure 3-5. Relative quantification of glycome from human adipocytes with insulin resistant conditions using ¹³C/¹²C labeling. (A) Upper left panel: a full FTMS spectrum of ¹³C/¹²C labeled N-linked glycans in HGINS and LG, upper right panel: a FTMS spectrum to calculate ¹³C/¹²C ratios from sum of isotopic peak area between the isotopic pairs, lower panel: a list of relative ratios in HGINS and LG for predominant N-linked glycans. (B) Upper left panel: a full FTMS spectrum of ¹³C/¹²C labeled O-linked glycans in LGPUG and LG, upper right panel: a FTMS spectrum to calculate ¹³C/¹²C ratios from sum of isotopic peak area between the isotopic pairs, lower panel: a list of relative ratios in LGPUG and LG for predominant O-linked glycans.

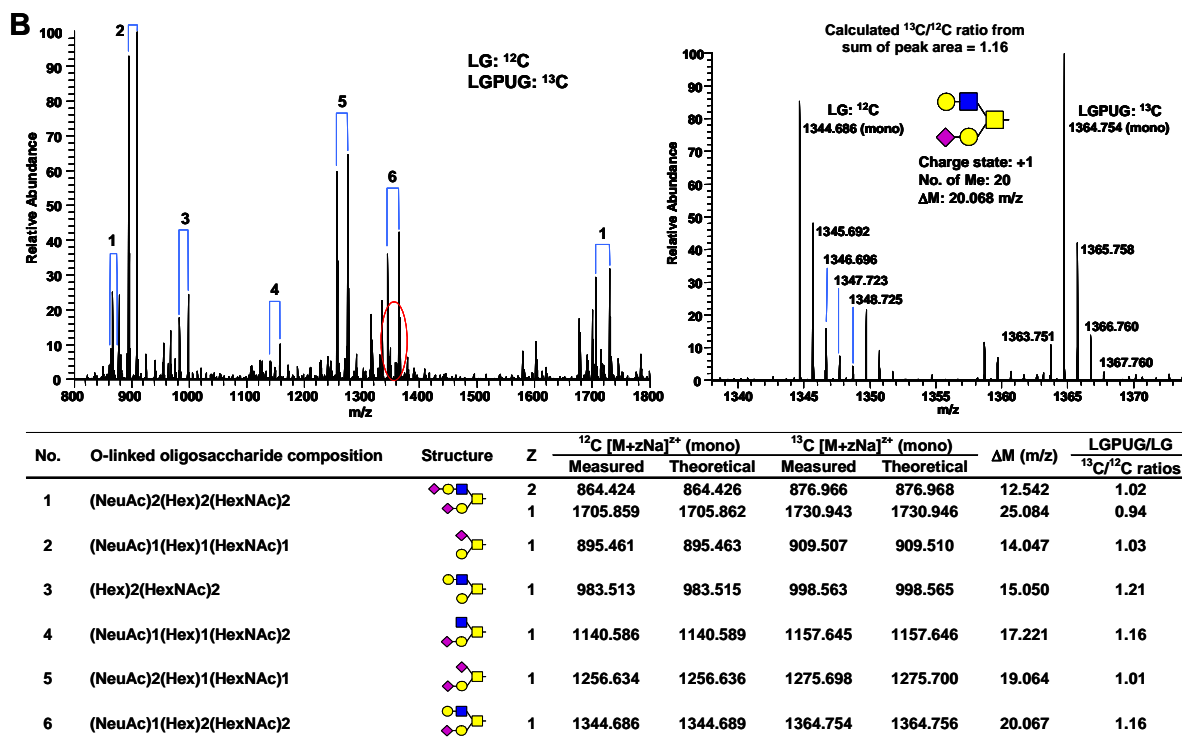


Figure 3-5. Continued.

SUPPORTING INFORMATION

Table 3-S1. The list of secreted proteins for single peptide detection from human adipose tissues

Table 3-S2. Human adipocytokines regulated a minimum of 150% under one of the insulin resistant conditions

Table 3-S3. Characterization of total N-linked glycans from human adipocytes by NS-MS and TIM scan

Table 3-S4. Characterization of total O-linked glycans from human adipocytes by NS-MS and TIM scan

Table 3-S1. The list of secreted proteins for a single peptide detection from human adipose tissues

No.	Protein ID	Identified Peptides	Subcellular Location ^a
1	O75882	Attractin	Extracellular
2	P15291	Beta-1,4-galactosyltransferase 1	Cytoplasm
3	P01034	Cystatin-C	Extracellular
4	P15502	Elastin	Extracellular
5	P19883	Follistatin	Extracellular
6	P17900	Ganglioside GM2 activator	Cytoplasm
7	P02788	Growth-inhibiting protein 12	Extracellular
8	P03956	Interstitial collagenase	Extracellular
9	P25391	Laminin subunit alpha-1	Extracellular
10	Q5VUM2	Laminin, alpha 2	Extracellular
11	P14174	Macrophage migration inhibitory factor	Extracellular
12	Q13361	Microfibrillar-associated protein 5	Extracellular
13	Q99497	Oncogene DJ1	Unknown
14	P45877	Peptidyl-prolyl cis-trans isomerase C	Cytoplasm
15	Q92954	Proteoglycan-4	Extracellular
16	Q9HCB6	Spondin-1	Extracellular
17	Q9NPK8	Tenascin XB	Extracellular

^a The subcellular location was determined for each protein based on the Ingenuity Pathway Analysis software (Ingenuity Systems).

Table 3-S2. Human adipocytokines regulated a minimum of 150% under one of the insulin resistant conditions

No.	Protein ID	Identified Proteins	LGPUG/LG	HGINS/LG	Ave. SC	SD	Ave. Peptides	SD
1	P17936	Insulin-like growth factor-binding protein 3	1.78	1.02	12.83	2.23	2.67	0.52
2	P41222	Prostaglandin-H2 D-isomerase	1.73	1.11	5.50	4.04	1.25	0.50
3	P04406	Glyceraldehyde-3-phosphate dehydrogenase	1.71	1.17	15.50	4.72	3.33	0.52
4	P10599	Thioredoxin	1.57	0.80	21.17	5.88	3.00	0.89
5	P26022	Pentraxin-related protein PTX3	1.46	1.30	74.67	16.37	8.00	1.67
6	Q07954	Low-density lipoprotein receptor-related protein 1	[3.84/0] ^a	[2.11/0]	5.50	0.58	2.50	0.58
7	P02787	Serotransferrin	1.35	3.67	16.75	7.23	5.00	2.31
8	Q92743	Serine protease HTRA1	1.10	3.65	7.40	1.52	2.80	0.84
9	P02649	Apolipoprotein E	0.82	2.90	19.67	13.68	5.00	2.68
10	P05121	Plasminogen activator inhibitor 1	0.70	2.58	13.25	1.50	2.00	1.15
11	Q08629	Testican-1	1.22	2.52	12.83	4.67	3.50	0.55
12	P06396	Gelsolin	1.18	2.52	23.17	12.16	4.50	2.07
13	P12110	Collagen alpha-2(VI) chain	0.78	2.26	17.00	6.84	4.17	0.98
14	P15289	Arylsulfatase A	1.41	2.10	6.33	2.34	1.83	0.75
15	P13611	Versican core protein	1.33	2.03	51.00	7.38	9.33	1.51
16	P12111	Collagen alpha-3(VI) chain	1.37	1.99	38.33	20.47	10.83	6.01
17	Q16363	Laminin subunit alpha-4	1.20	1.98	41.33	29.37	8.67	3.67
18	P08758	Annexin A5	1.44	1.89	13.20	9.26	4.20	2.05
19	Q12841	Follistatin-related protein 1	1.27	1.85	82.83	15.22	11.00	1.67
20	Q14767	Latent-transforming growth factor beta-binding protein 2	1.12	1.81	40.67	6.68	10.00	1.55
21	Q08380	Galectin-3-binding protein	1.44	1.78	68.33	4.72	10.17	1.17
22	Q02818	Nucleobindin-1	1.01	1.60	33.33	1.97	6.83	1.47
23	P27797	Calreticulin	0.92	1.59	44.50	28.59	4.83	1.17
24	P07355	Annexin A2	0.90	1.56	29.75	0.96	6.50	0.58
25	P35052	Glypican-1	0.84	1.54	5.75	0.50	2.25	0.50
26	Q99715	Collagen alpha-1(XII) chain	1.30	1.53	106.67	51.02	21.67	7.31
27	O95967	EGF-containing fibulin-like extracellular matrix protein 2	0.43	1.51	7.67	1.15	2.33	0.58
28	P98095	Fibulin-2	1.13	1.46	101.83	34.75	16.33	3.01

Table 3-S2. Continued.

No.	Protein ID	Identified Proteins	LG/LGPUG	LG/HGINS	Ave. SC	SD	Ave. Peptides	SD
1	P07093	Glia-derived nexin	4.03	0.92	5.00	1.73	2.00	0.00
2	Q9Y4K0	Lysyl oxidase homolog 2	2.44	1.07	16.00	5.66	4.75	1.71
3	O95967	EGF-containing fibulin-like extracellular matrix protein 2	2.32	0.66	7.67	1.15	2.33	0.58
4	O14549	Osteoblast specific cysteine-rich protein	1.73	1.44	19.00	11.21	4.00	0.89
5	P20908	Collagen alpha-1(V) chain	1.62	1.30	35.17	18.49	7.17	2.04
6	Q9BRK5	Stromal cell derived factor 4	1.21	3.00	11.80	8.87	1.80	1.10
7	P23284	Peptidylprolyl isomerase B	0.96	1.83	25.33	12.89	3.00	1.55
8	P62937	Peptidyl-prolyl cis-trans isomerase A	0.75	1.64	18.00	6.98	2.50	0.58

^a Brackets indicate the average number of normalized spectral counts assigned to the proteins when no peptides were detected under a given condition.

Table 3-S3. Characterization of total N-linked glycans from human adipocytes by NS-MS and TIM scan

No.	N-linked oligosaccharide composition	Z	$\frac{[M+zNa]^{z+}}{m/z \text{ (mono)}}$	No.	N-linked oligosaccharide composition	Z	$\frac{[M+zNa]^{z+}}{m/z \text{ (mono)}}$
1	(Man)1(GlcNAc)2	1	763.384	82	(Gal)2(GlcNAc)3(Fuc)1(Man)3(GlcNAc)2(Fuc)1	2	1343.165
2	(Man)1(GlcNAc)2(Fuc)1	1	937.473	83	(NeuAc)1(Gal)2(GlcNAc)3(Man)3(GlcNAc)2	2	1349.663
3	(Man)2(GlcNAc)2	1	967.484	84	(Gal)3(GlcNAc)3(Man)3(GlcNAc)2(Fuc)1	2	1358.171
4	(Man)2(GlcNAc)2(Fuc)1	1	1141.573	85	(Gal)1(GlcNAc)4(Fuc)1(Man)3(GlcNAc)2(Fuc)1	2	1363.679
5	(Man)3(GlcNAc)2	1	1171.583	86	(NeuAc)1(Gal)1(GlcNAc)4(Man)3(GlcNAc)2	2	1370.176
6	(Man)3(GlcNAc)2(Fuc)1	1	1345.673	87	(Gal)4(GlcNAc)3(Man)3(GlcNAc)2	2	1373.176
7	(Man)4(GlcNAc)2	1	1375.683	88	(Gal)2(GlcNAc)4(Man)3(GlcNAc)2(Fuc)1	2	1378.684
8	(GlcNAc)1(Man)2(GlcNAc)2(Fuc)1	1	1386.699	89	(NeuAc)2(Gal)1(GlcNAc)2(Man)3(GlcNAc)2(Fuc)1	2	1392.681
9	(GlcNAc)1(Man)3(GlcNAc)2	1	1416.710	90	(Gal)3(GlcNAc)4(Man)3(GlcNAc)2	2	1393.689
		2	719.850	91	(Gal)1(GlcNAc)5(Man)3(GlcNAc)2(Fuc)1	2	1399.197
10	(Man)4(GlcNAc)2(Fuc)1	1	1549.772	92	(NeuAc)1(Gal)2(GlcNAc)2(Fuc)1(Man)3(GlcNAc)2(Fuc)1	2	1401.189
		1	1579.783	93	(NeuAc)2(Gal)2(GlcNAc)2(Man)3(GlcNAc)2	2	1407.687
		2	801.386			3	946.121
12	(GlcNAc)1(Man)3(GlcNAc)2(Fuc)1	1	1590.799	94	(NeuAc)1(Gal)3(GlcNAc)2(Man)3(GlcNAc)2(Fuc)1	2	1416.194
		2	806.894	95	(Gal)1(GlcNAc)1(Man)8(GlcNAc)2(Fuc)1	2	1419.194
		1	1620.810	96	(GlcNAc)6(Man)3(GlcNAc)2(Fuc)1	2	1419.710
13	(Gal)1(GlcNAc)1(Man)3(GlcNAc)2	2	821.900	97	(NeuAc)1(Gal)1(GlcNAc)3(Fuc)1(Man)3(GlcNAc)2(Fuc)1	2	1421.702
14	(GlcNAc)2(Man)3(GlcNAc)2	1	1661.836	98	(Gal)2(GlcNAc)3(Fuc)2(Man)3(GlcNAc)2(Fuc)1	2	1430.210
15	(Man)5(GlcNAc)2(Fuc)1	1	1753.872	99	(NeuAc)1(Gal)2(GlcNAc)2(Man)2(Man)3(GlcNAc)2	2	1431.199
		1	1783.883	100	(NeuAc)1(Gal)2(GlcNAc)3(Man)3(GlcNAc)2(Fuc)1	2	1436.707
		2	903.436	101	(Gal)3(GlcNAc)3(Fuc)1(Man)3(GlcNAc)2(Fuc)1	2	1445.215
17	(Gal)1(GlcNAc)1(Man)3(GlcNAc)2(Fuc)1	1	1794.899	102	(NeuAc)1(Gal)3(GlcNAc)3(Man)3(GlcNAc)2	2	1451.713
		2	908.944			3	975.472

Table 3-S3. Continued.

No.	N-linked oligosaccharide composition	Z	$\frac{[M+zNa]^{z+}}{m/z \text{ (mono)}}$	No.	N-linked oligosaccharide composition	Z	$\frac{[M+zNa]^{z+}}{m/z \text{ (mono)}}$
18	(GlcNAc)1(Man)5(GlcNAc)2	1	1824.909	103	(NeuAc)1(Gal)1(GlcNAc)4(Man)3(GlcNAc)2(Fuc)1	2	1457.221
		2	923.950	104	(Gal)2(GlcNAc)3(Man)2(Man)3(GlcNAc)2(Fuc)1	2	1460.220
19	(GlcNAc)2(Man)3(GlcNAc)2(Fuc)1	1	1835.925	105	(Gal)4(GlcNAc)3(Man)3(GlcNAc)2(Fuc)1	2	1460.220
		2	929.458	106	(Gal)2(GlcNAc)4(Fuc)1(Man)3(GlcNAc)2(Fuc)1	2	1465.728
20	(Gal)1(GlcNAc)2(Man)3(GlcNAc)2	1	1865.936	107	(NeuAc)1(Gal)2(GlcNAc)4(Man)3(GlcNAc)2	2	1472.226
		2	944.463	108	(Gal)3(GlcNAc)4(Man)3(GlcNAc)2(Fuc)1	3	989.147
21	(GlcNAc)3(Man)3(GlcNAc)2	1	1906.963	109	(NeuAc)2(Gal)2(GlcNAc)2(Man)3(GlcNAc)2(Fuc)1	2	1480.734
		2	964.976	110	(Gal)4(GlcNAc)4(Man)3(GlcNAc)2	2	1494.731
22	(Man)6(GlcNAc)2(Fuc)1	1	1957.972	111	(Gal)4(GlcNAc)4(Man)3(GlcNAc)2	2	1495.739
		2	990.481	112	(NeuAc)1(Gal)1(GlcNAc)2(Fuc)1(Man)5(GlcNAc)2(Fuc)1	2	1503.239
23	(Gal)1(GlcNAc)1(Fuc)1(Man)3(GlcNAc)2(Fuc)1	1	1968.988	113	(NeuAc)2(Gal)3(GlcNAc)2(Man)3(GlcNAc)2	2	1509.736
		2	995.989	114	(NeuAc)2(Gal)1(GlcNAc)3(Man)3(GlcNAc)2(Fuc)1	3	1014.154
24	(NeuAc)1(Gal)1(GlcNAc)1(Man)3(GlcNAc)2	1	1981.983	115	(NeuAc)2(Gal)1(GlcNAc)3(Man)3(GlcNAc)2(Fuc)1	2	1515.244
		2	1002.487	116	(NeuAc)2(Gal)1(GalNAc)1(GlcNAc)2(Man)3(GlcNAc)2(Fuc)1	3	1017.826
25	(Man)7(GlcNAc)2	1	1987.983	117	(Man)12(GlcNAc)2	2	1515.244
		2	1005.486	118	(Gal)3(GlcNAc)5(Man)3(GlcNAc)2	3	1017.826
26	(GlcNAc)1(Man)5(GlcNAc)2(Fuc)1	1	1998.999	119	(NeuAc)1(Gal)2(GlcNAc)3(Fuc)1(Man)3(GlcNAc)2(Fuc)1	2	1515.736
		2	1010.994	120	(Gal)3(GlcNAc)5(Man)3(GlcNAc)2	2	1516.252
27	(Gal)1(GlcNAc)1(Man)5(GlcNAc)2	1	1025.999	119	(NeuAc)1(Gal)2(GlcNAc)3(Fuc)1(Man)3(GlcNAc)2(Fuc)1	2	1523.752
		2	1031.507	120	(NeuAc)2(Gal)2(GlcNAc)3(Man)3(GlcNAc)2	2	1530.250
28	(Gal)1(GlcNAc)2(Man)3(GlcNAc)2(Fuc)1	1	1031.507	119	(NeuAc)2(Gal)2(GlcNAc)3(Man)3(GlcNAc)2	2	1538.757
		2	1046.513	120	(NeuAc)1(Gal)3(GlcNAc)3(Man)3(GlcNAc)2(Fuc)1	3	1033.502
29	(Gal)2(GlcNAc)2(Man)3(GlcNAc)2	1	1046.513	120	(NeuAc)1(Gal)2(GlcNAc)4(Fuc)1(Man)3(GlcNAc)2	2	1559.271
		2	1052.021	120	(GlcNAc)3(Man)3(GlcNAc)2(Fuc)1	3	1047.177
30	(GlcNAc)3(Man)3(GlcNAc)2(Fuc)1	1	1052.021				
		2	1067.026				
31	(Gal)1(GlcNAc)3(Man)3(GlcNAc)2	1	1067.026				
		2	1089.531				
32	(NeuAc)1(Gal)1(GlcNAc)1(Man)3(GlcNAc)2(Fuc)1	1	1089.531				
		2					

Table 3-S3. Continued.

No.	N-linked oligosaccharide composition	Z	$\frac{[M+zNa]^{z+}}{m/z \text{ (mono)}}$	No.	N-linked oligosaccharide composition	Z	$\frac{[M+zNa]^{z+}}{m/z \text{ (mono)}}$
33	(NeuAc)1(Gal)1(GlcNAc)1(Man)1 (Man)3(GlcNAc)2	2	1104.536	121	(Gal)5(GlcNAc)3(Man)3(GlcNAc)2(Fuc)1	2	1562.270
34	(Man)8(GlcNAc)2	2	1107.536	122	(NeuAc)1(Gal)3(GlcNAc)4(Man)3(GlcNAc)2	3	1574.276
35	(Gal)1(GlcNAc)1(Man)5(GlcNAc)2 (Fuc)1	2	1113.044	123	(NeuAc)2(Gal)2(GlcNAc)3(Man)3(GlcNAc)2 (Fuc)1	2	1617.294
36	(Gal)1(GlcNAc)2(Fuc)1(Man)3 (GlcNAc)2(Fuc)1	2	1118.552	124	(Gal)4(GlcNAc)5(Man)3(GlcNAc)2	3	1085.860
37	(NeuAc)1(Gal)1(GlcNAc)2(Man)3 (GlcNAc)2	2	1125.050	125	(Gal)2(GlcNAc)2(Man)3(GlcNAc)2 (Fuc)1	2	1632.300
38	(Gal)1(GlcNAc)1(Man)3(Man)3 (GlcNAc)2	2	1128.049	126	(NeuAc)2(Gal)3(GlcNAc)3(Man)3(GlcNAc)2	3	1095.863
39	(Gal)2(GlcNAc)2(Man)3(GlcNAc)2 (Fuc)1	2	1133.557	127	(NeuAc)1(Gal)3(GlcNAc)4(Man)3(GlcNAc)2 (Fuc)1	2	1661.321
40	(Gal)3(GlcNAc)2(Man)3(GlcNAc)2	2	1148.563	128	(NeuAc)1(Gal)4(GlcNAc)4(Man)3(GlcNAc)2	2	1676.326
41	(Gal)1(GlcNAc)3(Man)3(GlcNAc)2 (Fuc)1	2	1154.071	129	(NeuAc)2(Gal)2(GlcNAc)3(Fuc)1(Man)3 (GlcNAc)2(Fuc)1	3	1125.214
42	(Gal)2(GlcNAc)3(Man)3(GlcNAc)2	2	1169.076	130	(NeuAc)1(Gal)3(GlcNAc)3(Fuc)2(Man)3 (GlcNAc)2(Fuc)1	2	1712.847
43	(Gal)1(GlcNAc)3(Man)4(GlcNAc)2	2	1169.076	131	(NeuAc)2(Gal)3(GlcNAc)3(Man)3(GlcNAc)2 (Fuc)1	3	1153.893
44	(GlcNAc)3(Man)5(GlcNAc)2	2	1169.076	130	(NeuAc)2(Gal)3(GlcNAc)3(Man)3(GlcNAc)2 (Fuc)1	2	1719.344
45	(GlcNAc)4(Man)3(GlcNAc)2(Fuc)1	2	1174.584	131	(NeuAc)1(Gal)2(GlcNAc)4(Fuc)2(Man)3 (GlcNAc)2(Fuc)1	2	1733.360
46	(NeuAc)1(Gal)1(GlcNAc)1(Fuc)1 (Man)3(GlcNAc)2(Fuc)1	2	1176.576	131	(NeuAc)1(Gal)2(GlcNAc)4(Fuc)2(Man)3 (GlcNAc)2(Fuc)1	3	1163.237
47	(Gal)1(GlcNAc)4(Man)3(GlcNAc)2	2	1189.589				
48	(NeuAc)1(Gal)2(GlcNAc)1(Man)3 (GlcNAc)2(Fuc)1	2	1191.581				
49	(Man)8(GlcNAc)2(Fuc)1	2	1194.581				
50	(Gal)1(GlcNAc)1(Fuc)1(Man)2 (Man)3(GlcNAc)2(Fuc)1	2	1200.089				

Table 3-S3. Continued.

No.	N-linked oligosaccharide composition	Z	$\frac{[M+zNa]^{z+}}{m/z \text{ (mono)}}$	No.	N-linked oligosaccharide composition	Z	$\frac{[M+zNa]^{z+}}{m/z \text{ (mono)}}$
51	(Gal)1(GlcNAc)2(Fuc)2(Man)3 (GlcNAc)2(Fuc)1	2	1205.597	132	(NeuAc)2(Gal)2(GlcNAc)4(Man)3(GlcNAc)2 (Fuc)1	2	1739.858
52	(NeuAc)1(Gal)3(GlcNAc)1(Man)3 (GlcNAc)2	2	1206.586			3	1167.568
53	(Man)9(GlcNAc)2	2	1209.586	133	(NeuAc)1(Gal)4(GlcNAc)4(Man)3(GlcNAc)2 (Fuc)1	2	1763.370
54	(GlcNAc)5(Man)3(GlcNAc)2	2	1210.103			3	1183.244
55	(NeuAc)1(Gal)1(GlcNAc)2(Man)3 (GlcNAc)2(Fuc)1	2	1212.094	134	(NeuAc)1(Gal)5(GlcNAc)4(Man)3(GlcNAc)2	2	1778.376
56	(Gal)2(GlcNAc)2(Fuc)1(Man)3 (GlcNAc)2(Fuc)1	2	1220.602			3	1193.247
57	(NeuAc)1(Gal)2(GlcNAc)2(Man)3 (GlcNAc)2	2	1227.100	135	(NeuAc)1(Gal)4(GlcNAc)5(Man)3(GlcNAc)2	2	1798.889
58	(Gal)1(GlcNAc)1(Man)4(Man)3 (GlcNAc)2	2	1230.099	136	(NeuAc)2(Gal)3(GlcNAc)3(Fuc)1(Man)3 (GlcNAc)2(Fuc)1	2	1806.389
59	(Gal)3(GlcNAc)2(Man)3(GlcNAc)2 (Fuc)1	2	1235.607			2	1812.887
60	(Gal)1(GlcNAc)3(Fuc)1(Man)3 (GlcNAc)2(Fuc)1	2	1241.115	137	(NeuAc)3(Gal)3(GlcNAc)3(Man)3(GlcNAc)2	3	1216.254
61	(NeuAc)1(Gal)1(GlcNAc)3(Man)3 (GlcNAc)2	2	1247.613	138	(NeuAc)2(Gal)3(GlcNAc)4(Man)3(GlcNAc)2 (Fuc)1	3	1235.602
62	(Gal)4(GlcNAc)2(Man)3(GlcNAc)2	2	1250.613			2	1850.415
63	(Gal)2(GlcNAc)3(Man)3(GlcNAc)2 (Fuc)1	2	1256.121	139	(NeuAc)1(Gal)4(GlcNAc)4(Fuc)1(Man)3 (GlcNAc)2(Fuc)1	3	1241.273
64	(GlcNAc)4(Fuc)1(Man)3(GlcNAc)2 (Fuc)1	2	1261.629			2	1856.913
65	(NeuAc)2(Gal)1(GlcNAc)1(Man)3 (GlcNAc)2(Fuc)1	2	1270.118	140	(NeuAc)2(Gal)4(GlcNAc)4(Man)3(GlcNAc)2	3	1245.605
66	(Gal)3(GlcNAc)3(Man)3(GlcNAc)2	2	1271.126	141	(NeuAc)1(Gal)3(GlcNAc)5(Fuc)1(Man)3 (GlcNAc)2(Fuc)1	3	1254.949
67	(Gal)1(GlcNAc)4(Man)3(GlcNAc)2 (Fuc)1	2	1276.634	142	(NeuAc)1(Gal)6(GlcNAc)4(Man)3(GlcNAc)2	3	1261.280

Table 3-S3. Continued.

No.	N-linked oligosaccharide composition	Z	$\frac{[M+zNa]^{z+}}{m/z \text{ (mono)}}$	No.	N-linked oligosaccharide composition	Z	$\frac{[M+zNa]^{z+}}{m/z \text{ (mono)}}$
68	(Gal)2(GlcNAc)4(Man)3(GlcNAc)2	2	1291.639	143	(NeuAc)2(Gal)3(GlcNAc)3(Fuc)2(Man)3 (GlcNAc)2(Fuc)1	3	1269.952
69	(NeuAc)1(Gal)1(GlcNAc)1(Man)2 (Man)3(GlcNAc)2(Fuc)1	2	1293.631	144	(NeuAc)3(Gal)3(GlcNAc)3(Man)3(GlcNAc)2 (Fuc)1	2	1899.931
70	(GlcNAc)5(Man)3(GlcNAc)2(Fuc)1	2	1297.147			3	1274.284
71	(NeuAc)1(Gal)1(GlcNAc)2(Fuc)1 (Man)3(GlcNAc)2(Fuc)1	2	1299.139	145	(NeuAc)3(Gal)4(GlcNAc)3(Man)3(GlcNAc)2	3	1284.288
72	(NeuAc)2(Gal)1(GlcNAc)2(Man)3 (GlcNAc)2	2	1305.637	146	(Gal)4(GalNAc)1(GlcNAc)5(Fuc)1(Man)3 (GlcNAc)2(Fuc)1	3	1284.300
73	(Gal)2(GlcNAc)2(Fuc)2(Man)3 (GlcNAc)2(Fuc)1	2	1307.647	147	(NeuAc)2(Gal)5(GlcNAc)3(Man)3(GlcNAc)2 (Fuc)1	3	1289.959
		3	879.428	148	(NeuAc)3(Gal)3(GlcNAc)4(Man)3(GlcNAc)2	2	1935.450
74	(Glc)1(Man)9(GlcNAc)2	2	1311.636			3	1297.963
75	(Gal)1(GlcNAc)5(Man)3(GlcNAc)2	2	1312.152	149	(NeuAc)2(Gal)4(GlcNAc)4(Man)3(GlcNAc)2 (Fuc)1	2	1943.957
		3	882.431			3	1303.635
76	(NeuAc)1(Gal)2(GlcNAc)2(Man)3 (GlcNAc)2(Fuc)1	2	1314.144	150	(NeuAc)3(Gal)3(GlcNAc)3(Fuc)1(Man)3 (GlcNAc)2(Fuc)1	3	1332.314
		3	883.759	151	(NeuAc)4(Gal)3(GlcNAc)3(Man)3(GlcNAc)2	2	1993.473
77	(Gal)1(GlcNAc)2(Fuc)1(Man)2(Man)3 (GlcNAc)2(Fuc)1	2	1322.652	152	(NeuAc)3(Gal)4(GlcNAc)4(Man)3(GlcNAc)2	3	1365.996
78	(Gal)3(GlcNAc)2(Fuc)1(Man)3 (GlcNAc)2(Fuc)1	2	1322.652	153	(NeuAc)3(Gal)4(GlcNAc)4(Man)3(GlcNAc)2 (Fuc)1	3	1424.026
79	(NeuAc)1(Gal)3(GlcNAc)2(Man)3 (GlcNAc)2	2	1329.150	154	(NeuAc)3(Gal)3(GlcNAc)5(Man)3(GlcNAc)2 (Fuc)1	3	1437.702
80	(NeuAc)1(Gal)1(GlcNAc)3(Man)3 (GlcNAc)2(Fuc)1	2	1334.658	155	(NeuAc)4(Gal)4(GlcNAc)4(Man)3(GlcNAc)2 (Fuc)1	3	1544.417
81	(Gal)4(GlcNAc)2(Man)3(GlcNAc)2 (Fuc)1	2	1337.657				

Table 3-S4. Characterization of total O-linked glycans from human adipocytes by NS-MS and

TIM scan

No.	O-linked oligosaccharide composition	Z	$[M+zNa]^{z+}$
			m/z (mono)
1	(Hex)1(HexNAc)1 (HexNAc)1(Hex)1	1	534.289
2	(Xyl)2(Glc)1	1	609.310
3	(NeuAc)1(Hex)1	1	650.337
4	(Hex)1(HexNAc)1(Hex)1	1	738.389
5	(HexNAc)2(Hex)1 (Hex)1(HexNAc)2	1	779.415
6	(NeuAc)1(Hex)1(HexNAc)1	1	895.463
7	(Hex)2(HexNAc)2	1	983.515
8	(NeuAc)1(Hex)1(HexNAc)1(Fuc)1	1	1069.552
9	(NeuAc)1(Hex)1(HexNAc)1(Hex)1	1	1099.563
10	(NeuAc)1(Hex)1(HexNAc)2	1	1140.589
11	(Hex)2(HexNAc)2(Hex)1 (Hex)3(HexNAc)2	1	1187.615
12	(NeuAc)2(Hex)1(HexNAc)1	1	1256.636
13	(NeuAc)1(Hex)1(Fuc)1(HexNAc)2	1	1314.678
14	(NeuAc)1(Hex)2(HexNAc)2	1	1344.689
15	(HexA)1(Hex)2(HexNAc)2(Hex)1	1	1405.694
16	(NeuAc)2(Hex)1(HexNAc)2	1	1501.763
17	(NeuAc)1(Hex)2(Fuc)1(HexNAc)2	1	1518.778
18	(NeuAc)1(Hex)2(HexNAc)3	1	1589.815
19	(NeuAc)2(Hex)1(Fuc)1(HexNAc)2	1	1675.852
20	(NeuAc)2(Hex)2(HexNAc)2	1 2	1705.862 864.426
21	(NeuAc)1(Hex)3(HexNAc)3	1	1793.915
22	(NeuAc)2(Hex)2(Fuc)1(HexNAc)2	1 2	1879.952 951.471
23	(NeuAc)2(Hex)2(Fuc)1(HexNAc)2(Hex)1	2	1053.521
24	(NeuAc)2(Hex)2(Fuc)1(HexNAc)2(HexNAc)1	2	1074.034
25	(NeuAc)2(Hex)3(HexNAc)3	2	1089.039
26	(NeuAc)1(Hex)4(HexNAc)4	2	1133.065
27	(NeuAc)2(Hex)4(Fuc)1(HexNAc)2	2	1155.570
28	(Hex)6(HexNAc)4	2	1156.578
29	(Hex)3(Fuc)1(HexNAc)6	2	1182.600

CHAPTER IV

CONCLUSION

The applications of systematic proteomic technologies using mass spectrometry to identify diagnostic, prognostic and mechanistic biomarkers have been widely utilized by scientific fields for high-throughput screening against a diverse set of disease-based cell culture models as well as clinical samples. Cultured adipocytes with chronically exposure to a combination of high glucose and insulin levels thereby increased glucose flux through HBP have been a well-characterized as a model system for insulin resistance research. Alternatively, elevation of O-GlcNAc by PUGNAc treatment can also lead to insulin resistance. Adipose tissue is an endocrine organ capable of controlling whole body glucose homeostasis and insulin sensitivity. Many adipocytokines (adipokines, adipocyte-secreted proteins), can act in an autocrine, paracrine, or endocrine fashions. More complete characterization of this secretome and glycome of adipocytes can contribute to the mechanism of how adipocytokines can regulate cellular processes such as energy homeostasis and insulin sensitivity. Using a combination of cell lines and treatment conditions, we have more completely defined the secretome and glycome of mammalian adipocytes. Several of the proteins that we identified have already been implicated in complications associated with metabolic diseases such as classical insulin resistance. While elevated O-GlcNAc levels impinge on insulin-dependent glucose uptake and modulate adipocytokine secretion, modulation of O-GlcNAc levels can serve as a potential therapeutic target in the treatment of insulin resistance-associated diseases such as metabolic syndrome and type 2 diabetes and their resulting complications.

Under insulin resistant conditions, we identified 8 and 20 interesting target proteins that showed increased expression profiles from 3T3 adipocytes (L1 and F442A lines) and primary rat adipocytes respectively. Several of these proteins have previously been associated with type 2 diabetes or known complications arising from the induction of insulin resistance. In the primary human adipocytes, 24 proteins were upregulated under both insulin resistant conditions. We also reported regulated proteins under either only one of insulin resistant conditions. A more significant increase was observed from classical insulin resistance.

Most secreted proteins are glycosylated and N-linked glycosylation is prevalent in the proteins of the extracellular matrix. We identified 37 sites on 21 proteins for 3T3s, 48 sites on 31 proteins for primary rat and 91 sites on 51 proteins from primary human respectively of N-linked glycosylation using PNGase F and ^{18}O water. We have focused on determining the full diversity and changes of major and minor glycans from the adipocytes under different insulin resistant conditions. We determined the changes of glycans under the insulin resistant conditions using $^{13}\text{C}/^{12}\text{C}$ ratio by permethylation and prevalence ratios. The results showed that changes of glycans under these conditions were moderately affected in mature adipocytes with the relatively short incubation periods used.

Understanding how perturbations in O-GlcNAc levels in adipocytes, that appear to play a major role in several key aspects of insulin-resistance, may provide novel insights into prognostics, diagnostics, and therapeutics for metabolic syndrome, type 2 diabetes, and the associated complications of these debilitating diseases. The experiments reported here can provide an avenue to identify possible prognostic/diagnostic markers for metabolic syndrome (insulin-resistance syndrome), type 2 diabetes, and complications such as cardiovascular disease resulting from these conditions. Future work is aimed at determining whether steady-state levels

of these proteins are altered in the serum of rodent models of diabetes and patients diagnosed with metabolic syndrome, type I diabetes, or resulting complications.

APPENDIX A

**MAPPING GLYCANS ONTO SPECIFIC N-LINKED GLYCOSYLATION SITES OF
PYRUS COMMUNIS PGIP REDEFINES THE INTERFACE FOR EPG-PGIP
INTERACTIONS**

Reproduced with permission from Jae-Min Lim, Kazuhiro Aoki, Peggi Angel, Derek Garrison,
Daniel King, Michael Tiemeyer, Carl Bergmann and Lance Wells, *Journal of Proteome
Research* **2009**, 8 (2), 673-680. Copyright 2009 American Chemical Society

ABSTRACT

Polygalacturonase inhibiting proteins (PGIPs) are members of the leucine rich repeat family of proteins, involved in plant defense against fungal pathogens. PGIPs exhibit a remarkable degree of specificity in terms of their ability to bind and inhibit their target molecules, the endopolygalacturonases (EPGs). This specificity has been attributed for certain EPG-PGIP combinations to differences in primary sequence, but this explanation is unable to account for the full range of binding and inhibitory activities observed. In this paper, we have fully characterized the glycosylation on the PGIP derived from *Pyrus communis* and demonstrated, using a combination of PNGase F and PNGase A in ^{18}O -water, that the *Pyrus communis* PGIP utilizes all seven potential sites of N-linked glycosylation. Further, we demonstrate that certain sites appear to be modified only by glycans bearing α 3-linked core fucosylation, while others are occupied by a mixture of fucosylated and nonfucosylated glycans. Modeling of the carbohydrates onto a homologous structure of PGIP indicates potential roles for glycosylation in mediating the interactions of PGIPs with EPGs.

Keywords: Glycosylation, mass spectrometry, glycomics, N-linked, PNGase A, PGIP

A.1. INTRODUCTION

The plant cell wall is a major barrier against attempted invasion by phytopathogenic fungi. Therefore, the plant cell wall-degrading enzymes produced by fungi play an important role in their pathogenicity (1). Many fungi use *endo* polygalacturonases (EPGs) to hydrolyze the cell wall polysaccharide homogalacturonan as one of the first steps in invasion (2). A variety of plant defense mechanisms have evolved, some of which are directed toward EPGs. During

pathogenesis, interactions between fungal EPGs and plant-derived polygalacturonase-inhibiting proteins (PGIPs) alter the hydrolytic activity of the EPG (3). PGIPs form high-affinity complexes with EPGs in a reversible, stoichiometric manner (3). The rate of hydrolysis of homogalacturonan by an EPG/PGIP complex is generally between 1 and 2 orders of magnitude slower than by the free EPG, depending on the source of the EPG and PGIP (4).

EPGs from a single strain of fungus may exist in a variety of isoforms (4-6). The EPG isoforms may each exist as a series of glycoforms, and may vary in their mode of action as well as in their ability to interact with, and be inhibited by, PGIPs (4, 7). For example, the EPGs from two *Fusarium moniliforme* isolates, though 91.7% identical, were completely different in their susceptibility to inhibition by specific PGIPs (8).

PGIPs exhibit specificity with respect to the EPGs to which they bind *in vitro* (4, 7, 9). The PGIPs of a single species may be present as a set of isoforms, each of which exists as a series of glycoforms (10, 11). Protein glycosylation has proven to be important in maintaining protein structure and function and can play a key role in protein-protein interactions (12, 13). This structural variability provides the potential for a wide range of specificity in EPG-PGIP interactions within any plant-pathogen pairing. The mode of action of a particular fungal EPG and its inhibition by PGIPs may be one of the critical factors in determining fungal pathogenicity. To fully understand the interactions of these two classes of molecules and their role in host-pathogen interactions, the mechanisms of EPG hydrolysis of homogalacturonan and of PGIP inhibition of EPG must be understood at the molecular level.

A crystal structure of a bean PGIP has been published (14). This is an excellent starting point to begin to locate critical points of contact on the surfaces of the two proteins within the enzyme-inhibitor (EPG-PGIP) complex. We previously identified nine amino acids in the PGIPs

and nine amino acids in the EPGs that are likely candidates for change due to selection pressure, thus, potentially altering the specificity of interaction of the two proteins (15). This study supported data from sitespecific mutation experiments (16), and indicated other regions on the PGIP that may be of importance for EPG-PGIP interaction (17). Work by others has indicated that single amino acid replacements in PGIP can alter specific EPG-PGIP interaction (16, 18), but the relevance of these findings for other EPG-PGIP combinations is currently unclear (8). Further, only a single study has investigated the role of N-linked glycosylation in EPG-PGIP binding¹⁰ and the functional role of O-linked glycosylation in EPG-PGIP interactions has not been addressed. To date, an undisputed model of the EPG-PGIP complex has not yet been proposed (18-20). Mass spectrometry utilizing amide deuterium exchange, differential proteolysis, and modeling studies enabled us to begin to describe the structure of an EPG-PGIP complex (19).

In this paper, we expand the parameters for understanding the molecular nature of the EGP-PGIP interaction by assigning N-linked glycosylation site utilization and by characterizing glycan heterogeneity at defined sites on PGIP. This study looks at seven predicted sites of N-glycosylation found on the PGIP from *Pyrus communis* (pear), and demonstrates that all seven consensus sequences are utilized but that certain sites only appear to be modified by 3-linked fucosylated core glycan structures. Modeling of the carbohydrates onto a homology structure of PGIP elucidates potential roles for glycosylation in mediating the interactions of PGIPs with EPGs.

A.2. EXPERIMENTAL PROCEDURES

Preparation of PGIP Peptides for N-Glycosylation Site Mapping. PGIP from pears (*P. communis*, cv Bartlett) was isolated and purified as described in past accounts (21). The purified protein (~10 μg) was resuspended in 40 mM NH_4HCO_3 (0.1 $\mu\text{g}/\mu\text{L}$ of PGIP), denatured with 1 M urea, reduced with 10 mM of DTT for 1 h at 56 °C, carboxyamidomethylated with 55 mM of iodoacetamide (Sigma) in the dark for 45 min, and then digested with 2 μg of sequencing-grade trypsin (Promega) in 40 mM NH_4HCO_3 overnight at 37 °C. After digestion, the peptides were acidified with 1% trifluoroacetic acid and desalted via C18 spin columns (Vydac Silica C18, The Nest Group, Inc.), and the resulting peptides were divided into two aliquots and dried down in a Speed-Vac. Resulting dried peptides were resuspended in 10 μL of sodium phosphate for PNGase F or 10 μL of citrate buffer for PNGase A and then dried back down. For N-linked glycosylation site analysis, peptides were resuspended in 9 μL of ^{18}O water (H_2^{18}O , 95%, Cambridge Isotope Laboratories, Inc.) and 1 μL of N-glycanase (PNGase F, Prozyme) and allowed to incubate for 18 h at 37 °C. To map the fucosylated N-linked glycosylation sites, peptides were resuspended in 9 μL of ^{18}O water and 1 μL of N-glycanase (PNGase A, Calbiochem) and allowed to incubate for 18 h at 37 °C. In either case, peptides were dried back down and resuspended in 50 μL of 40 mM of NH_4HCO_3 , with 1 μg of trypsin, to remove any possible C-terminal incorporation of ^{18}O from residual trypsin activity for 4 h (22) and then dried down and stored at -20 °C until analyzed.

Liquid Chromatography Tandem Mass Spectrometry (LC-MS/MS) Analysis. The peptides were resuspended with 19.5 μL of mobile phase A (0.1% formic acid, FA, in water) and 0.5 μL of mobile phase B (80% acetonitrile, ACN, and 0.1% FA in water) and filtered with 0.2 μm filters

(Nanosep, PALL). Proteins were analyzed as previously described (23). Briefly, the samples were loaded off-line onto a nanospray tapered capillary column/emitter ($360 \times 75 \times 15 \mu\text{m}$, PicoFrit, New Objective) self-packed with C18 reverse-phase (RP) resin (8.5 cm, Waters) in a Nitrogen pressure bomb for 10 min at 1000 psi ($\sim 5 \mu\text{L}$ load) and then separated via a 160 min linear gradient of increasing mobile phase B at a flow rate of $\sim 200 \text{ nL/min}$ directly into the mass spectrometer. One-dimensional LC-MS/MS analysis was performed on a linear ion trap mass spectrometer (LTQ, Thermo Fisher Scientific, Inc., San Jose, CA) equipped with a nanoelectrospray ion source. A full MS spectrum was collected (m/z 350-2000) followed by 8 MS/MS spectra following CID (34% normalized collision energy) of the most intense peaks. Dynamic exclusion was set at 2 for 30 s exclusion.

Data Analysis. The resulting data was searched against a database containing the polygalacturonase-inhibiting protein (PGIP, gi|33087512 and *Pyrus communis*) fasta sequence, obtained from NCBI, and the common contaminants database (ThermoFisher) using the TurboSequest algorithm (BioWorks 3.1, Thermo Fisher Scientific, Inc.). Spectra with a threshold of 15 ions and a TIC of 2×10^3 were search. Charge state analysis using ZSA, correct ion, combion, and ionquest (all as part of the Bioworks work flow) were applied over a range of $[\text{MH}]^+ = 600\text{-}4000$. The SEQUEST parameters were set to allow 2.0 Da of precursor ion mass tolerance and 0.5 Da of fragment ion tolerance with monoisotopic mass. Only fully tryptic peptides were allowed with up to three missed internal cleavage sites. Dynamic mass increases of 15.99 and 57.02 Da were allowed for oxidized methionine and alkylated cysteine, respectively. Carbamylation, due to the presence of urea, was scanned for but not observed. In the cases where sites of N-linked glycosylation were investigated with N-glycanase and ^{18}O

water, a dynamic mass increase of 3.00 Da was allowed for Asn residues as previously described (24). The results of the SEQUEST search were filtered at 2.0/2.3/2.8 Xcorr (Cross correlation) with charge states of +1/+2/+3, respectively. Only Asn residues in consensus sites were identified as being modified by +3 Da and all peptide fragmentation data indicative of a site of modification were manually validated following automated filtering. All spectra leading to assignments are available upon request.

N-Glycan Release, Permethylation, and Analysis. Glycans were released from PGIP by sequential enzymatic digestion, first with PNGase F (Prozyme) and subsequently with PNGase A (Calbiochem). Preparation and analysis of N-linked glycans was performed as previously described (25). Briefly, between 5 and 10 μg of PGIP was denatured by boiling and incubated with trypsin. The resulting digest was subjected to reverse phase chromatography to enrich for glycopeptides, which were then concentrated to dryness by vacuum centrifugation before treatment with PNGase F. Exhaustive digestion with PNGase F was performed in 20 mM sodium phosphate, pH 7.5. The reaction mixture was subjected to reverse phase chromatography to separate the PNGase F-sensitive glycans from residual glycopeptide and from deglycosylated peptide. The residual glycopeptide/peptide mixture was then digested with PNGase A in 0.2 M citrate phosphate buffer, pH 5.0. Released glycans were separated from residual peptide by reverse phase chromatography, yielding PNGase A-sensitive glycans. Both pools of glycan were permethylated and analyzed by nanospray ionization tandem mass spectrometry, NSI-MSⁿ, using a linear ion trap mass spectrometer (LTQ, ThermoFisher). All spectra leading to assignments are available upon request.

Homology Modeling. To create a homology model for PGIP, the mature amino acid sequence of pear PGIP was threaded onto the crystal structure of PGIP from *Phaseolus vulgaris* (14) using the Swiss PDB Viewer, DeepView v. 3.7. The homology structure was then optimized with molecular mechanics, MM3, using the protein modeling suite, BioMedCache v. 6.1 (BMC). The optimized structure was then allowed to move using molecular dynamics, simulating 300 K for 2 ps, before it was again optimized with molecular mechanics. Seven glycosylation, three M3XN2 (Man3XylGlcNAc2) and four M3XN2F (Man3XylGlcNAc2Fuc) were created using BMC, and their structures were optimized using the semiempirical method, PM5. The N-linked glycosylations were attached to the appropriate residues and the entire glycosylated PGIP model was optimized by applying several iterations of molecular mechanics and molecular dynamics computations as before.

A.3. RESULTS

N-Linked Site Mapping of PGIP with PNGase F. *P. communis* PGIP has seven potential N glycosylation sites (N-X-S/T, where X is not P). To determine whether consensus sites were being utilized, purified, digested PGIP-derived peptides were treated with PNGase F in ¹⁸O-water to convert modified Asn residues to heavy Asp (a mass shift of 3 Da). Following enzymatic treatment, peptides were analyzed by LC-MS/MS and 3 of the potential 7 Asn were determined to be sites of N-linked glycosylation (Figure A-1, Table A-1). However, it was noted that complete coverage of the protein was only 61% and that tryptic peptides containing the other 4 potential sites of modification were not identified in this experiment (Table A-1).

N-Linked Site Mapping of PGIP with PNGase A. It is well-established that both plants and insects, unlike mammals, are capable of α 3-linked fucose modification of the reducing terminal GlcNAc residue in N-linked structures (26). Furthermore, PNGase F is unable to cleave N-linked glycans containing α 3-linked fucose in the chitobiose core (27). Therefore, we utilized PNGase A to incorporate ^{18}O at glycosylated Asn sites. This enzyme is able to cleave 3-linked fucose on the reducing end GlcNAc of N-linked structures (27). Following PNGase A treatment in ^{18}O -water of the PGIP-derived peptides, coverage increased to 81% and all 7 sites of N-linked glycosylation were shown to be utilized (Figure A-2, Table A-1).

Glycan Analysis Following PNGase F and PNGase A Release from PGIP. To determine the full range of structures that might be found at the 7 N-linked glycosylation sites of PGIP, glycans were released by PNGase F or by PNGase A (following PNGase F). Released, permethylated glycans were analyzed by tandem mass spectrometry (25). The profile of glycans released from PGIP by PNGase F digestion is dominated by a single structure, the xylosylated trimannosyl core glycan M3XN2 (Figure A-3, $m/z = 1331$). Fragmentation analysis places the Xyl residue onto the branched Man residue, as previously described for plant N-linked glycans (28). In addition to the dominant PNGase F-sensitive glycan, 14 other detectable glycans were released by PNGase F digestion. A full series of high-mannose glycans, ranging from M9N2 to M3N2, as well as hybrid (NM3N2, NM3XN2) and complex (N2M3N2) glycans were released by PNGase F, but were detected at very low levels (Table A-2). Following exhaustive treatment with PNGase F, digestion of residual glycoprotein with PNGase A identified a single dominant PNGase F resistant, PNGase A-sensitive glycan as M3XN2F, where the Fuc residue was detected in α 3 linkage to the reducing terminal GlcNAc residue (Figure A-2B, $m/z = 1506$). The remaining

detectable, but minor, PNGase A-sensitive glycans all share a characteristic α 3-linked Fuc on the reducing terminal core GlcNAc residue (Table A-2). Both paucimannose (M3N2, M2N2) and hybrid-type (NM3XN2) glycans are modified with core Fucose on PGIP. The diversity of minor glycans released by PNGase F or PNGase A is consistent with the microheterogeneity inherent in N-linked glycosylation. However, the overwhelming predominance of M3XN2 and M3XN2F indicates that PGIP exhibits a significant level of glycosylation homogeneity.

A.4. DISCUSSION

The differences in the specificities of EPGs for PGIPs have generally been attributed to changes in individual amino acids within individual PGIPs (29) and EPGs (30). These single site changes are unlikely to account for the wide spectrum of binding and inhibitory activities observed, and little emphasis has been placed on the potential for glycosylation to effect the ability of PGIPs to bind, and/or to inhibit EPGs. We have previously discovered that several of the EPGs we have studied (PG I, PGA, PGC from *Aspergillus niger*, along with PG 2 and PG 3 from *Botrytis cinerea*) contain O-linked mannose (31-33). These modifications are located near the N-terminus in close proximity to the sites where we hypothesize PGIP binding occurs. This has led us to speculate that O-mannosylation may play an important role in EPG/PGIP interaction, as the O-Man-initiated modification has been previously observed to have a dramatic impact on the α -dystroglycan/laminin interaction in animals (13).

An earlier study provided partial characterization of the carbohydrate structures present on two N-linked sites in *P. vulgaris* (bean) PGIP by MALDI-TOF MS (34). Here, we have demonstrated that the *P. communis* PGIP utilizes all seven sites of glycosylation by using a combination of PNGase F and PNGase A to sequentially release differentially sensitive glycans.

By digesting PGIP with PNGase F or A in ^{18}O -water, modified Asn residues are converted to ^{18}O -Asp, tagging the site of modifications with a mass label (+3 Da, Figures A-1 and A-2, Table A-1). Our methodology clearly illustrates the need to use the less commonly used N-glycanase, PNGase A, to fully site-map and characterize the N-linked glycans in plants (and insects). Interestingly, 4 of the 7 sites appear to be exclusively modified by fucosylated N-linked glycans as they were not detected following PNGase F treatment. While the major PNGase F sensitive glycan was M3XN2 and the major PNGase A sensitive glycan was M3XN2F (with the fucose in α 3-linkage), several other minor glycan structures, including those observed in the earlier study on *P. vulgaris* PGIP were observed (Table A-2).

A homology model with the most abundant glycan structures was generated and energy minimized to better understand the impact of N-linked glycosylation on the interaction interface (Figure A-4). Inspection of the model generated indicates that the N-linked glycans of *P. communis* PGIP lie on either side of the binding surface, greatly increasing the surface area available for interaction with the target EPG, but also increasing the potential for steric modulation of binding by glycosylation. The striking dominance of α 3-fucosylated glycans at specific N-linked sites suggests that this Fuc residue imparts protein conformation that is favored for interactions with EPG. Extremely little is known about the factors that influence whether individual N-linked glycans are modified by core Fuc. Elucidation of PGIP glycosylation lays a groundwork for investigating whether specific protein motifs favor, or perhaps inhibit, the elaboration of α 3-Fuc.

P. communis PGIP is relatively heavily glycosylated, yet it also appears to be designed to allow for additional glycosylation. The asparagines running down either side of the molecule are components of what is termed an asparagine ladder which is believed to add stability to the

structure (14). Not all of these asparagines fall into an N-linked glycosylation consensus sequence (NXS/T), but each asparagine provides a site for evolution toward the generation of a new glycosylation site. The situation is similar for the *P. vulgaris* PGIP which also displays an asparagine ladder (14), and PGIPs are known to exist in multiple glycosylation states (14, 15). Whether glycosylation directly impacts the ability to bind and/or inhibit EPGs awaits further analysis, but the significant presence of specific N-linked glycans flanking the PGIP/EPG interaction region requires that their contribution be considered in elucidating the biological specificity of this host-pathogen interaction.

REFERENCES

1. Cooper, R. M., The mechanisms and significance of enzymic degradation of host cell walls by parasites. In *Biochemical Plant Pathology*; Wiley; New York, **1985**, p135.
2. Jones, T. M.; Anderson, A. J.; Albersheim, P. Host-Pathogen Interactions IV. Studies of the polysaccharide-degrading enzymes. *Physiol. Plant Pathol.* **1972**, *2*, 153-166.
3. Cervone, F.; De Lorenzo, G.; Aracri, B.; Bellincampi, D.; Caprari, C.; Devoto, A.; Mattei, B.; Nuss, L.; Salvi, G. The PGIP Family: Extracellular proteins specialized for recognition. In *Biology of Plant-Microbe Interactions*; International Society for Molecular Plant-Microbe Interactions: St. Paul, MN, **1996**, p93-98.
4. Cook, B. J.; Clay, R. P.; Bergmann, C. W.; Albersheim, P.; Darvill, A. G. Fungal polygalacturonases exhibit different substrate degradation patterns and differ in their susceptibilities to polygalacturonase-inhibiting proteins. *Mol. Plant-Microbe Interact.* **1999**, *12* (8), 703-711.
5. Centis, S.; Dumas, B.; Fournier, J.; Marolda, M.; Esquerre-Tugaye, M. T. Isolation and sequence analysis of Clpg1, a gene coding for an endopolygalacturonase of the phytopathogenic fungus *Colletotrichum lindemuthianum*. *Gene* **1996**, *170* (1), 125-129.
6. Parenicova, L.; Benen, J. A.; Kester, H. C.; Visser, J. pgaA and pgaB encode two constitutively expressed endopolygalacturonases of *Aspergillus niger*. *Biochem. J.* **2000**, *345*, 637-644.
7. Kemp, G.; Stanton, L.; Bergmann, C. W.; Clay, R. P.; Albersheim, P.; Darvill, A. Polygalacturonase-inhibiting proteins can function as activators of polygalacturonase. *Mol. Plant-Microbe Interact.* **2004**, *17* (8), 888-894.

8. Sella, L.; Castiglioni, C.; Roberti, S.; D'Ovidio, R.; Favaron, F. An endo-polygalacturonase (PG) of *Fusarium moniliforme* escaping inhibition by plant polygalacturonase-inhibiting proteins (PGIPs) provides new insights into the PG-PGIP interaction. *FEMS Microbiol. Lett.* **2004**, *240* (1), 117-124.
9. Kemp, G.; Bergmann, C. W.; Clay, R.; Van der Westhuizen, A. J.; Pretorius, Z. A. Isolation of a polygalacturonase-inhibiting protein (PGIP) from wheat. *Mol. Plant-Microbe Interact.* **2003**, *16* (11), 955-961.
10. Bergmann, C.; Cook, B. J.; Darvill, A.; Albersheim, P.; Bellincampi, D.; Caprari, C. The effect of glycosylation of EPG and PGIP on the production of oligogalacturonides. In *Pectins and Pectinases*; Elsevier Science: New York, **1996**, p275-282.
11. Desiderio, A.; Aracri, B.; Leckie, F.; Mattei, B.; Salvi, G.; Tigelaar, H.; Van Roekel, J. S.; Baulcombe, D. C.; Melchers, L. S.; De Lorenzo, G.; Cervone, F. Polygalacturonase-inhibiting proteins (PGIPs) with different specificities are expressed in *Phaseolus vulgaris*. *Mol. Plant-Microbe Interact.* **1997**, *10* (7), 852-860.
12. Haltiwanger, R. S.; Lowe, J. B. Role of glycosylation in development. *Annu. Rev. Biochem.* **2004**, *73*, 491-537.
13. Martin, P. T. Dystroglycan glycosylation and its role in matrix binding in skeletal muscle. *Glycobiology* **2003**, *13* (8), 55R-66R.
14. Di Matteo, A.; Federici, L.; Mattei, B.; Salvi, G.; Johnson, K. A.; Savino, C.; De Lorenzo, G.; Tsernoglou, D.; Cervone, F. The crystal structure of polygalacturonase-inhibiting protein (PGIP), a leucinerich repeat protein involved in plant defense. *Proc. Natl. Acad. Sci. U.S.A.* **2003**, *100* (17), 10124-10128.

15. Stotz, H. U.; Bishop, J. G.; Bergmann, C.; Koch, M.; Albersheim, P.; Darvill, A.; Labavitch, J. M. Identification of target amino acids that affect interactions of fungal polygalacturonases and their plant inhibitors. *Physiol. Mol. Plant Pathol.* **1999**, *56*, 117-130.
16. Leckie, F.; Mattei, B.; Capodicasa, C.; Hemmings, A.; Nuss, L.; Aracri, B.; De Lorenzo, G.; Cervone, F. The specificity of polygalacturonase-inhibiting protein (PGIP): a single amino acid substitution in the solvent-exposed beta-strand/beta-turn region of the leucine-rich repeats (LRRs) confers a new recognition capability. *EMBO J.* **1999**, *18* (9), 2352-2363.
17. Bishop, J. G. Directed mutagenesis confirms the functional importance of positively selected sites in polygalacturonase inhibitor protein. *Mol. Biol. Evol.* **2005**, *22* (7), 1531-1534.
18. Federici, L.; Caprari, C.; Mattei, B.; Savino, C.; Di Matteo, A.; De Lorenzo, G.; Cervone, F.; Tsernoglou, D. Structural requirements of endopolygalacturonase for the interaction with PGIP (polygalacturonase-inhibiting protein). *Proc. Natl. Acad. Sci. U.S.A.* **2001**, *98* (23), 13425-13430.
19. King, D.; Bergmann, C.; Orlando, R.; Benen, J. A.; Kester, H. C.; Visser, J. Use of amide exchange mass spectrometry to study conformational changes within the endopolygalacturonase II-homogalacturonan-polygalacturonase inhibiting protein system. *Biochemistry* **2002**, *41* (32), 10225-10233.
20. Sicilia, F.; Fernandez-Recio, J.; Caprari, C.; De Lorenzo, G.; Tsernoglou, D.; Cervone, F.; Federici, L. The polygalacturonaseinhibiting protein PGIP2 of *Phaseolus vulgaris* has

- evolved a mixed mode of inhibition of endopolygalacturonase PG1 of *Botrytis cinerea*. *Plant Physiol.* **2005**, *139* (3), 1380-1388.
21. Stotz, H. U.; Powell, A. L.; Damon, S. E.; Greve, L. C.; Bennett, A. B.; Labavitch, J. M. Molecular characterization of a polygalacturonase inhibitor from *Pyrus communis* L. cv Bartlett. *Plant Physiol.* **1993**, *102* (1), 133-138.
22. Angel, P. M.; Lim, J. M.; Wells, L.; Bergmann, C.; Orlando, R. A potential pitfall in ¹⁸O-based N-linked glycosylation site mapping. *Rapid Commun. Mass Spectrom.* **2007**, *21* (5), 674-682.
23. Lim, J. M.; Sherling, D.; Teo, C. F.; Hausman, D. B.; Lin, D.; Wells, L. Defining the regulated secreted proteome of rodent adipocytes upon the induction of insulin resistance. *J. Proteome Res.* **2008**, *7* (3), 1251-1263.
24. Koles, K.; Lim, J. M.; Aoki, K.; Porterfield, M.; Tiemeyer, M.; Wells, L.; Panin, V. Identification of N-glycosylated proteins from the central nervous system of *Drosophila melanogaster*. *Glycobiology* **2007**, *17* (12), 1388-1403.
25. Aoki, K.; Perlman, M.; Lim, J. M.; Cantu, R.; Wells, L.; Tiemeyer, M. Dynamic developmental elaboration of N-linked glycan complexity in the *Drosophila melanogaster* embryo. *J. Biol. Chem.* **2007**, *282* (12), 9127-9142.
26. Tomiya, N.; Narang, S.; Lee, Y. C.; Betenbaugh, M. J. Comparing N-glycan processing in mammalian cell lines to native and engineered lepidopteran insect cell lines. *Glycoconjugate J.* **2004**, *21* (6), 343-360.
27. Maley, F.; Trimble, R. B.; Tarentino, A. L.; Plummer, T. H., Jr. Characterization of glycoproteins and their associated oligosaccharides through the use of endoglycosidases. *Anal. Biochem.* **1989**, *180* (2), 195-204.

28. Kurosaka, A.; Yano, A.; Itoh, N.; Kuroda, Y.; Nakagawa, T.; Kawasaki, T. The structure of a neural specific carbohydrate epitope of horseradish peroxidase recognized by anti-horseradish peroxidase antiserum. *J. Biol. Chem.* **1991**, *266* (7), 4168-4172.
29. Di Matteo, A.; Bonivento, D.; Tsernoglou, D.; Federici, L.; Cervone, F. Polygalacturonase-inhibiting protein (PGIP) in plant defence: a structural view. *Phytochemistry* **2006**, *67* (6), 528-533.
30. Raiola, A.; Sella, L.; Castiglioni, C.; Balmas, V.; Favaron, F. A single amino acid substitution in highly similar endo-PGs from *Fusarium verticillioides* and related *Fusarium* species affects PGIP inhibition. *Fungal Genet. Biol.* **2008**, *45* (5), 776-789.
31. Colangelo, J.; Licon, V.; Benen, J.; Visser, J.; Bergmann, C.; Orlando, R. Characterization of the glycosylation of recombinant endopolygalacturonase I from *Aspergillus niger*. *Rapid Commun. Mass Spectrom.* **1999**, *13* (14), 1448-1453.
32. Woosley, B.; Xie, M.; Wells, L.; Orlando, R.; Garrison, D.; King, D.; Bergmann, C. Comprehensive glycan analysis of recombinant *Aspergillus niger* endo-polygalacturonase C. *Anal. Biochem.* **2006**, *354* (1), 43-53.
33. Woosley, B. D.; Kim, Y. H.; Kumar Kolli, V. S.; Wells, L.; King, D.; Poe, R.; Orlando, R.; Bergmann, C. Glycan analysis of recombinant *Aspergillus niger* endo-polygalacturonase A. *Carbohydr. Res.* **2006**, *341* (14), 2370-2378.
34. Mattei, B.; Bernalda, M. S.; Federici, L.; Roepstorff, P.; Cervone, F.; Boffi, A. Secondary structure and post-translational modifications of the leucine-rich repeat protein PGIP (polygalacturonaseinhibiting protein) from *Phaseolus vulgaris*. *Biochemistry* **2001**, *40* (2), 569-576.

Table A-1. Sites of N-Linked Glycosylation and Sequence Coverage of PGIP

PNGase F	Coverage: 61%
<p>DLCNPDDKK VLLQIK KAFGDPYVLASWKSDTDCCDWYCVTCDSTTNRINSLTIF AGQVSGQIPALVGDLPYLETLEFHK QPNLTGPIQPAIAKLGKGLK SLRLSWTMLSGS VPDFLSQLK NLTFLDLSFNLTGAIPSSSELPNLGALRLDRNKLTGHIPISFGQFIGN VPDLYLSHNQLSGNIPTSFQMDFTSIDLSR NKLEGDASVIFGLNKTTQIVDLSR NLLEFNLSK VEFPTSLSLDINHNI YGSIPVEFTQLNFQFLMVSYNRLCGQI PVGGKLQSFDEYSYFHNRLCGAPLPSCK</p>	
PNGase A	Coverage: 81%
<p>DLCNPDDKKVLLQIKKAFGDPYVLASWKSDTDCCDWYCVTCDSTTNRINSLTIF AGQVSGQIPALVGDLPYLETLEFHKQPLTGPIQPAIAK LKGLKSLR LSWTNLSGS VPDFLSQLKNLTFDLSFNNLTAIPSSSELPNLGALR LDRNKLTGHIPISFGQFIGN VPDLYLSHNQLSGNIPTSFQMDFTSIDLSR NKLEGDASVI FGLNKTTQIVDLSR NLLEFNLKVEFPTSLSLDINHNIYGSIPVEFTQLNFQFLNVSYNRLCGQI PVGGKLQSFDEYSYFHNRLCGAPLPSCK</p>	
<p>Bold represents assigned coverage by LC-MS/MS. <i>Red Asn</i> are assigned as +3 (PNGase F sensitive N-linked glycosylation sites), <i>Blue Asn</i> are assigned as +3 (PNGase A sensitive N-linked glycosylation sites), <u><i>Underlined Green Asn</i></u> were identified as being sensitive to both PNGase A and PNGase F.</p>	

Table A-2. N-Linked Glycans of PGIP

Glycan Structure	Permethylated Mass (m/z)		Glycan Prevalence (% Total Profile)	
	Singly charged [m+Na] ⁺	Doubly charged [m+2Na] ²⁺	Released by PNGaseF	Released by PNGaseA after PNGaseF
M3N2	1171	nd ¹	1.9	nd
M4N2	1375	nd	1.6	nd
M5N2	1579	800	5.6 ³	nd
M6N2	1783	903	17.4	nd
M7N2	1987	1005	3.3	nd
M8N2	2191	1107	1.5	nd
M9N2	2395	nd	<0.3 ⁴	nd
NM3N2	1416	nd	<0.3	nd
NM4N2	1620	nd	<0.3	nd
NM5N2	1684	nd	<0.3	nd
N2M3N2	1661	nd	<0.3	nd
M2XN2	1127	nd	1.3	nd
M3XN2	1331	677	61.8	nd
NM3XN2	1576	800	5.6 ³	nd
M2N2F ³ or ⁶	1141	nd	<0.3	<0.3
M3N2F ³ or ⁶	1345	nd	nd	1.3
M2XN2F ³	1302	nd	nd	3.8
M3XN2F ³	1506	nd	nd	87.5
NM3XN2F ³	1750	nd	nd	5.5
M2N2F ^{2,6}	1315	nd	nd	0.6
M3N2F ^{2,6}	1519	nd	nd	1.4

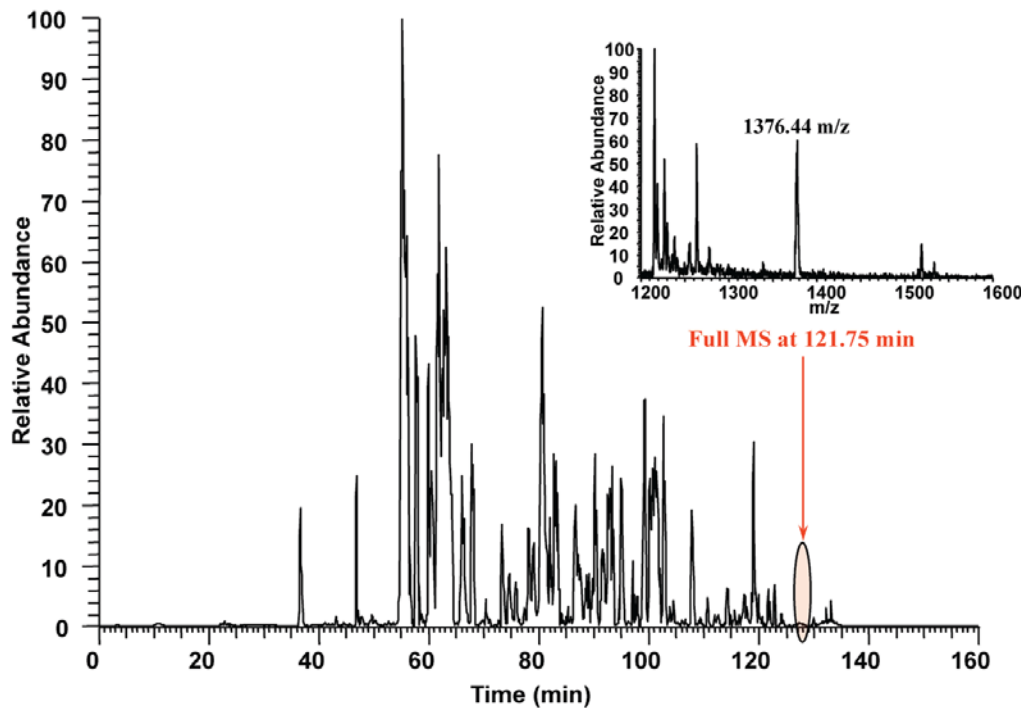
¹"nd" denotes "not detected"

²Superscripted "3" or "6" indicates the Fuc linkage position onto GlcNAc.

³The M5N2 and NM3XN2 glycans were primarily detected as doubly-charged ions, which were unresolved (m/z = 800 for both). Therefore, the calculated prevalence was divided equally between the two glycans.

⁴Glycans with prevalence indicated as "<0.3" were detected below the threshold of quantification, which was taken as 2 times background.

A. PNGaseF



B.

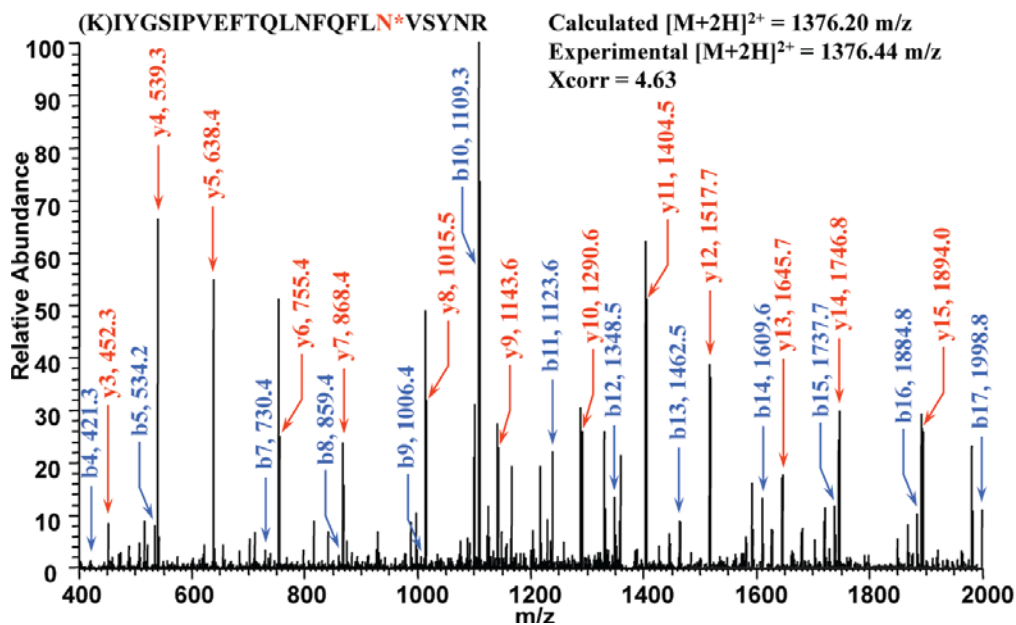
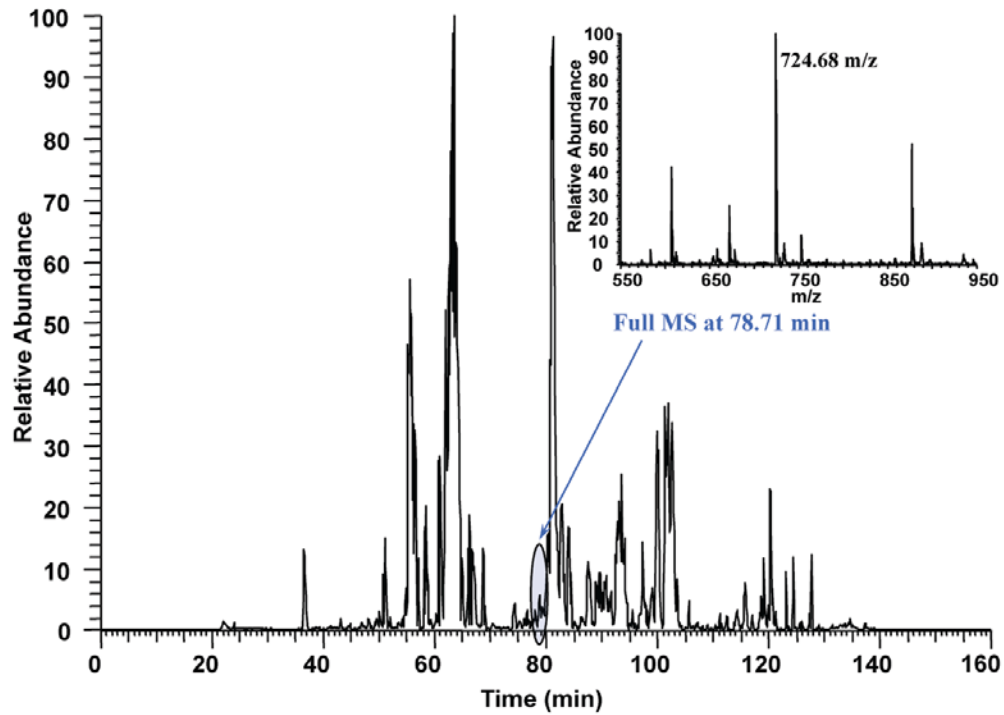


Figure A-1. Tandem mass spectrometry following PNGase F treatment in ^{18}O -water to map sites of N-linked glycosylation on PGIP. (A) Full chromatogram of LC-MS/MS run. (B) MS/MS fragmentation leading to the identification of a site of modification ($N^* = +3$ Da).

A. PNGaseA



B.

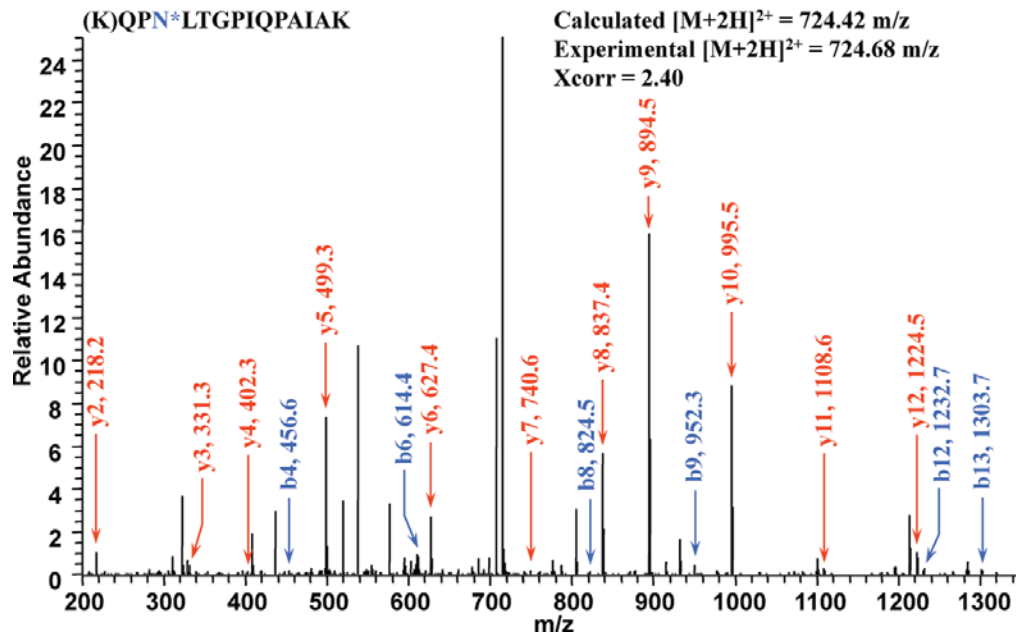


Figure A-2. Tandem mass spectrometry following PNGase A treatment in ^{18}O -water to map sites of N-linked glycosylation on PGIP. (A) Full chromatogram of LC-MS/MS run. (B) MS/MS fragmentation leading to the identification of a site of modification ($N^* = +3$ Da).

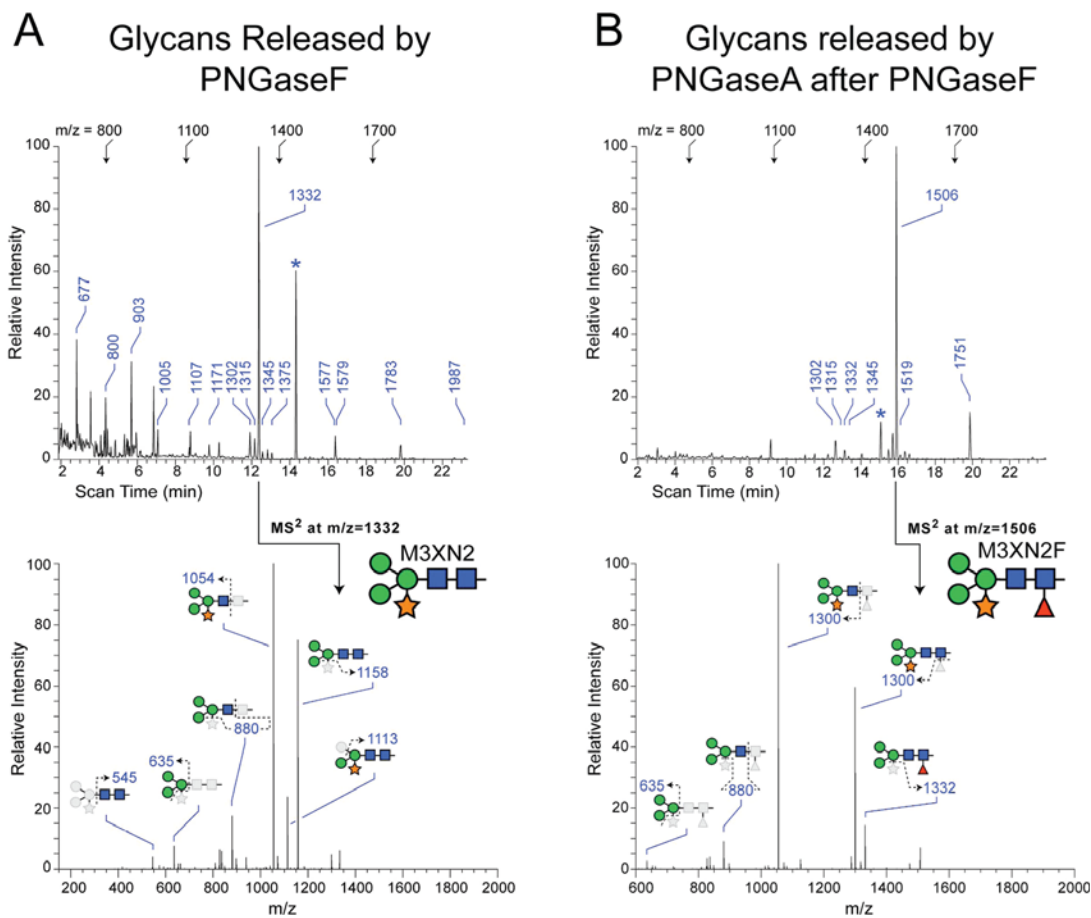


Figure A-3. N-linked glycan analysis of PGIP. (A) Total ion mapping (TIM) profile and MS/MS fragmentation of most abundant glycan following PNGase F release. (B) TIM profile and MS/MS fragmentation of most abundant glycan following PNGase A release after removal of PNGase F released glycans. For TIM scans in A and B, landmark m/z values are shown across the top at their equivalent scan times for each sample. For detected glycans, m/z values are indicated along the scan. Asterisks indicate a nonglycan contaminant at $m/z = 1452$, which is routinely detected following permethylation. For MS/MS spectra, glycan representations are consistent with the nomenclature recommendations of the Consortium for Functional Glycomics (Man, green circle; GlcNAc, blue square; Fuc, red triangle; Xyl, orange star). The dominant glycan released by PNGase F is M3XN2. For PNGase A, the dominant glycan is the α 3-fucosylated version of the same structure, M3XN2F.

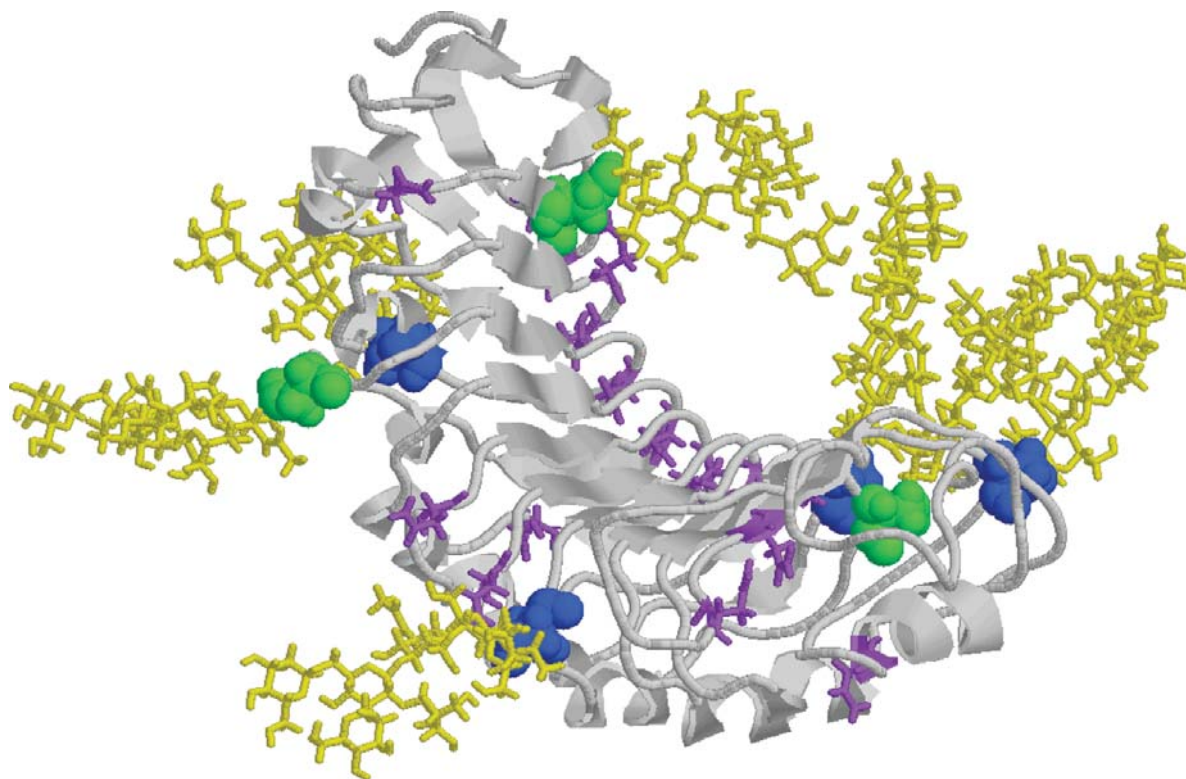


Figure A-4. Homology model of N-glycosylated PGIP. PNGase A-only sensitive sites are shown in blue with M3XN2F attached in yellow and PNGase F and A sensitive sites are shown in green with M3XN2 attached in yellow. The peptide backbone is shown in gray with all unmodified Asn residues labeled in purple.